Properties and dynamics of suspended load and near-bed fine cohesive sediments in highly impacted estuaries

Case studies from the Weser, Ems and Elbe estuaries (Germany)

Dissertation

zur Erlangung des Doktorgrades

der Mathematischen-Naturwissenschaftlichen Fakultät

der Christian-Albrechts Universität

zu Kiel

vorgelegt von

Svenja Papenmeier

Kiel, 2012

Erste Gutachterin: Prof. Dr. Kerstin Schrottke

Zweiter Gutachter: Prof. Dr. Karl Stattegger

Tag der mündlichen Prüfung: 24.10.2012

Zum Druck genehmigt: 24.10.2012

gez. (Prof. Dr. Wolfgang J. Duschl), Dekan

Contents

Abstract

Estuaries are often used as transport ways to cities and harbours in the hinterland and have emerged as an important focus in coastal research. Mankind aspires to understand and control the complex hydro- and sediment dynamics in order to optimize the system due to social-economic demands. In this process, river regulations (e.g. dredging activities) change the natural dynamics of the environment sustainably. This study provides new knowledge about near bed cohesive sediment dynamics as well as of fine cohesive sediment dynamics not only under 'natural' tidal flow but also under the influence of Water Injection Dredging (WID).

In-Situ Particle Size Distributions (ISPSDs) and Primary Particle Size Distributions (PPSDs) measured in the German Elbe and Weser estuaries indicate that the organic and inorganic Suspended Particulate Matter (SPM) is in a flocculated state. The substrate for the organic matter, which is needed for flocculation processes, is mainly transported from the seaside into the estuaries. Regional differences in PPSD have been observed in winter when the freshwater discharge is high and the extension of the Turbidity Maximum Zone (TMZ) is large. Individual sorting between the seaward and landward section as well as in the TMZ has not been observed in summer when the TMZ extension is small. Regional differences in the PPSD have no influence on the ISPSD. The latter is controlled primarily by the particle collision frequency powered by tidal forces and increased Suspended Sediment Concentrations (SSCs). Although, flocs break-up due to shear stress with progressing tidal current they do not change their PPSD. Knowledge about floc size and composition is important to estimate settling velocities of the SPM. Increased particle settling can lead to enhanced near bed fine cohesive sediment concentrations. High resolution vertical sampling of near bed SPM in the Weser and Ems estuaries indicates that the widely accepted 3-layer models, often used to describe vertical, cohesive sediment distribution is evidently incomplete. Sedimentological and rheological parameters, statistically proven by a cluster analysis, have shown that the intermediate fluid mud layer has to be subdivided in a low-viscosity fluid mud layer (I) and high-viscosity fluid mud layer (II). On the basis of a multi-parameter analysis it was possible to define the exact SSC-limits of both fluid mud types. The upper boundary of the fluid

mud (I) is characterised by a strong SSC-gradient (lutocline) which is detected with the low frequency channel of a parametric sediment echo sounder. The amplitude of the acoustic interface correlates with the SSC-gradient sampled at the acoustic interface which had not been quantified before in literature. Decreasing SSC-gradients with progressing tidal currents indicate an interfacial mixing but significant changes do not occur in areas of smooth bed morphology until one hour after slack water. Fluid mud (II) layers are suggested to represent recurrent, cohesive sediment accumulations which frequently have to be dredged in harbours and navigation channels. Over the last few decades the hydraulic WID technique has gained increased interest for the removal of mud shoals and subaqueous sand dunes in tidal controlled environments. Extensive hydroacoustical, optical and ground-truthing data collected during WID in the brackish- and freshwater reach of the Weser estuary shows that the crests of subaqueous sand dunes were exactly removed at the demanded height. Potential dredging effects are restricted to the approximate dredging site. Destruction of the internal sediment structure is limited to the upper decimetres and mobilized sandy sediments are accumulated on the dune slopes or in the adjacent troughs. Significant variations in the SSC or floc size are neither observed in the brackwater nor in the freshwater reach although acoustic interferences suggest increased turbulences over a distance of some hundreds of metres at the current lee-side of the dredging device.

Zusammenfassung

Tidedominierte Flussmündungen, sogenannte Ästuare, werden häufig als Transportwege zu Häfen und Städten im Hinterland genutzt. Um wirtschaftlichen und sozialen Interessen gerecht zu werden ist der Mensch bestrebt die komplexe Hydro- und Sedimentdynamik des Systems zu verstehen und zu kontrollieren. Bedingte Maßnahmen zur Flussregulierungen (z.B. Baggeraktivitäten) führen meist zu nachhaltigen Veränderungen der natürlichen Dynamik des Ästuars. Diese Arbeit untersucht die Dynamik von kohäsiven Schwebstoffen in der Wassersäule und im bodennahen Bereich, sowohl unter natürlichen Tidebedingungen als auch unter dem Einfluss von Wasserinjektions (WI)-Baggerung.

Die Korngrößenverteilung von in-situ Partikeln und Primärpartikeln im Weser und Elbe Ästuar zeigen, dass die organischen und anorganischen Schwebstoffe sich in einem aggregierten Zustand befinden und sogenannte Flocken bilden. Das Trägermaterial für organische Substanzen, die für das Zusammenhaften der einzelnen Partikel benötigt wird, wird von der Seeseite in die Ästuare transportiert. Im Winter, unter hohem Oberwasserabfluss und einer ausgedehnten Trübungszone, wurden unterschiedlich große Primärpartikel in der Trübungszone sowie im see- als auch im landwärtigen Bereich gemessen. Entsprechende Verteilungsmuster existieren im Sommer unter geringem Oberwasserabfluss und einer kurzen Trübungszone nicht. Die regionalen Unterschiede in der Primärpartikelgröße haben keine Auswirkungen auf das Größenspektrum der in-situ Partikel. Die in-situ Größe wird maßgeblich durch die Kollisionsrate der Partikel bestimmt die wiederum vom Tidestrom und der Schwebstoffkonzentration abhängig ist. Obwohl die in-situ Partikel im Laufe eines Tidenzykluses unter der Wirkung von Schubspannung zerfallen und sich unter ruhigeren Strömungsbedingungen wieder neu aufbauen, verändert sich deren Primärpartikel-Zusammensetzung nicht. Erkenntnisse über in-situ Partikelgrößen und Zusammensetzung sind wichtig um das Sinkverhalten von Schwebstoffen abzuschätzen zu können. Hohe Sinkgeschwindigkeiten können zu erhöhten Schwebstoffkonzentrationen in Bodennähe führen. Vertikal hoch auflösende Beprobungen der bodennahen Schwebstoffkonzentrationen und kohäsiven Ablagerungen zeigen, dass allgemeingültige 3-Schichten Modelle für vertikale Schwebstoffverteilungen unvollständig sind. Sedimentologische und rheologische Parameter beweisen, dass die

mittlere Schicht der Modelle – die Fluid Mud Lage – in eine gering-viskose Fluid Mud (I) Lage und in einen hoch-viskose Fluid Mud (II) Lage unterteilt werden muss. Anhand von einer Clusteranalyse konnten die Grenzen der Schwebstoffkonzentration beider Fluid Mud Typen genau bestimmt werden. Die obere Grenze der Fluid Mud (I) Lage ist geprägt durch einen abrupten Anstieg in der Schwebstoffkonzentration, die als akustischer Reflektor mit der niedrigen Frequenz eines parametrischen Sedimentecholots detektiert wurde. Gegenüber früheren Studien kann zum ersten Mal die Beziehung zwischen der Amplitude des akustischen Reflektors und dem Schwebstoffgradienten am Reflektor quantifiziert werden. Die Abnahme des Gradienten mit zunehmender Strömungsgeschwindigkeit belegt einen Schwebstoffaustausch an der Grenzschicht. In Bereichen der Weser wo die Morphologie sehr plan ist, findet der Austausch an der Grenzschicht allerdings frühestens eine Stunde nach Stauwasser statt. Kohäsive Sedimente, vorzugsweise des Typs Fluid Mud (II), die mit der Tideströmung nicht wieder in Schwebe gebracht werden, führen zu Ablagerungen, die regelmäßige Baggeraktivitäten erfordern. Um Untiefen in tidedominierten Fahrwasserrinnen und Häfen zu beseitigen, hat das hydraulische WI-Verfahren in den letzten Jahrzehnten an Bedeutung gewonnen. Umfassende hydroakustische und optische Messungen, gekoppelt mit Sediment- und Wasserprobenentnahmen fanden begleitend zu WI-Maßnahmen im Brack- und Frischwasserbereich der Weser statt. Die Daten zeigen, dass die Kuppen von sandigen Unterwasserdünen exakt auf die angeforderte Höhe abgetragen wurden. Hydroakustische Messungen zeigen, dass sich der Einfluss der Baggeraktivitäten lediglich auf die direkte Baggerumgebung beschränkt. Die internen Sedimentstrukturen werden nur in den obersten Dezimetern zerstört und die mobilisierten Sedimente akkumulieren auf den angrenzenden Dünenflanken oder im nächsten Dünental. Signifikante Änderungen im Schwebstoffgehalt und in der in-situ Partikelgröße in der Wassersäule wurden nicht beobachtet obwohl akustische Interferenzen, assoziiert mit Turbulenzen, über mehrere hundert Meter auf der strömungsabgewandten Seite des Baggers zu beobachten waren.

Chapter 1: General introduction

Tidal estuaries as a link between river and sea have emerged as an important focus in coastal research. To mankind, estuaries have always been important, both as a source of food and as a transport route to cities and harbours in the hinterland. Therefore, man is aspired to understand and control the hydro- and sediment-dynamics, which is very complex due to the interaction of sea and freshwater as well as the influence of wave and tides (Dalrymple et al. 2012). Only a few estuaries today still have their original shape because they are often deepened, broadened and regulated by man in order to be able to meet the demand of increasing ship size and passages. At the same time the rivers are separated from the hinterland by dykes so that it is protected against high water levels. Construction and maintenance work involve risks because the modification of the river geometry results in changes of hydro- and sediment-dynamics (Savenije 2005, Talke & de Swart 2006). Natural dynamics attempt to compensate the anthropogenic modifications which again results in shoals, comprising subaqueous bed forms or mud accumulations (de Jonge 1983, Talke & de Swart 2006). Regular dredging activities are necessary to guarantee safe ship access. Local and short-term effects on the natural suspended sediment concentrations (SSCs) have been observed in context with dredging activities whereas the strength of the effect depends on the dredged material (Meyer-Nehls 2000, Mikkelsen & Pejrup 2000). Generally it is known, that finer sediments are transported about a larger distance than coarser ones (Meyer-Nehls 2000) but detailed information about transport distances and routes as well as the impact on the suspended sediment dynamics is in literature very sparsely reported.

The natural SSCs are highest in the so called turbidity maximum zones (TMZ) where sea- and freshwater suspended sediment loads are mixed. The geographical location and expansion of the TMZ is controlled by the freshwater discharge and tidal current (e.g. Grabemann & Krause 2001, Spingat 1997). Estuaries with a low tidal range (< 2 m, e.g. Mediterranean Sea) have a highly stratified TMZ whereas high tidal ranges (> 2 m, e.g. North Sea) lead to a partially or well-mixed TMZ (Brown et al. 2006). In the course of a tidal cycle the suspended particulate matter (SPM) dynamics are characterized by resuspension, advection and sedimentation. With increasing current

velocities during the flood and ebb phase SPM is suspended through the entire water column. As long as current velocity is fast enough, an advective sediment transport takes place in the direction of current flow. As soon as the current velocity is too low to keep the SPM in suspension (around slack water), the SPM starts to settle down (e.g. Brown et al. 2006, Grabemann et al. 1997, Spingat & Oumeraci 2000). The SPM is quite often organized into so called 'flocs' or 'aggregates' (e.g. Eisma 1986, Fugate & Friedrichs 2003, Uncles et al. 2006a) and consists of inorganic ('primary') particles (mostly of quartz, feldspars and carbonates of silt to sand size) glued together by Particulate Organic Matter (POM) (McAnally et al. 2007). The flocculation is a dynamic process which reacts to changes in turbulent hydrodynamic conditions (Manning & Bass 2006). The suspended particles are preferentially brought together by Brownian motion (Eisma 1986), differential settling or turbulent flow (Eisma 1986, Whitehouse et al. 2000) and decrease in size with increasing shear stress (e.g. by increasing current velocity) because they are very fragile and break into smaller particles (Whitehouse et al. 2000). This makes particle-size and dynamic investigations without in-situ measurements very complicated.

Despite larger flocs being less dense than their constituents, they have higher settling rates and are much more rapidly deposited than smaller flocs (Manning & Bass 2006). The settling velocity is again slowed down with the onset of hindered settling at high SSCs which is associated with a lutocline and the development of a space-filling network (Winterwerp 2002). This state is often referred to as fluid mud which is a thixotropic behaving mixture of water, clay, silt and POM (McAnally et al. 2007). Most studies describe fluid mud only on the basis of SSC or density data whereas the limits vary strongly between the studies. For example, the upper limit has been reported by Faas (1984) at 10 g/l and by Kendrick & Derbyshire (1985) at 200 g/l. The lower fluid mud boundary is described at around some hundreds of gram per litre (Ross et al. 1987). Fluid mud accumulations have been found all over the world: e.g. Ems estuary (Wurpts & Torn 2005), the Weser estuary (Schrottke et al 2006), the James estuary (Nichols 1984), on the Amazon shelf (Kineke et al. 1996), the Eel river (Traykovski et al. 2000), Humber estuary (Uncles et al. 2006a) and the Tamar estuary (Uncles et al. 1985). In estuarine environments fluid mud can reach a thickness of a few metres depending on the SSC of the water column as well as on the settling time (Schrottke et al. 2006). Preferentially

fluid muds have been described during low current velocities (mainly around slack water). Initially, when the accumulations are only weakly consolidated, they are susceptible to resuspension with ongoing tidal current and the effect of shear stress (McAnally et al. 2007). In this state conventional echo sounders installed on commercial vessel have problems to detect such accumulations adequately (Schrottke et al. 2006). Thicker or consolidated layers can represent a critical management problem as is it buries benthic communities, impedes navigation and contributes to the eutrophication (McAnally et al. 2007). To optimize dredging strategies or to control the formation of permanent accumulations, high resolution detection techniques are necessary which can easily be used for spatial large scale measurements.

Chapter 2: Motivation

The previous chapter has shown that fine cohesive sediment dynamics in estuarine environments is a complex interaction of aggregation and disaggregation, resuspension and accumulation as well as advection which are highly variable on spatial and temporal scales. Understanding the single processes is absolutely necessary to evaluate the whole system for ecological and socio-economic aspects but this is only possible on the basis of consistent definitions as well as with high resolution and state of the art measuring techniques.

This thesis combines information on high resolution timescales about fine cohesive sediment processes in the water column and near bed of the Weser, Ems and Elbe estuaries. The changing properties and dynamics of the aggregated SPM, which can influence the settling velocity, are described in chapter 5. For this purpose the size distribution of undisturbed in-situ particles and their inorganic constituents were measured and compared on different temporal and spatial scales. The vertical characteristics of near bed fine cohesive sediment suspensions and accumulations including fluid mud are examined in chapter 6. Here, a statistical substantive definition on basis of several sedimentological and rheological parameters is developed (chapter 6) which is applied in chapter 7. Acoustical interfaces within the water column, representing the upper fluid mud layer, are used to describe the near bed cohesive sediment dynamics over a tidal cycle. In chapter 8 suspended sediment dynamics and sedimentological bed characteristics are considered under the influence of water injection dredging (WID).

Chapter 3: Geological settings

The Weser, Ems and Elbe estuaries (located along the German North Sea coast), are the seaward accesses to the most important German seaports located in the German hinterland (fig. 3.1). The three estuaries belong to the category of coastal plain or drowned river estuaries and were formed after the last glacial maximum at the end of the Middle Weichselian (ca. 15,000 yrs BP) (Streif 1990, 2004). At the beginning, when sea-level was 100 to 130 meters below present sea level, retreat of glaciers created initially shallow lagoons at the edge of the continental shelf (Streif 1990). With ongoing rise, sea level increased faster and flooded the fluvial valleys between 12,000 and 6,000 yrs BP (Kappenberg & Fanger 2007). The downstream freshwater sections of the rivers were shortened due to brackwater advancing. Maximum expansion of the estuaries was reached between 5,000 to 3,000 yrs BP, when sea level rise slowed down again (Kappenberg & Fanger 2007). The river mouth systems are to this day under steady influence of wave and tidal energy or storm surges. Especially in case of the Ems estuary, a series of storm surges flooded since the 14th century over the natural banks of the Ems. These events created in combination with polderization or diking of the foreland, the Dollard Basin (Streif 1990, Talke & de Swart 2006). Also within the estuaries, the impact of

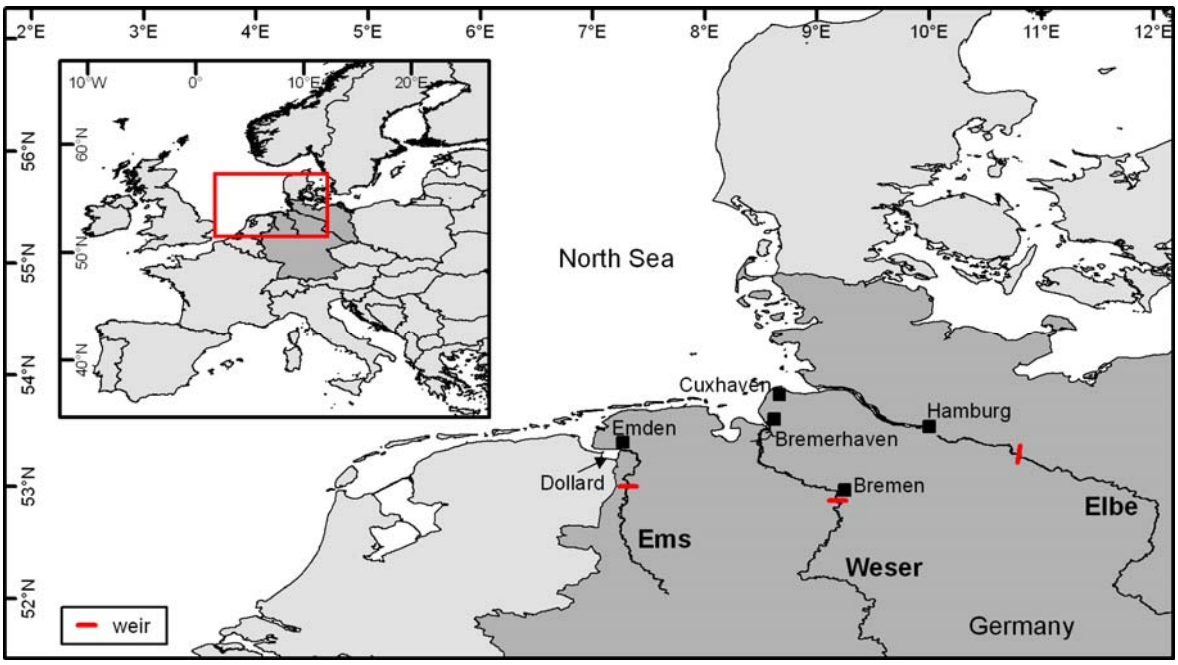

Figure 3.1: *Locations of the Ems, Weser and Elbe rivers along the German North Sea coast. The tidal influenced sections are restricted by weirs (red bars) 100 -160 km stream-up of the river mouths.*

human activities (e.g. diking, river regulation and deepening as well as river constructions) due to increasing ship size and access are influencing the river geometry and hydrodynamics (Kappenberg & Fanger 2007, Wienberg 2003). Regular dredging is necessary to guarantee save ship access. The tidal influenced reach is nowadays restricted in all three estuaries by a weir 100 – 160 km up-stream of the river mouth (details see chapter 6 & 7). Despite their geographic vicinity, differences in the size of their catchment areas or the amount of freshwater make physical and hydrodynamic characteristics of Weser, Ems and Elbe estuaries different (more details about tidal range, river-currents, suspended sediment concentration, etc., see chapter 6 & 7).

Chapter 4: Methodology

This work is based on a combination of a number of multi parameter probes, acoustical and optical methods as well as sedimentological and rheological investigations. Data collection and sampling took place from a research vessel. Geographical positions were received with a Digital Global Position System (DGPS). The fundamental principles of the field methods (section 4.1), the sampling devices (section 4.2) and the laboratory methods (section 4.3) are described in this chapter. Further description can be found in the chapter 5 to 8.

4.1: Field Methods

4.1.1: Laser in-situ scattering and transmissometry

Early in-situ particle size sampling methods such as pumping systems, settling tubes or hydrographic sampling bottles had the problem that the fragile aggregates were disrupted during sampling or analysis of underwater photography was very time consuming (Bale & Morris 2007). In this work a 'Laser In-Situ Scattering and Transmissometry' ('LISST-100X') instrument manufactured by Sequoia® Scientific Inc. (Bellevue, Washington) was used for quick and undisruptive information about the in-situ particle size distribution and volume concentration obtained by laser diffraction as well as beam transmission. The advantage of the laser diffraction is that the method is mostly independent of particle composition and does not require a particle refractive index which is in aquatic science poorly known (Agrawal & Pottsmith 2000). Figure 4.1 shows the schematic optical geometry of the device. With a 10 mW diode laser, a red 670 nm laser beam is produced and collimated by a coupled single-mode optical fibre in the endcap of the device. Before the laser leaves the pressure housing through a window, a portion of the beam is splitted and directed to a reference beam detector. The reference is used to normalize out effects of laser power drifts by e.g. long-term variations of laser characteristics or temperature (Agrawal & Pottsmith 2000). The beam diameter in the water is 6 mm and is scattered by suspended particles. In case of high SSCs, path reduction modules can be installed to reduce the 5 cm long optical path and hence the

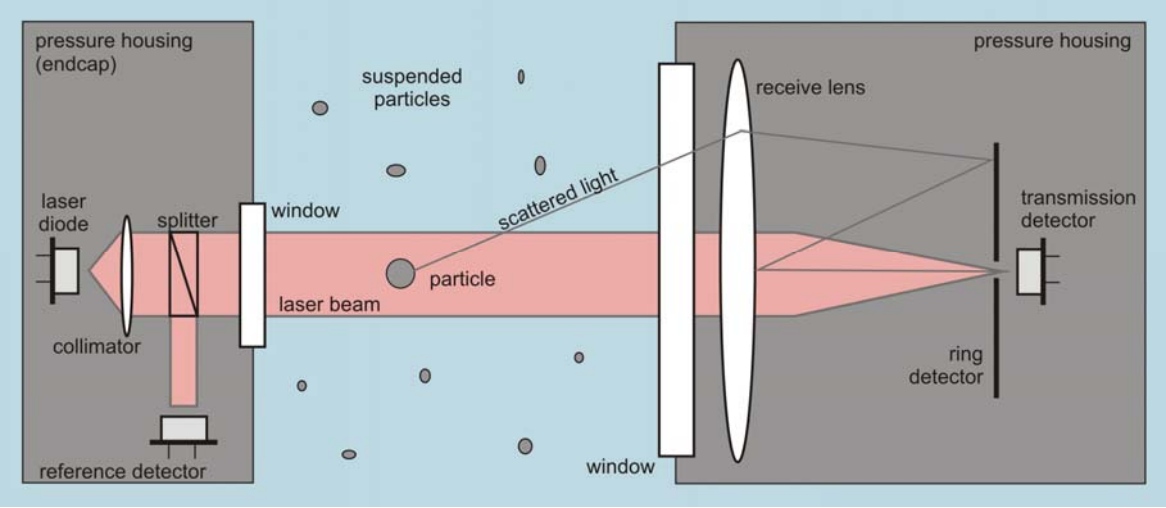

Figure 4.1: *Scheme of the optical geometry of the 'Laser In-Situ Scattering and Transmissometry' sensor ('LISST-100X') (modified after Agrawal & Pottsmith 2000).*

sampling volume. The scattered light enters the pressure housing through a window on the other side of the measuring chamber. Both windows within the optical train are polished to a very high degree and the air sides are anti-reflection coated (Agrawal & Pottsmith 2000). A spherical constructed multi-ring detector placed at the focal plane of the receiving lens senses the intensity of the scattered light. The radii of the 32 rings increase logarithmically. In case of the instrument used in this study (type C), an angular range of 0.00085 – 0.17 radians corresponding to a size range of 2.5 – 500 µm is covered by the rings. The scattered ring-signature is a weighted sum of size distribution and the corresponding scattering for each size which can be converted to particle size distribution (PSD) by a mathematical inversion. Particles beyond the measuring range are assigned either to the finest or largest size class, respectively (Agrawal & Pottsmith 2000). Direct beams which are not scattered or absorbed are passed through a 75 µm large hole in the centre of the ring-detector. Behind the array the transmitted beam power is detected with a silicon photo-diode which provides the optical transmissometer function. A full mathematical and technical description is given by Agrawal and Pottsmith (2000) and Agrawal et al. (2007, 2008). To avoid artificial scattering by micro-roughness on the optics, background scattering distributions with distilled water have to be measured and stored. The particle size distribution is presented in the data output as volume concentration (VC) of each size class which can be summed-up to a total volume concentration (TVC).

In this work (chapter 5 & 8) the device was applied from the drifting vessel in a profiling mode. Data was collected in real-time with a sampling rate of 1 Hz. At the beginning of each measuring day a background scatter was acquired to check the overall instrument health. A path reduction module (50 and 90%) was installed when SSCs were high. For deployment details see section 5.3 and 8.4. During data processing values with transmissions smaller than 30% were interpreted with caution due to multiple scattering which can lead to an overestimation of small particles (Agrawal & Pottsmith 2000). TVCs were calibrated with the SSC, calculated by dry mass per unit volume of vacuum-filtered water samples (see section 4.3.1).

4.1.2: Acoustic Doppler current profiler

For flow measurements in oceanography, estuarine, river and stream sciences, acoustic methods using the Doppler principle have been established. The principle refers to a frequency shift (compression or expansion) of the transmitted sonar signal caused by the relative motion between the transmitter and the scattering material (e.g. SPM or air bubbles) floating with the water currents. The difference in frequency between the transmitted and reflected sound wave is directly proportional to the current velocity (Gordon 1996). Since a single acoustic beam can only measure the velocity component parallel to the beam, the so called ADCPs (Acoustic Doppler Current Profiler) are using a ring of four transducers facing angled to the horizontal and angled at right angles to each other (Janus configuration). They transmit a burst of fixed frequency sound along a narrow acoustic beam. 'One facing beam pair records one horizontal component and the vertical velocity component. The second pair measures a second, perpendicular horizontal component as well as a second vertical velocity component' (Gordon 1996). By trigonometric relations (assuming horizontally homogenous currents) current speed can be converted into direction components. At least three beams are required to determine the three current components (e.g. east, north and down) but the fourth beam can be used to check data quality. The error velocity, the difference between the two vertical velocities, allows estimation whether the assumption of horizontal homogeneity is reasonable.

The echo intensity of the backscattered signal can be used as a measure for the amount of scatterers in the water column. The echo intensity depends on the transmitted power, the acoustic characteristics of the transducer and the resulting acoustic beam, sound absorption (by water and SPM) and the backscatter coefficient (Gordon 1996, Guerrero et al. 2011). It has to be kept in mind that the relationship of echo intensity to the SSC strongly depends on the particle size. To get absolute SSC values, data has to be calibrated with in-situ measurements (e.g. SSC data by water sample filtration, see section 4.3.1).

In contrast to conventional mechanic methods (e.g. hydrometric vanes) an ADCP has the ability to measure a 'profile' of the water currents throughout the water column. Profiles are produced by range-gating the echo signal (Gordon 1996). By turning the receivers on and off at regular intervals, the received signals are broken in successive depth cells. Depending on the travel time between transmitting and receiving of the signal, one gets information about the current at various depth cells of the water column. Within each depth cell velocities are averaged by a weight function (Gordon 1996). Data from distances too close to the surface (when looking up) or the bottom (when looking down) should normally be rejected. Echoes from sea surface or seafloor are so much stronger than the echo from scatterers in the water that it can overwhelm the backscatter signal. The larger the beam angel, the thicker the contaminated layer is. For example: a 20° transducer has a contaminated range of the last 6% of the water column and a 30° transducer a range of 15% (Gordon 1996). To approach comparable profiles with conventional mechanic methods, a bunch of hydrometric vanes on a moored line were necessary. With an ADCP mounted on a moving ship, transects of vertical current velocity can be achieved relatively quick.

During this work (chapter 5, 7 & 8) a 1,200 kHz 'Workhorse-ADCP' (RDI-Teledyne™, Poway, California) was mounted downward-looking on the starboard side of the '*RV Littorina*' at a depth of 2.7 m and in the moon pool of the working vessel '*Scanner*' at a depth of approximately 0.2 m, respectively. The beam angel was 20° and a cell size of 25 cm and 50 was chosen, respectively. The standard deviation for the current flow velocity amounts to 0.129 cm/s (Gordon 1996). Data was recorded with the software WinRiver® (RDI-Teledyne™, Poway, California).

4.1.3: Sediment echo sounder

For high resolution sub-bottom profiling in shallow water environments, it is recommended to use a parametric (nonlinear) sub-bottom profiler (Wunderlich et al. 2005). Two slightly different high frequencies are transmitted simultaneously at a very high sound pressure. During nonlinear sound propagation these two primary frequencies interact and generate a lower, second frequency which corresponds to the differences of the transmitted primary frequencies. The secondary frequency has the same narrow beam like the primary frequencies (resulting in a small footprint), short pulses and has no significant side lobes (Wunderlich et al. 2005). This improves the signal to noise ratio and results in a high vertical and lateral resolution which is in shallow waters not possible with common linear sub-bottom profilers because the data quality is limited by reverberation effects.

The operation of two frequencies enables the precise detection of the sediment surface (primary frequency) and internal sedimentary structures (secondary frequency) simultaneously. Additionally, Schrottke et al. (2006) have proved the detection of acoustical interfaces within the water column by means of the low secondary frequency.

For this work (chapter 7 & 8) a 'SES-2000® standard' of Innomar Technology GmbH (Warnemünde, Germany) was used. The primary frequency is of about 100 kHz and the secondary frequency was set on 12 kHz with a ping rate of approximately 63 pps, depending on the ship speed. The sound velocity was set on 1,500 m/s. Heave, roll and pitch movements were corrected with data provided by a motion sensor (Seatex MRU-6). Sediment structures up to 5 m depth were detected with a resolution of approximately 6 cm (Schrottke & Bartholomä 2008). The device was firmly mounted midships on the star board side of the '*RV Littorina*' in 3.03 m water depth and at the bow of the working vessel '*Scanner*' in approximately 0.5 m water depth, respectively.

To indicate the properties of the acoustical interfaces within the water column, the amplitude (A) of the received echo signal is used. To take different gain settings as well as geometrical and physical attenuation into account, the amplitude is normalized (A_N) on these factors:

$$A_N = A_2 * A + 2\,TL + WA \quad (1)$$

where A_2 is the amplification factor (2), *TL* the geometric attenuation or transmission loss (3) and *WA* physical attenuation or the acoustic sound absorption in the water (4). The amplification factor A_2 is calculated by:

$$A_2 = A_1\left(10^{\left(\frac{G_{dB}}{20}\right)}\right) \quad (2)$$

where A_1 is the reference amplitude level (ingoing amplitude) and G_{dB} the gain in dB (Lurton 2002). The transmission loss (*TL*) induced by geometrical spreading during sound propagation increases with increasing distance (*d*) to the signal source and can be calculated by:

$$TL = 20\,log\,(d) \quad (3)$$

The acoustic sound absorption in water (*WA*) is calculated on the basis of the propagation distance to signal source and the attenuation coefficient α (dB/km) of water (5):

$$WA = 2 * d * \frac{\alpha}{1000} \quad (4)$$

α (dB/km) is depending on the seawater properties such as temperature, salinity as well as the frequency of the sound which is calculated with the empirical formula for sea water at frequencies between 3 kHz and 0.5 MHz after *Marsch* and *Schulkin* (Brekhovskikh & Lysanov 2003):

$$\alpha = 8.68 * 10^3\left(\frac{SAf_T f^2}{f_T^2 + f^2} + \frac{Bf^2}{f_T}\right)(1 - 6.54 * 10^{-4}P) \quad (5)$$

where A = 2.34*10^{-6}, B = 3.38*10^{-6}, S is salinity, P is hydrostatic pressure (kg/cm²), f is frequency (kHz) and f_T is the relaxation frequency (kHz) which is depending on the temperature T (°C):

$$f_T = 21.9 * 10^{6-1520/(T+273)} \quad (6)$$

4.1.4: Side scan sonar

Side Scan Sonar (SSS) mapping is the most commonly used technique to image large areas of the seafloor. A few metres up to some tenth of kilometres can be ensonified

perpendicular to the tow direction (Blondel 2009). A transducer / receiver unit transmits on each side of the tow fish beams in a wide angle (to cover as much range as possible) and narrow horizontal directivity (to get high resolution) (Blondel 2009). The portion scattered back towards the sonar is small due to most of the energy being reflected specularly as well as a small portion being lost in the ground. The intensity of the backscattered signal from the seafloor is dependent basically on three factors: 1) The geometry of the sensor and ensonificated target. Surfaces inclined and declined towards the SSS increase and decrease the strength of the sonar signal, respectively. In this manner, bed forms like subaqueous dunes can be imaged and objects like boulders or artificial objects can be identified by means of their acoustical shadow. 2) The physical characteristics of the surface (e.g. roughness). Coarser sediments generally produce higher backscatter than finer sediments. 3) The intrinsic nature of the surface (e.g. composition or density). The acoustic penetration and thus the acoustic attenuation are higher in soft sediments (e.g. unconsolidated mud) than in compacted, dense sediments or even rocks.

For sedimentological interpretation of the backscattered sonar signal, ground-truthing via sediment sampling or under water visualization is necessary. Apart from seafloor mapping, objects within the water column can be detected and visualized on the side scan sonar image. Objects like fish swarms or just turbulences in the water column emit the acoustic signal.

In this study (chapter 8) a digital dual-frequency SSS system of type 'Sportscan® 881' (Imagenex, Port Coquitlam, Canada) was used with a frequency of 330 kHz. The range was set on 60 m and the gain on 8 dB. The sonar was deployed firmly over the starboard site of the working vessel '*Scanner*' at a depth of approximately 0.5 m. Ground-truthing was done with a Van-Veen-grab sampler and grain size analysis were performed with a settling tube (see section 4.3.2.1) and a SediGraph (see section 4.3.2.2).

4.1.5: Optical back scatter sensor

For vertical SSC profiling in aquatic environments turbidity or transmission sensors are often used. Most of the devices are based on the principle of transmission loss over a defined measuring distance. The disadvantage of this technique is that at higher SSCs the emitted optical signal is completely absorbed. Today, Optical Back Scatter sensors (OBS) are used increasingly in natural environments for example in the TMZs of estuaries where SSCs can exceed several grams per litre. The sensors transmit an optical signal which is scattered and reflected by the total suspended particulate matter and detected by a lens which is orientated in a distinct angle to the sensor axis.

In this study (chapter 8) an OBS sensor of type 'ViSolid® 700 IQ' (WTW, Weilheim, Germany) was used. This sensor was originally designed for use in wastewaters. Depending on the backscatter intensity the transmitting angle of the infrared light (860 nm) is adapted automatically between 15 and 90° towards the sensor axis. The backscatter intensity corresponds to an equivalent SiO_2 concentration. To get absolute concentration values, the data has to be calibrated with SSCs derived from filtered and weighted suspended sediment samples (see section 4.3.1). The data is measured in a profiling mode and recorded online every second from the working vessel '*Rüstersiel*' and '*Scanner*', respectively.

4.2: Suspended and solid sediment sampling

4.2.1: Rumohr-type gravity corer

Suitable for vertical water-solid bed interface sampling is a light-weight, high-momentum gravity corer according to Meischner & Rumohr (1974) (in the following called Rumohr-type gravity corer). This construction is comprised by a transparent Perspex core barrel, several weights and a flap valve system at the top of the corer. The flap valve is closed by a lever mechanism when the core is pulled out of the sediment. The resulting vacuum prevents the core slipping out of the barrel without using a core catcher. The latter has the disadvantage that the sample material is disturbed. The transparent barrel enables a visual inspection immediately after core recovery and makes the construction very light.

On the one hand the system is through the light weight very easy to handle, even from small boats or by man power, but on the other hand the instrument is very susceptible to drifting due to water currents. In tidal environments application is only practicable around slack water. To sample the water-solid bed interface during low or moderate current velocities (up to 1.5 m/s near surface and 0.9 m/s near bed) a special, weighted steel frame was constructed for this work (fig. 4.2). The corer hangs in the middle of an approximate 3 x 3 x 3 metre frame while each of the edges is weighted with concrete blocks of approximately 36 kg. Below the corer a table with a closure mechanism is installed. When pulling the core out of the sediment, a slide is pushed below the core, sealing it against possible leakage.

Figure 4.2: *Rumohr-type gravity corer (2 m length) with a special constructed weighted steel frame (~3 x 3 x 3 m) and a closure system for sampling at current velocities up to 1.5 m/s.*

To record the core penetration depth, a pressure sensor 'P-LOG520-PA-INT' manufactured by Driesen and Kern (Bad Bramstedt, Germany) is installed at the top of the corer. The absolute pressure (sum of water and atmospheric pressure) can be

recorded in a range of 0 to 10 bar and the temperature in a range of -10 to 80°C. The resolution is 0.1 mbar and up to 0.001°C, respectively. The accuracy is ± 0.1% of the pressure range and ± 0.2°C for the temperature. The data is recorded with a frequency of two seconds.

For high vertical sampling resolution, core barrels of this study (chapter 6 & 7) are prepared with holes spaced in ten centimetres intervals and closed with water-resistant tape (see also section 6.3 and Schrottke et al. 2006). Sampling is done through the holes immediately after recovery. For samples with SSC approximately < 500 g/l temperature and salinity is measured using a multimeter of the type 'Cond 340i' by WTW (Weilheim, Germany). The salinity is given as Practical Salinity Unit (PSU, unitless). The accuracy is for salinities is ± 0.1 and for temperature ± 0.1°C. The samples are analysed on SSC (section 4.3.1), POM (section 4.3.1) and grain size (section 4.3.2) in the laboratory after the survey.

4.2.2: Horizontal water sampler

As previously described, acoustical and optical devices used for the SSC measurements often present only a measure of concentration but not absolute concentration values. A common practice for calibration is the use of water samples. Diverse water sampling techniques have been established on the market; e.g. pumping systems, bottles or tubes aligned vertically or horizontally and applied either separately or as groups in a rosette.

During this study a horizontal water sampler manufactured by Hydro-Bios GmbH (Kiel, Germany) with and approximate volume of 2 litres was used. The sampler can be lowered to each depth; even near bed sampling is possible. The advantage of the horizontal technique is that the device is orientated in the current flow direction and thus enables an undisturbed flow of the water with its suspended sediment load through the sampler. The samples are analysed on SSC (section 4.3.1), POM (section 4.3.1) and grain size (section 4.3.2) in the laboratory after the survey.

4.3: Laboratory methods

4.3.1: SSC and POM determination

The SSC of water samples or Rumohr-type gravity cores were recorded as dry weight per unit sample volume. Depending on the sample consistency, an aliquot was prepared for vacuum filtration using a glass fibre filter (pore diameter 1.2 µm) or by taking 2 ml of consolidated sediment. In a next step, the aliquot was dried for about 12 hours at 60 °C. After weighing, the dried samples were analysed for POM content by weight-loss on ignition, only leaving the clastic mineral components (Dean 1974). This was done by combustion in a muffle furnace at 550°C for 2 h (filter samples) and 6 h (solid samples), respectively.

4.3.2: Grain size analysis

Due to logistical reasons, samples obtained with the Rumohr-type gravity corer on surveys between the year 2005 and 2007 were measured depending on the grain size with different hydraulic methods (settling tube: section 4.3.2.1 or SediGraph: section 4.3.2.2) at the Senckenberg Institute (Wilhelmshaven, Germany). Rumohr-type gravity cores and water samples obtained after 2007 were measured with an optical method (4.3.2.3 Beckman Coulter particle sizer) at the University of Kiel (Germany). The influence of particulate organic carbon and carbonate can cause aggregation of particles, resulting in greater falling rates than single particles (Coakley & Syvitski 1991). Thus these components were removed before analysis by hydrochloric acid and hydrogen peroxide, respectively. For a detailed description of sample preparation see section 5.3 and 6.3. Hydraulic measured samples were additionally desalinated. The grain size classification is attached to the scale of Friedman & Sanders (1978) and statistical grain size data is based on Folk & Ward (1957).

4.3.2.1: Settling tube

Conventional mechanical particle size analysis (e.g. sieving) often do not represent the grain size of aquatic environments accurately due to geometrical effects. In the hydrodynamic environments is the mobility of particles depending on the ratio between shear velocity and settling velocity (Syvitski et al. 2007). With so called settling tubes, settling velocity and grain size of sands can be measured on a hydraulic way, considering particle characteristics (size, density and shape) as well as characteristics of fluid (density and viscosity) which are not considered during sieving (Syvitski et al. 2007). Basically the method bases on the Stokes' law where the settling of a spherical particle is calculated in relation to the frictional resistance of a turbulent-free liquid:

$$w = \left[\frac{(\rho_f - \rho_p)g}{18\eta}\right] d^2 \qquad (7)$$

where *w* is the settling velocity (m/s), ρ_f is the fluid density (kg/m), ρ_p is the particle density (kg/m), *g* is the gravitational force (m/s), η is the viscosity of the liquid (Pa·s) and *d* is the diameter of the spherical particle (m).

Settling tubes mainly consist of a vertical, liquid filled cylinder and a measuring system at the bottom. Important is that the liquid, preferentially purified water, is free of air bubbles and turbulence as well as the temperature and salinity being defined. Accurate results are achieved with tubes with minimum dimensions of 140 cm in length and 12 cm as an internal diameter (Gibbs 1974). Only by maintaining these minimum dimensions can a complete separation of the size components into their hydraulic components be guaranteed and wall affects can be avoided. A small portion of lab processed sediment sample is introduced at the same time in the upper end of a vertical water column with a defined length. Particles are settling assumedly individually through the water (Syvitski et al. 2007), neither hindered by other settling particles, nor involved in convective plumes of high concentration, nor retarded by up flow of displaced fluid. This is only valid for low concentrations (< 1 g) and sand sized sediments (Syvitski et al. 2007). Within the settling tube particles are stratified according to their respective settling velocities. The most precise data is achieved by an electrical underwater balance

recording the voltage increase over the time induced by the load of the settled sediment. From the measured time-coupled voltage increase, the settling velocity can be calculated.

In this study (chapter 6 & 8) an autonomous settling tube of the type 'MacroGranometer^{TM}' (Neckargemuend, Germany) (h = 1.8 m; d = 0.2 m) was used to analyse grain-sizes in a range between 5 and -2 Phi [φ] with a resolution of 0.1 φ (Brezina 1979). With the program 'SedVar 6.2^{TM}' the increase of voltage, recorded by an electrical underwater balance, was converted after Brezina (1979) into the binary logarithm of particle size *Phi* [φ] (8) and the binary logarithmical settling rate *Psi* [cm/s] (9).

$$Phi = -log_2 d \tag{8}$$

where d (mm) represents the grain diameter.

$$Psi = -log_2 v_p \tag{9}$$

where v_p (cm s^{-1}) is the settling velocity of the particles.

The data are normalized on the international used standard values: 24°C water temperature, salinity = 30, quartz density = 2.65 g/cm³, hydraulic particle shape factor = 1.18 and local gravitational acceleration = 981.37 cm/s².

4.3.2.2: SediGraph

The principle of particle settling is also a widely used method for particles < 63 µm. In the 1970s a system, the so called 'SediGraph' manufactured by Micromeritics Instruments (Norcross, Georgia), was introduced. The SediGraph determines the relative concentration change of suspended particles at a selected vertical distance in a selected time, and thus the size distribution of the settling particles (Coakley & Syvitski 2007, McCave & Syvitski 2007). Similar to the settling tube method (section 4.3.2.1), the SediGraph assumes that particles settle in accordance with Stokes' law (7). The relative concentration change is measured with a collimated X-ray beam (14 W) of 0.0051 cm height and 0.9525 cm width (Coakley & Syvitski 2007) placed in front of an analytical cell. The amount of absorption by particles located in the beam bath is detected by a scintillation counter behind the cell and converted into particle concentration. At the

beginning of an analysis cycle an X-ray reference beam is projected through a clear liquid medium. The so called baseline represents 0% concentration. Afterwards suspended sediment, heated to 30°C, is pumped through the analysis cell. Under flowing condition a full-scale X-ray absorption value (or maximum absorption) is detected for each point along the cell. This value is set to 100% concentration. Measurement of particle falling rates and the amount of X-ray absorption is started when fluid circulation is stopped, and the suspended particles start to settle under the influence of gravity. The measured concentration is the concentration of particles smaller than or equal to that size associated for that height and elapsed time. Larger particles, with higher falling rates, have fallen to a lower point in the cell. To minimize analytical time, the analysis cell is moved downward with the time thus small particles do not have to settle over the whole height of the cell. The advantage over conventional techniques, such as pipette and hydrometer, is that this method is less time consuming, needs less sample material and is reversible.

In the beginning of this study a Micromeritics Instrument (Norcross, Georgia) SediGraph of the type '5100™' was used. Later on the newer model '5120^{TM}' was available. Both devices have a particle size range of 10.75 to 4 φ with a resolution of 0.25 φ.

4.3.2.3: Laser diffraction particle sizer

Today, laser diffraction is a standard method for measuring particle size. This technique is based on the principle that particles scatter light forwards at a specific angle depending on their size (Agrawal et al. 2007, McCave & Syvitski 2007). The angle increases with decreasing particle size. However, this technique is inapplicable for particles in the submicron range. The ratio of particle dimension to light wavelength is reduced and thus the scattering pattern becomes less angular dependent. Very similar scattering patterns make it difficult to obtain correct size values with an appropriate resolution.

The laser diffraction particle sizer ('LS 13 320') manufactured by Beckman Coulter (Krefeld, Germany) enables size measurements of particles in the submicron range by applying additionally the patented 'Polarized Intensity Differential Scattering' (PIDS)

technology (Pye & Blott 2004). PIDS uses single frequency polarized light of three different wavelengths. The difference of the scattering intensity between the vertically and horizontally polarized light directly correlates with the particle size.

For the laser diffraction method a laser beam with a wavelength of 750 nm, produced by a 5 mW monochromatic laser diode, is passed through a spatial filter and projection lens to get constant beam intensity. The beam is scattered by suspended particles in characteristic patterns according to their size. A Fourier lens behind the analysis cell is used to focus the scattered signal. The scattering pattern is measured by 126 silicon photo-detectors placed on three arrays, which are arranged up to ~35° from the optical axis. The PIDS technology uses an incandescent tungsten-halogen source. The light is transmitted alternating through three sets of band-pass filters (450 nm = blue, 600 nm = orange and 900 nm = near-infrared), each horizontally as well as vertically polarized. Before projecting the monochromatic light through the PIDS sample cell, it is formed into a narrow, slightly diverging beam by sending it through a slit. The scattered light is sensed by six photodiode detectors arranged between 0 through 146°. The amount of absorption is measured by a seventh detector.

The laser diffraction unit as well as the PIDS unit are running simultaneously and are put in one matrix to give a continuous size distribution between 0.04 through 2000 µm. Different optical models can be chosen to convert the scattering pattern into particle size distributions. For sand sized particles the Fraunhofer diffraction theory is most frequently used. Mie Theory becomes important for samples containing significant amount of material finer than ~10 µm (Blot & Pye 2006).

In this study (chapter 5 & 7), sampling modules, comprising the sample cell and the circulation system, were exchanged depending on the sample amount. For samples with a SSC of < 1 mg a ‘Universal Liquid Module’ (120 ml) was used and for samples with SSC > 1 mg an ‘Aqueous Liquid Module’ (800 ml) was used. The sample was circulated through the system at a pump speed of 60 through to 70%.

4.3.3: Rheological investigations

Although, the term 'rheology' – the science of deformation and flow of matter - was invented for the first time at the beginning of the 20th Century by Eugen Bingham (Mezger 2011), the historical development of rheological studies goes back at least some hundreds years before Christ, when the mathematician Archimedes investigated hydrostatistics (buoyancy) and described the 'Archimedean Principle'. The basic law of solid-state physics was described by Robert Hooke in 1676 and shortly thereafter Isaac Newton introduced the basic law of fluid mechanics in 1687 (Barnes et al. 1989, Mezger 2011). According to the law of fluid mechanics, liquids are differentiated between Newtonian and the more complex non-Newtonian liquids to which cohesive sediment suspensions belong. In contrast to Newtonian fluids are the non-Newtonian fluids a function of shear stress or shear rate and of time (Mezger 2000, 2011). Rotational instruments are widely used in industry and science (Barnes et al. 1989, Barnes & Nguyen 2001, Mezger 2011) to measure flow behaviour of non-Newtonian fluids (Barnes et al. 1989). The measuring systems consist of a bob and cup showing the same symmetry or rotation axis (Mezger 2011). The arrangement can be operated in two modes: 1) the 'Searle' mode where the bob is set in motion and the cup is stationary; 2) the 'Couette' mode where the bob is fixed and the cup is rotating (Mezger 2011). Almost all rotational measuring systems in industrial and scientific laboratories work under the 'Searle' mode (Mezger 2011, Tabilo-Munizaga & Barbosa-Cánovas 2005) because its configuration and handling is much easier than the 'Couette' systems. The disadvantage of the 'Searle' method is that in low-viscous liquids, when rotational speeds are high, turbulent flow conditions ('Taylor vortices') may occur (Mezger 2011). A vane rotor as a measuring tool in non-Newtonian fluids has achieved great popularity (Barnes & Nguyen 2001). Especially applicable are vane tools for gel-like samples or materials of high solid content like muds and clay suspensions. The arrangement of several rectangular thin blades fixed around a shaft, allows the insertion of the device into the sample without significant structural disturbance before measurement (Krulis & Rohm 2004, Barnes & Nguyen 2001, James et al. 1987, Mezger 2011). A further advantage of this geometry is that slip effects at smooth walls do not occur as often observed with rotating cylinders (James et al 1987). However, yield stress can be simply calculated on

the basis of an equivalent solid cylinder (Barnes & Nguyen 2001), circumscribed by the tips of the blades, with a surface area *A* (m²) of:

$$A = 2\pi r(r + h) \tag{10}$$

where *r* (m) is the radius and *h* (m) the height of the vane tool.

The total torque M_t (N·m) which is needed to overcome the yield stress τ_y (Pa), is proportional to the shear stress τ (Pa). The torque M_c acting on the cylindrical vane surface can be expressed by:

$$M_c = 2\pi r^2 h\tau \tag{11}$$

and the torque M_e acting on both end faces (top and bottom) of the vane can be described by:

$$M_e = 2\left[2\pi \int_0^r r^2 \tau dr\right] = \frac{4}{3} r^2 \pi\tau \tag{12}$$

The total torque M_t acting on a vane tool is achieved by combining Eq. (11) and (12):

$$M_t = 2\pi r^2 h\tau + \frac{4}{3} r^2 \pi\tau \tag{13}$$

The total shear stress τ_t (Pa) would then be given by:

$$\tau_t = M_t \frac{1}{2\pi r^2}\left(\frac{h}{r} + \frac{2}{3}\right)^{-1} \tag{14}$$

The viscosity η (Pas) cannot be directly measured. It has to be calculated from the relationship between shear stress τ (Pa) and shear rate $\dot{\gamma}$ (s^{-1}):

$$\eta = \frac{\tau}{\dot{\gamma}} \tag{15}$$

The shear rate at the inner cylinder is proportional to the angular velocity ω (s^{-1}):

$$\dot{\gamma} = \omega \frac{2R^2}{R^2 - r^2} \tag{16}$$

where *R* (m) is the radius of the cup. The angular velocity is calculated by the rotational speed *n* (min^{-1}):

$$\omega = \frac{2\pi n}{60} \tag{17}$$

To assume for non-Newtonian fluids a linear shear rate in the gap between the inner cylinder (circumscribed by the tips of the blades) and the outer cylinder (cup), an infinitely small ration of the radii δ is necessary:

$$\delta = \frac{R_a}{R_i} \tag{18}$$

where R_a is the radius of the outer cylinder and R_i the radius of the inner cylinder. The German DIN and international standards recommend a ratio δ between 1.00 and 1.10. The closer the ratio comes to 1.00 the better the rheological quality. Greater ratios lead to higher viscosities (Schramm 2000).

Rheological data presented in this work (chapter 6) were measured with a rotational rheometer (Haake 'Rotovisco®RV20', Berlin, Germany) equipped with a four bladed vane tool, operating under the 'Searle' mode. The torque produced by the vane tool is detected by a spring which is placed between the drive motor and the shaft of the vane tool. Its twist angle is a direct measure of the viscosity of the sample (Schramm 2000) and is displayed as percentage torque *M%* (%) of the maximum torque M_d (0.049 N m). The accuracy of the measured torque is mainly dependent on the linearity of the spring-coefficient which is rated as 0.5% of the maximum torque (Schramm 2000). To assume a linear shear rate between the inner cylinder circumscribed by the vane tool and the outer cylinder (cup), an arrangement with a radii ratio of δ = 1.08 was chosen. The detailed dimensions and arrangement can be gathered from section 6.3 and figure 4.3.

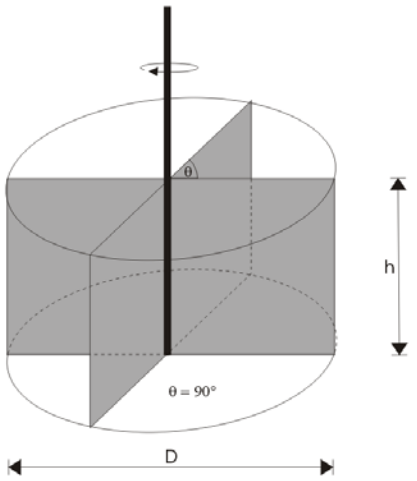

Figure 4.3: *Scheme of four bladed vane tool (d=36 mm; h=20 mm).*

Rheological measurements are dependent on the shear rate, thus to get comparable data, the vane was rotated by an electric motor with a constant rotational speed of 0.0065 s^{-1} corresponding to a shear rate $\dot{\gamma}$ of 0.548 s^{-1}. The flow behaviour of chosen samples was tested with controlled shear rates between 0.07 and 30 s^{-1}. When measuring with shear rates $\dot{\gamma}$ < 1 s^{-1} it must be guaranteed that the measurement duration is long enough, otherwise start-up effects or time-dependent transition effects e.g. transient viscosity are recorded instead of steady state conditions (Mezger 2011). Repeated measurements have shown a standard deviation of 0.25 Pas.

Chapter 5: Changing characteristics of estuarine suspended particles in the German Weser and Elbe estuaries

Svenja Papenmeier[1], Kerstin Schrottke[2], Alexander Bartholomä[3]

[1] Corresponding author: Institute of Geosciences & Cluster of Excellence „The Future Ocean“, at Kiel University, Otto-Hahn Platz 1, 24118 Kiel, Germany, sp@gpi.uni-kiel.de

[2] Institute of Geosciences & Cluster of Excellence „The Future Ocean“, at Kiel University, Otto-Hahn Platz 1, 24118 Kiel, Germany, ks@gpi.uni-kiel.de

[3] Senckenberg Institute, Dept. of Marine Research, Suedstrand 40, 26382 Wilhelmshaven, Germany, abartholomae@senckenberg.de

Submitted in May 2012 to the Journal of Sea Research.

Abstract

Fine cohesive, suspended sediments appear in all estuarine environments in a predominately flocculated state. The transport and deposition of these flocs is influenced by their in-situ and primary particle size distribution. Especially the size of the inorganic particles influences the density and hence the settling velocity of the flocculated material. To describe both the changes in primary particle size of suspended particulate matter as well as the variability of floc sizes over time and space, the data of In-Situ Particle-Size Distributions (ISPSDs), Primary Particle Size Distributions (PPSDs) and Suspended Sediment Concentrations (SSCs) were collected. For this, Laser In-Situ Scattering and Transmissometry (LISST) measurements as well as the water samples were collected in the German Elbe and Weser estuaries, covering seasonal variability of the SSC.

The data of the ISPSDs show that the inorganic and organic Suspended Particulate Matter (SPM), as found in the Elbe and Weser estuaries, mostly appears in a flocculated state. The substrate (inorganic particles < 8 µm) for organic matter (gluing inorganic particles

together) is mainly imported from the seaside and transported into the estuaries as indicated by an upstream decrease of the amount of fine particles. In winter, when the freshwater discharge is high, different PPSDs are found in case of the Elbe estuary in the Turbidity Maximum Zone (TMZ) as well as in the landward and in the seaward sections close to the TMZ. In summer, the distance between the seaward and the landward section is too low to obtain an individual PPSD within the Elbe TMZ.

A missing correlation between the PPSD and ISPD shows that the inorganic constituents do not have an influence on the in-situ floc size. Although flocs aggregate and disaggregate over a tidal cycle and with changing SSC, they do not change their PPSD. The microflocs are therefore strong enough to withstand further breakage into their inorganic constituents.

Keywords: *in-situ particle size, primary particles size, flocculation, LISST, Weser Estuary, Elbe Estuary*

5.1: Introduction

In tidal estuarine environments fine cohesive sediments, supplied from rivers and the sea, are mainly transported in suspension. They are quite often organized in so called ‘flocs’ or ‘aggregates’ (e.g. Eisma 1986, Fugate & Friedrichs 2003, Uncles et al. 2006). Flocculation is a consequence of particles sticking together as they are brought into contact with each other (Whitehouse et al. 2000). Processes whereby particles are brought together are multifarious. The most relevant ones are Brownian motion (Eisma 1986), differential settling and turbulent shear (Eisma 1986, Whitehouse et al. 2000). The probability of collision is increased under conditions of turbulent flow (Eisma 1986, Whitehouse et al. 2000) as well as under increased Suspended Sediment Concentrations (SSCs) (Chen et al. 1994, Eisma 1986, Manning et al. 2006, Whitehouse et al. 2000). To allow the formation of flocs (Chen et al. 1994, Eisma 1986; Whitehouse et al. 2000), the brought together particles have to either be cohesive (e.g. electro-chemical attraction, (van Olphen 1991, Whitehouse et al. 2000, Winterwerp & van Kesteren 2004)) and / or there has to be sticky organic substances present.

Electro-chemical forces of suspended cohesive sediments can be strongly influenced by the addition of salts. A negative particle charge is compensated by adding positively charged ions to the surrounding water. This process, known as salt flocculation, has been demonstrated by laboratory experiments (e.g. Thill et al. 2001). In the past salt was thought to cause particle flocculation within the brackwater zone of estuaries (van der Lee, 2001) where riverine freshwater and salty seawater mix. Especially when the vertical salinity structure within this zone is well stratified. Up to now, salt flocculation has only been shown for colloid ironhydroxydes, humates and associated substances < 1 µm (Sholkovitz 1976, Sholkovitz et al. 1978). In the case of salt flocculation for particles > 1 µm no evidence has yet been found (Eisma 1980, 1986). In contrast, an increased amount of small flocs at the salt water - fresh water contact have been observed and interpreted as de-flocculation (Eisma 1986, Puls et al. 1988).

Organic matter, such as bacterial polysaccharides, algae and higher plants serves as a ‘glue’ by providing fibrous structures around the inorganic particles (Fennessy et al. 1994). However, knowing that biological activity significantly depends on temperature, the strength of biological effects may differ on seasonal scales. Thus, concurring with Eisma (1986) and Eisma et al (1991, 1994) that more intensive biological activity in spring and summer leads to stronger inter-particle bindings than in winter. The preferred inorganic particle size (substrate size) for organic matter has been reported to be 8 µm (Chang et al. 2007).

Krone (1963) (summarized by Mikes 2011) described with his conceptual aggregation model that each floc is built from flocs of the next lower order. Single inorganic grains or so called ‘primary particles’ (mostly quartz, feldspars and carbonates) represent the zero order ‘flocs’. These inorganic grains together with organic matter form flocs of low order, also known as microflocs. They are mostly irregular shaped (Eisma 1986) and are considered to be sufficiently dense and strong enough to withstand disaggregation (Chen et al. 1994, Manning et al. 2006). The only way to break up microflocs in their inorganic constituents is by the artificial use of ultrasonics and / or by the removal of organic matter (Eisma 1986). The maximum size limit for microflocs is proposed to be between 100 µm (van Leussen 1999), 125 µm (Eisma 1986), 150 µm (Dyer et al. 1996) and 160 µm (Manning et al. 2006). Larger particles with a porous and fragile structure are

known as macroflocs. Eisma (1986) described macroflocs or higher order flocs as somewhat irregularly shaped and more or less rounded, but in some cases they are elongated and curved, almost sickle-shaped. Maximum sizes of up to 600 µm (surface water) and 800 µm (bottom water) are known from sampling in the Elbe estuary around slack water (Chen et al. 1994). Macroflocs with diameters of even up to 3-4 mm were observed in the Gironde estuary (Eisma 1986). However, these large flocs are fairly loose bound and can easily break up under turbulent conditions (Whitehouse et al. 2000). In this work, flocs < 125 µm are proposed as microflocs and particles larger than 125 µm as macroflocs, similar to the work of Eisma (1986).

The size distribution of flocs is a dynamic process that depends on the rates of aggregation and disaggregation of single particles and particle agglomerations, respectively (Chen et al. 1994). Size variation over space and time is related to tidal induced flow and turbulence. In many cases, largest flocs occur around slack water when fluid shear is small (e.g. Eisma et al. 1994, Fugate & Friedrichs 2003, Uncles et al. 2006). With increasing current velocity floc size tends to decrease (Chen et al. 1994, Eisma et al. 1994), and with the approach of the next slack water phase, when current intensity diminishes, floc sizes again begin to increase rapidly (Chen et al. 1994). Besides this general tendency in floc size variation, more voluminous flocs can occasionally be found during the flood or ebb current, when high SSCs result in an increased particle collision frequency (Chen et al. 1994, Eisma 1986, Manning et al. 2006, Whitehouse et al. 2000).

So far, the PPSD of the flocs has been poorly quantified, especially on spatial and temporal scales. Mikkelsen et al. (2006) for example, simply assume in their study in the Adriatic Sea, that all particles < 36 µm represent the primary particles. Size analyses of the inorganic fraction were not separately done in their studies. Nevertheless, the size quantification of the inorganic particles is important because they increase the density and hence the settling velocity of flocs by orders of magnitude (van Leussen 1988). The following studies show that partially a relation between primary particle size and floc size does exist. Kranck (1981) proposed a linear relationship between inorganic particle size (after ashing and de-flocculation) and in-situ sizes when total SSC is high, often in response with changes in current speed. In contrast, van Leussen (1999) describes an

increase of primary particle size while microfloc size (in this case < 100 µm) increases only at the seaward boundary of the Ems estuary where mucopolysaccharides are mobilized.

A problem occurring with studies about flocculation processes is the susceptibility of flocs concerning physical disturbance, especially during sampling. The work of Bale & Morris (1991) illustrates how prone flocs are with respect to physical disruption during sampling. Here, the 'real' in-situ size (87-188 µm) differs in comparison to pumped samples (10-20 µm) and primary particles (considerably smaller). To get undisturbed floc sizes it is important to use in-situ techniques which do not physically disturb the fragile flocs. Laser In-Situ Scattering and Transmissometry techniques (LISST, Sequoia® Scientific Inc., Bellevue, Washington) have been proved to be very useful for correct identification of in-situ particle size distributions (ISPSDs) (Agrawal & Pottsmith 2000, Mikkelsen & Pejrup 2001, Mikkelsen et al. 2005, Traykovski et al. 1999).

The objective of this paper is to describe both, undisturbed ISPSDs measured with a LISST and the size distribution of their inorganic constituents, the primary particles. Furthermore, the ISPSDs and the Primary Particle Size Distributions (PPSDs) are necessary to know for quantifying the transport and deposition of fine cohesive sediments. Especially, the size of the inorganic particles which influences the density and hence the settling velocity of flocculated material. To describe the variability of flocculation and changes in PPSD on different spatial and temporal scales measurements were done from several tidal cycles during the summer and winter seasons in the Elbe and Weser estuaries.

5.2: Regional settings

The upper meso- to lower macro-tidal coastal plain estuaries of the Weser and Elbe rivers are located along the southern North Sea coast of Germany (fig. 5.1). The tidally influenced parts, which extend from the open North Sea to the weir at Bremen in the case of the Weser river and up to Geesthacht in the case of the Elbe river, are about 120 and 160 km long, respectively (tab. 5.1). The geometry of the upper estuarine section of the Weser (south of Bremerhaven) and the Elbe (south of Cuxhaven) is channel-like,

whereas the lower estuarine sections are funnel-shaped. Morphology of both estuaries is strongly anthropogenically influenced by repeated deepening, ongoing maintenance and constructional work in and along the navigation channel. The sustained navigable depth in the channel-like section of the Weser estuary is currently 9 m (Schrottke et al. 2006), and 14.4 m in the Elbe estuary (Kerner 2007) at low-springs. As a consequence of man-induced changes in river geometry over the last decades, the tidal range has substantially increased in both estuaries (tab. 5.1). Today, the mean tidal range in the Weser estuary varies from 3.6 m in Bremerhaven to 4 m in Bremen (Grabemann & Krause 2001), while it currently amounts to 3 m in Cuxhaven, 2.7 m in Glückstadt and 3.5 m in Hamburg (Kerner 2007).

Both estuaries are characterised by semidiurnal tides but differ in tidal dominance, river run-off and mixing despite their geographical proximity (tab. 5.1). The long-term, mean

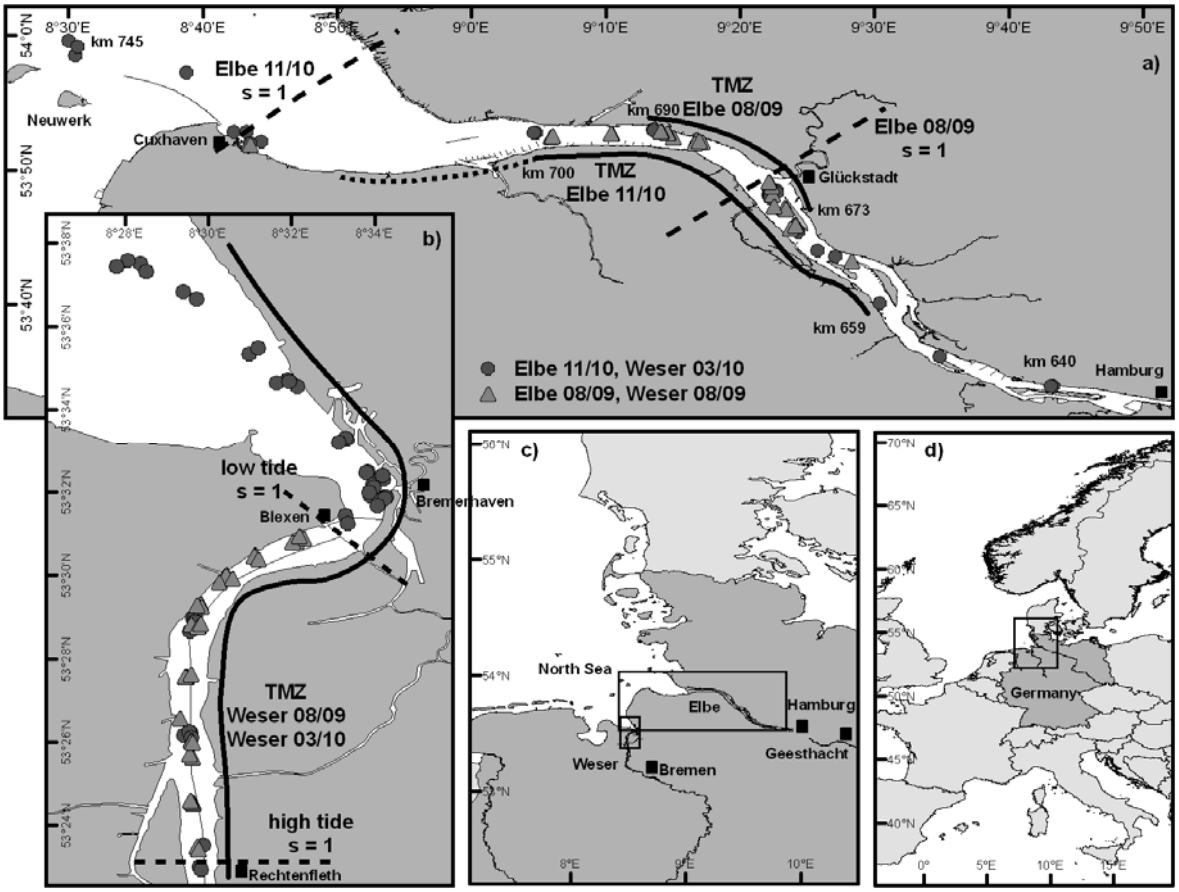

Figure 5.1: *Location of the study areas along the German North Sea coast (c-d). Detailed charts of the study areas within the Elbe (a) and Weser (b) estuaries showing sample positions, seaward directed brackwater boundary with a salinity (s) of 1 (dashed line) and TMZ location (black line). The downstream boundary of the TMZ could not exactly be determined during the Elbe 11/10 survey (dotted line).*

annual freshwater discharge of the ebb-dominated Weser estuary is about 326 m³/s and around 713 m³/s in the flood-dominated Elbe estuary (NLWKN 2009, NLWKN 2011). The mean current velocity in the Weser estuary amounts to 1-1.3 m/s with maximum values of 2.6 m/s being achieved during the ebb-tidal phase (BfG 1992). In the main navigation channel of the Elbe estuary mean current velocities vary between 0.6 and 1.5 m/ with maximum current velocities of up to 2.2 m/s (Projektbüro Fahrrinnenanpassung 2007).

The Weser estuary is a partially mixed (Grabemann et al. 1997) and the Elbe estuary partially to well mixed system depending on the freshwater discharge (Kappenberg & Fanger 2007). Both estuaries exhibit a well-developed Turbidity Maximum Zone (TMZ). The 15-20 km long TMZ of the Weser estuary is located during the mean fresh water discharge around Blexen (Grabemann & Krause 2001). The Elbe TMZ is approximately 30 km long and is usually located between Glückstadt and Cuxhaven (Duinker et al. 1982, Kappenberg & Grabemann 2001). The locations of both TMZs differ with varying fresh water discharge (Grabemann et al 1995).

Values of the SSC in the water column of the TMZs differ markedly between both estuaries. In the fairway of the Weser TMZ, the SSC ranges between 0.03 and 1.5 g/l (Grabemann & Krause 2001), with average values of 0.13 g/l (Schuchardt et al. 1993). Outside of the Weser TMZ, values do generally not exceed 0.05 g/l (Grabemann & Krause 2001, Schuchardt et al. 1993). SSCs in the Elbe TMZ exceed the riverine values (0.035 g/l) by a factor of 10 to 30 (Kappenberg & Grabemann 2001). Seaward of the Elbe TMZ mean concentrations of 0.01 g/l are known (BfG 2008).

In both estuaries, the Suspended Particulate Matter (SPM) is often found in a flocculated state. In the Weser estuary, the mean particle size ranges between 33 – 250 µm in the TMZ and between 102 – 268 µm in the freshwater section (Papenmeier et al. 2009, Papenmeier et al. 2010). On average, a downward coarsening of approximately 40 µm has been observed in the TMZ whereas a vertical size gradient does not exist in the freshwater section (Papenmeier et al. 2009). The mean floc size in the Elbe TMZ ranges between 150 and 200 µm near the surface and between 160 and 280 µm within the bottom water (Eisma et al. 1994). Maximum sizes of up to 600 – 800 µm have been

Table 5.1: *Physical settings of the estuaries of the German river Weser and Elbe.*

	Weser	**Elbe**
estuary type:	coastal plain	coastal plain
length:		
total	477 km	~1.091 km
tidal influenced part	~120 km (Intschede to Wadden Sea) [(*1)]	160 km (Geesthacht to Wadden Sea) [(*2)]
shape:		
inner estuary	channel-like (Bremen – Bremerhaven)	channel like (Geesthacht – Cuxhaven)
outer estuary	funnel-shaped, double channel (Bremerhaven – Wadden Sea)	funnel-shaped (Cuxhaven – Wadden Sea)
depth:		
channel like section at low-springs	9 m [(*3)]	14.4 m [(*4)]
tide:	semidiurnal [(*5)] ebb-dominated [(*5)]	semidiurnal with diurnal asymmetry [(*2)] flood-dominated [(*4)]
range changes	0.13 m (1882) – 4 m (1990) [(*3)]	
mean range	~4 m (Bremen; macrotidal) [(*5)] ~3.6 m (Bremerhaven; mesotidal) [(*6)]	3 m – 2.7 m – 3.5 m - 2m (Cuxhaven – Glücksstadt – Hamburg - Geesthacht) (max. 4 m) [(*2)]
freshwater discharge measured at…:	…Intschede	… Neu Darchau
Mean (MQ)	326 m³/s [(*6)]	713 m³/s [(*7)]
Low mean (MLQ)	118 m³/s [(*6)]	278 m³/s [(*7)]
High mean (MHQ)	1,230 m³/s [(*6)]	1920 m³/s [(*7)]
catchment area:	45.800 km² [(*1)]	~132.000 km² [(*2)]
currents:	partially mixed [(*8)]	partially to well mixed [(*9)]
mean velocity	1-1.3 m/s [(*3)]	0.6-1.5 m/s [(*10)]
maximum velocity	2.6 m/s [(*3)]	2.2 m/s [(*10)]
TMZ:		
length	15-20 km [(*5)]	30 km [(*11)]
location	around Blexen	between Glückstadt & Cuxhaven
SSC:		
fresh water reach:	< 0.05 g/l [(*5, 12)]	0.035 g/l [(*2)]
TMZ:	0.03 – 1.5 g/l [(*5)]	10-30 x fresh water values [(*2)]
salt water reach:	< 0.05 g/l [(*5)]	0.01 g/l [(*13)]
bottom material:	*TMZ:* mud (up to 25% silt & clay, 5% organic matter) [(*5, 14)] *outside TMZ:* fine & medium sand (silt & clay < 1%, organic matter < 0.1%) [(*5, 14)]	*generally:* fine – middle sand, partially with 5 – 30% silt [(*13)]

[(*1)] Seedorf & Meyer (1992), [(*2)] Kappenberg & Grabemann (2001), [(*3)] Schrottke et al. (2006), [(*4)] Kerner (2007), [(*5)] Grabemann & Krause (2001), [(*6)] NLWKN (2011), dataset from 1941-2007, [(*7)] NLWKN (2009), dataset from 1926-2003, [(*8)] Grabemann et al (1997), [(*9)] Kappenberg & Fanger (2007), [(*10)] Projektbüro Fahrrinnenanpassung (2007), [(*11)] Duinker et al. (1982), [(*12)] Schuchardt et al. (1993), [(*13)] BfG (2008), [(*14)] Grabemann & Krause (1989)

observed in the Elbe TMZ (Chen et al. 1994, Dyer et al. 1996), while particles sizes outside of the Elbe TMZ have so far not been reported.

Surface sediments of the river bed in the Weser TMZ are mainly characterised by mud and fine- to coarse-grained sands, whereas the mud content locally reaches 98% (Schrottke et al. 2006). The consolidation levels of the mud deposits range from the fluid phase to highly compacted mud layers (Schrottke et al. 2006). Outside of the Weser TMZ, bottom sediments in the fairway generally consist of fine to medium sand with clay and

silt contents < 1% and Particulate Organic Matter (POM) contents < 0.1% (Grabemann & Krause 1989, 2001). The river bed within the Elbe estuary originally consisted of highly compacted, erosion resistant clay and marl layers in a depth of 6 m and 10 m below sea level. Due to the success of navigational deepening, those sediments were almost completely removed from the river bed (BfG 2008). Recent outcrop exist only at steep riverbanks. Nowadays, sediments of the river bed in the Elbe navigation channel mainly consist of fine to medium sands, partly with 5 – 30 % silt (BfG 2008).

5.3: Material and Methods

Data from four surveys with the '*RV Littorina'*, representing summer and winter seasons, are discussed in this paper: 6-8 August 2009 (Weser 08/09), 9-13 August 2009 (Elbe 08/09), 9-11 March 2010 (Weser 03/10) and 25-30 November 2010 (Elbe 11/10). The summer surveys took place during quite normal fresh water discharge conditions (Elbe 08/09 = 396 m^3/s, Weser 08/09 = 117 m^3/s) whereas high discharge events took place during the winter surveys (Elbe 11/10 = 1,504 m^3/s, Weser 03/10 = 650 m^3/s) (tab. 5.2).

Table 5.2: *Mean freshwater discharge (Q) during the survey and long time mean (1990-2010) for the survey time span at Intschede (Source: Wasser- und Schifffahrtsamt Verden) and Neu Darchau (Source: Wasser- und Schifffahrtsdirektion Nord), respectively. Minimum, mean and maximum value of current velocity, Suspended Sediment Concentration (SSC), salinity and temperature during the water sampling campaigns in the Weser and Elbe estuary.*

	Mean Q [m^3/s]				current velocity [m/s]			SSC [mg/l]			salinity [PSU]			temperature [°C]		
	survey	long time	section	n	min	mean	max	min	mean	max	min	mean	max	min	mean	max
Elbe 08/09	396	402	landside	2	1.1	1.2	1.2	112	117	121	0.4	0.4	0.4	22.2	22.3	22.3
			TMZ	51	0.2	1.0	1.5	12	217	918	0.4	2.0	6.9	20.3	21.4	22.3
			seaside	7	0.4	1.2	1.5	13	54	176	2.2	4.8	7.3	21.0	21.3	21.6
Elbe 11/10	1504	774	landside	6	-	-	-	19	86	397	0.3	0.3	0.3	6.5	6.8	7.0
			TMZ	19	0.6	0.9	1.2	38	158	447	0.3	0.5	0.7	5.0	6.4	7.2
			seaside	15	0.3	0.6	0.9	32	128	316	0.6	16.7	28.2	5.5	6.1	7.7
Weser 08/09	117	152	landside	-	-	-	-	-	-	-	-	-	-	-	-	-
			TMZ	63	0.2	0.7	1.5	28	321	3060	4.3	10.2	20.2	21.2	22.3	23.2
			seaside	-	-	-	-	-	-	-	-	-	-	-	-	-
Weser 03/10	650	558	landside	-	-	-	-	-	-	-	-	-	-	-	-	-
			TMZ	41	0.3	0.6	1.3	33	215	1330	1.1	7.2	14.3	2.9	3.6	4.7
			seaside	-	-	-	-	-	-	-	-	-	-	-	-	-

In-situ particle sizing, current velocity measurements and water sampling was done in the Weser estuary within the TMZ between Rechtenfleth and the Northern end of the Container Terminal of Bremerhaven (fig. 5.1 b). The marine and riverine sections close to the TMZ were not sampled. Surveys in the Elbe estuary comprised the marine, brackwater and riverine sections of the Elbe estuary between Hamburg and the outer estuary, North of the Island Neuwerk (fig. 5.1 a).

The ISPSD was collected by means of laser diffraction with a 'Laser In-Situ Scattering & Transmissometry' system 'LISST-100X' (type-C, Sequoia® Scientific Inc., Bellevue, Washington) applied in a profiling mode from the drifting vessel. The ISPSD is displayed in 32 logarithmically-spaced size classes, ranging from 2.5 to 500 µm. Particles outside this range are assigned to either the finest or largest size class, respectively (Agrawal & Pottsmith 2000). A full technical description of the LISST was done by Agrawal & Pottsmith (2000) and Agrawal et al. (2008). For measurements in water with higher SSCs a path reduction module (50% & 90%) was installed to reduce the optical path length and thus the sample volume (Papenmeier et al. 2010). ISPSD is given as Volume Concentration (VC) for each size of the 32 classes, summed-up to Total Volume Concentration (TVC). The TVC was calibrated with SSC, which was calculated by dry mass per unit volume, based on values of vacuum-filtered water samples (Papenmeier et al. 2010). Water samples were taken with a horizontal water sampler (Hydro-Bios GmbH, Kiel, Germany) at 4 m (Weser) and 5 m (Elbe) water depth as well as 1 m above the river bed in both estuaries. Temperature and salinity of the water samples were measured directly after recovery using a Cond 3310 by WTW multimeter (Weilheim, Germany).

Primary particles were extracted by the centrifugation of 0.5 – 1 litre water samples. The carbonate components were removed by treating the sample with 10 ml 10% hydrochloric acid for four hours in a 60°C water basin and the organic components were removed by treating the samples with 10 ml 30% hydrogen peroxide for 24 hours in a 60°C water basin. The remaining inorganic material was measured with a Beckman Coulter laser diffraction particle sizer ('LS 13320'. Krefeld, Germany) using an 'Aqueous Liquid Module' or a 'Universal Liquid Module'. The device simultaneously uses two different techniques to analyse Particle Size Distribution (PSD) in a range of 0.04 – 2000 µm. The principle of light scattering was used for particles larger than 0.4 µm. The

resulting scattering pattern is converted into particle size by the Fraunhofer Diffraction theory (Blott & Pye, 2006). Particles smaller than 0.4 µm were detected by PIDS (Polarized Intensity Differential Scattering) technology (Pye & Blott, 2004) and converted by the Mie theory. To obtain representative data sets, 12 runs each taking 60 seconds were performed. However for data analysis, the average of only the last six runs was used to exclude size anomalies by effects of possible initial aggregations. Grain size classification is attached to the scale of Friedman & Sanders (1978) and statistical data is based on Folk & Ward (1957).

Current velocity was recorded with a 1,200 kHz 'Workhorse-ADCP' (Acoustic Doppler Current Profiler, RDI-Teledyne^{TM}, Poway, California) with a beam angle of 20° and a cell size of 25 cm step interval (Schrottke et al. 2011). The standard deviation for the current flow velocity amounts to 0.129 cm/s (Gordon 1996). Due to the water sampler was not going straight down under high current velocities, current data were averaged for the depth intervals of 3.5-4.5 m (Weser) and 4.5-5.5 m (Elbe). Current velocities for samples one meter above bed were not extracted, knowing that data quality within the lowermost 6% of the water column is reduced due to bottom induced signal interferences (Gordon 1996).

5.4: Results

5.4.1: Hydrological condition

Generally, the Weser and Elbe estuaries are partially to well mixed during the winter and summer surveys. In the Weser estuary, the location of the seaward boundary of the brackwater zone (salinity = 1), vary between Rechtenfleth and Blexen depending on the direction of the tidal current (fig. 5.1). The TMZ (mean SSC > 150 mg/l) is located around Blexen. A shift of the Weser TMZ (> 30 km) is not observed because sampling did not include the seaward and landward margins of the TMZ (fig. 5.1). The location of the marine brackwater boundary in the Elbe estuary is strongly dependent on the seasonal freshwater discharge. In summer, under high discharge conditions of 1,504 m³/s, the boundary is located near Cuxhaven. Under low discharge conditions of 396 m³/s, as

appeared in summer, the marine influence reaches till Glückstadt (fig. 5.1). The TMZ of the Elbe estuary (mean SSC > 150 mg/l) is located around Glückstadt; whereas in winter its length, 30 km, is twice as long as during summer time.

In general, the Weser TMZ has higher SSCs than the Elbe estuary (tab. 5.2). Here, maximum values can be up to three grams per litre. In the Elbe TMZ, SSCs do not exceed one gram per litre. In the seaward and landward sections close to the Elbe TMZ SSC values are mostly < 100 mg/l. Only near bed SSC values of some hundreds of milligram per litre were observed.

5.4.2: In-situ particle size distributions

In the Elbe and Weser estuaries, in-situ particle sizes vary between very coarse silt to medium sand size classes (exemplary shown for the Elbe estuary in figure 5.2). Open PSDs at the coarse end indicate the presence of particles larger than the measurement range of (> 500 µm). PSDs are mostly unimodal and fine skewed to very fine skewed (-0.14 to -0.51). Depth related size changes are not observed as shown in the example of the Elbe 08/09 survey in figure 5.3.

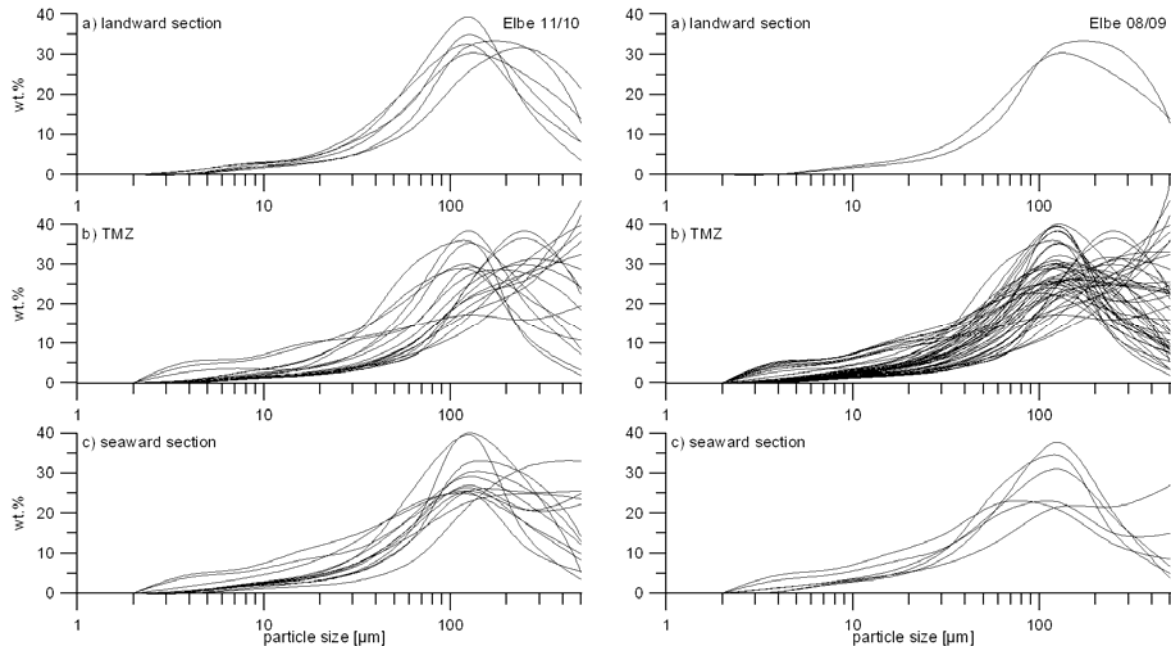

Figure 5.2: *In-situ particle size distribution for (a) the landward section, (b) TMZ and (c) seaward section of the Elbe 11/10 survey (left) and the Elbe 08/09 survey (right). The data are based on samples from 4 m (Weser) and 5 m (Elbe) water depth as well as 1 m above bed in both estuaries; corresponding to the water sampling depth.*

Three populations with peaks of around 125 µm, 250 µm and > 500 µm can be figured out in the TMZ of the Elbe and Weser estuaries as shown exemplary for the Elbe surveys in figure 5.2. Within the landward section of the Elbe estuary mainly PSDs with a mode of around 125 µm are present and in the seaward section PSDs with modes of around 125 µm as well as > 500 µm.

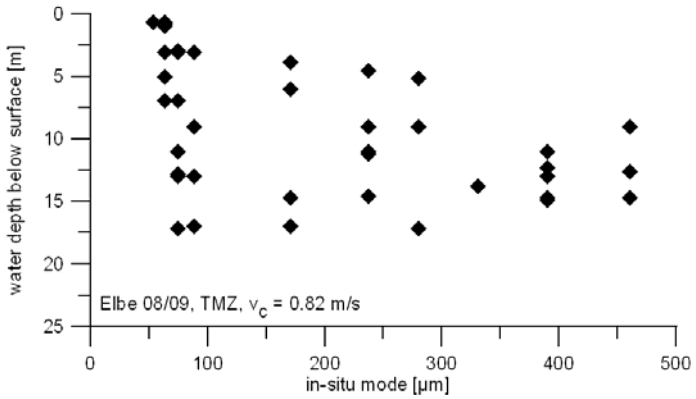

Figure 5.3: *In-situ mode vs. water depth exemplary shown for one station of the Elbe 08/09 survey within the TMZ at a current velocity (vc) of 0.82 m/s.*

During the winter survey on the Elbe (11/10) ISPSDs were strongly influenced by the current velocity (fig. 5.4). At low current velocities of (< 0.5 m/s) 50% or more of the particles are characterized by PSDs with modes of 250 µm or larger while the frequencies of large particles decrease with an increase in current velocity. At current velocities > 1.1 m/s PSDs with modes of > 250 µm are nearly absent (< 7%). During the above mentioned instances, 70% of the PSDs have a mode around 125 µm. During the summer surveys in the Elbe and Weser estuaries a similar trend with decreasing particle size at increasing current velocities can be observed in a weakened form. The difference between low and high current velocity is relatively small. Even at the highest current speeds, more than 10% (Elbe 08/09) and 30% (Weser 08/09) of the PSDs have a mode > 250 µm (fig. 5.4). The dependence of PSDs on the current velocity is less clear during the Weser 03/10 survey (fig. 5.4). The decreased frequency of 63 – 125 µm particles at a current velocity of 0.7 m/s is related to a data deficit. Despite the observed trends of decreasing PSD with increasing current speed, a correlation between current velocity and in-situ mode does not exist, as the example of the Elbe 11/10 survey in figure 5.5 shows.

Nevertheless, a relation between floc size and SSC exists. The frequency of ISPSDs with modes in a size spectrum of 250 to 500 µm increases with increasing SSC while the frequency of particles < 250 µm decreases (fig. 5.6). In winter, IPSDs with modes > 250 µm do not exist for a SSC < 15 mg/l.

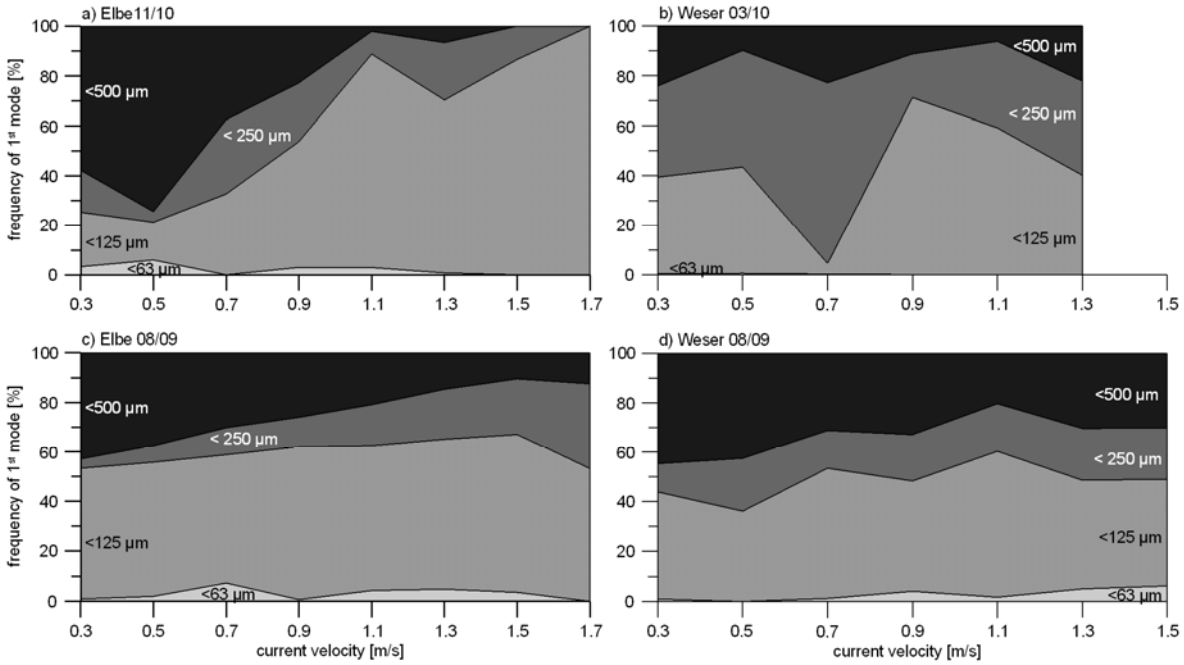

Figure 5.4: *The frequency of the first in-situ mode for different current velocities. The data are based on measurements covering the whole water column, retrieved from the landward section, TMZ and seaward section surveyed in August 2009 (Elbe & Weser) as well as March (Weser) and November (Elbe) 2010.*

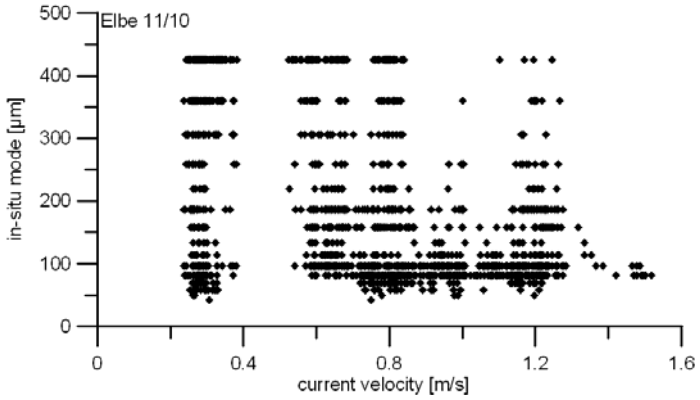

Figure 5.5: *Current velocity vs. in-situ mode of data covering the whole water column, retrieved from the landward section, TMZ and seaward section for the Elbe 11/10 survey.*

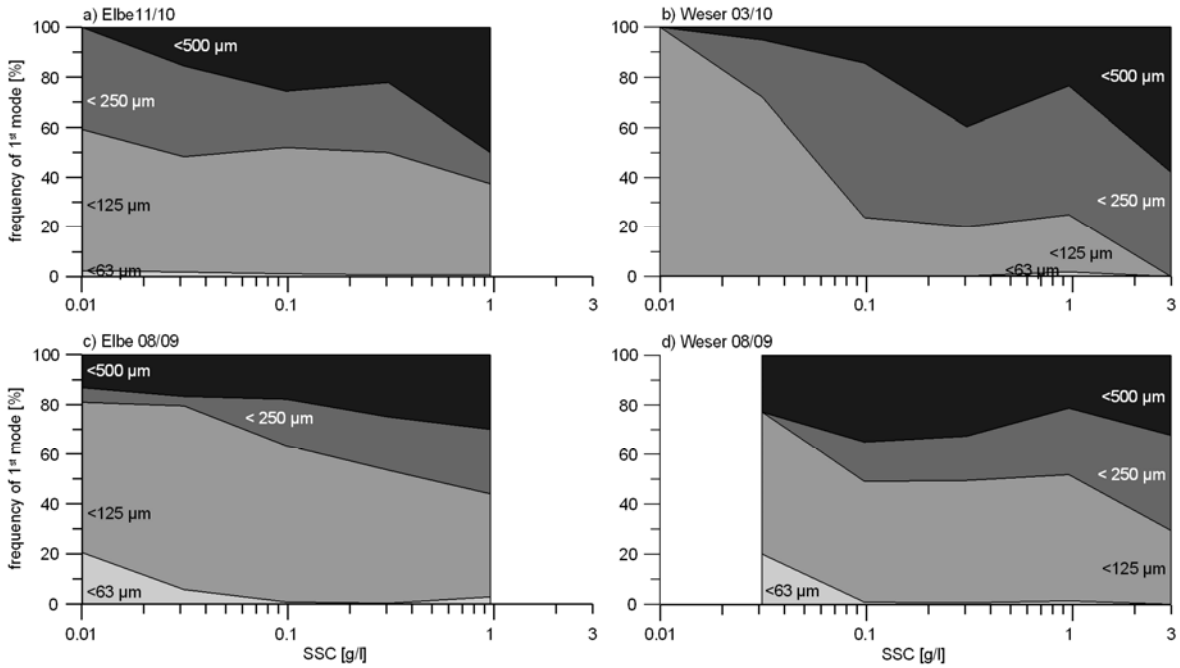

Figure 5.6: *The frequency of the first in-situ mode for different SSCs. The data are based on measurements covering the whole water column, retrieved from the landward section, TMZ and seaward section surveyed in August 2009 (Elbe & Weser) as well as March (Weser) and November (Elbe) 2010.*

5.4.3: Primary particle size distributions

The size spectrum of the primary particles ranges from clay to coarse sand (fig. 5.7). In both estuaries the most dominant fraction is silt (fig. 5.8), a slightly coarser component can be measured in the Elbe estuary. In both estuaries the clay content is less than 30 wt.% and sand-sized particles account for less than 25 wt.%.

PSDs of the Elbe 11/10 survey vary between the TMZ and the seaward and landward sections close to it (fig. 5.9). The maximum particle sizes is measured in the landward section and in the TMZ with a mode of almost 70 µm. Clay and very fine silt content is generally less than 15 wt.%. However, PSDs show different characteristics for the two sections as such that the ones of the TMZ are unimodal whereas landwards they tend to be polymodal. PSDs of the landward section are less negative skewed (-0.18 to -0.33) than those from the TMZ (-0.22 to -0.49) resulting in a larger mean particle size within the TMZ (fig. 5.10). Smallest mean particle sizes were observed in the seaward section. Here, the PSDs are slightly polymodal shaped. The first mode peak appears at around 10 µm. The clay content is always larger than 15 wt.%. The PSD is less skewed (-0.07 to -0.15) than

further downstream (fig. 5.10). Actually, the clay content can be linked to the salinity in case of the samples taken during the Elbe 11/10 survey (fig. 5.11). Samples with < 15 wt.% clay are linked to salinities < 1 and samples with > 15 wt.% to salinities > 5.

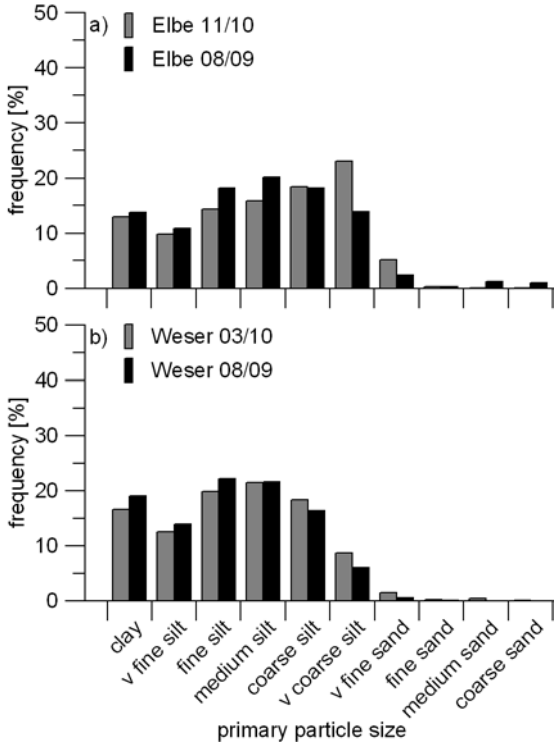

Figure 5.7: *Averaged primary particle size distribution of all samples, representing the situation during winter and summer in the Elbe estuary (a) and Weser estuary (b).*

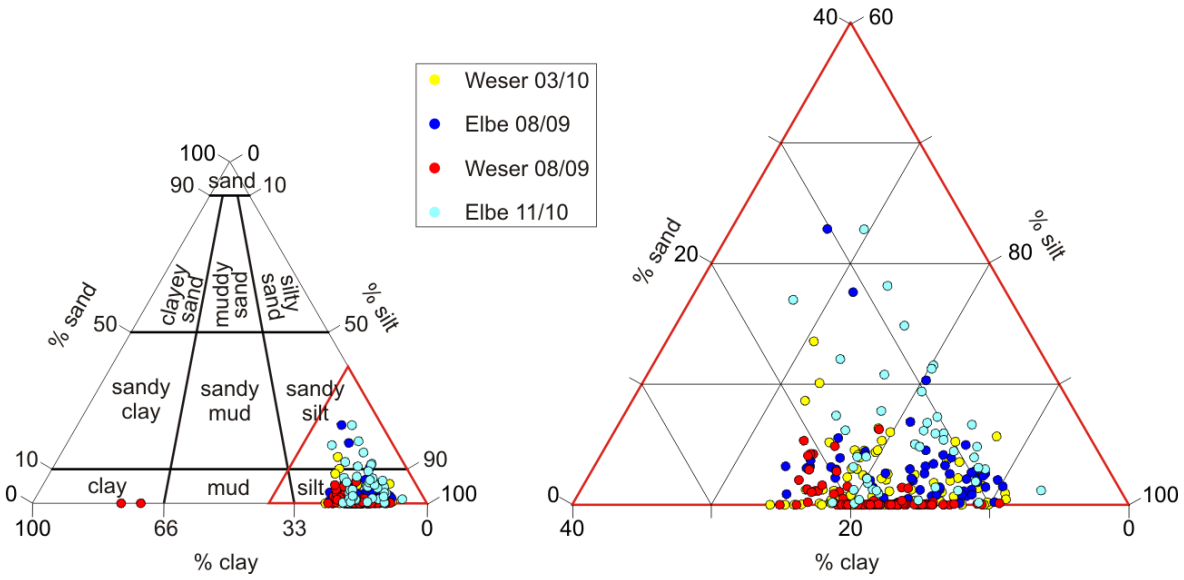

Figure 5.8 Left: *Ternary diagram on the basis of sand/silt/clay ratios of the primary particles. The classification is after Folk and Ward (1957).* ***Right:*** *Zoom of the data range.*

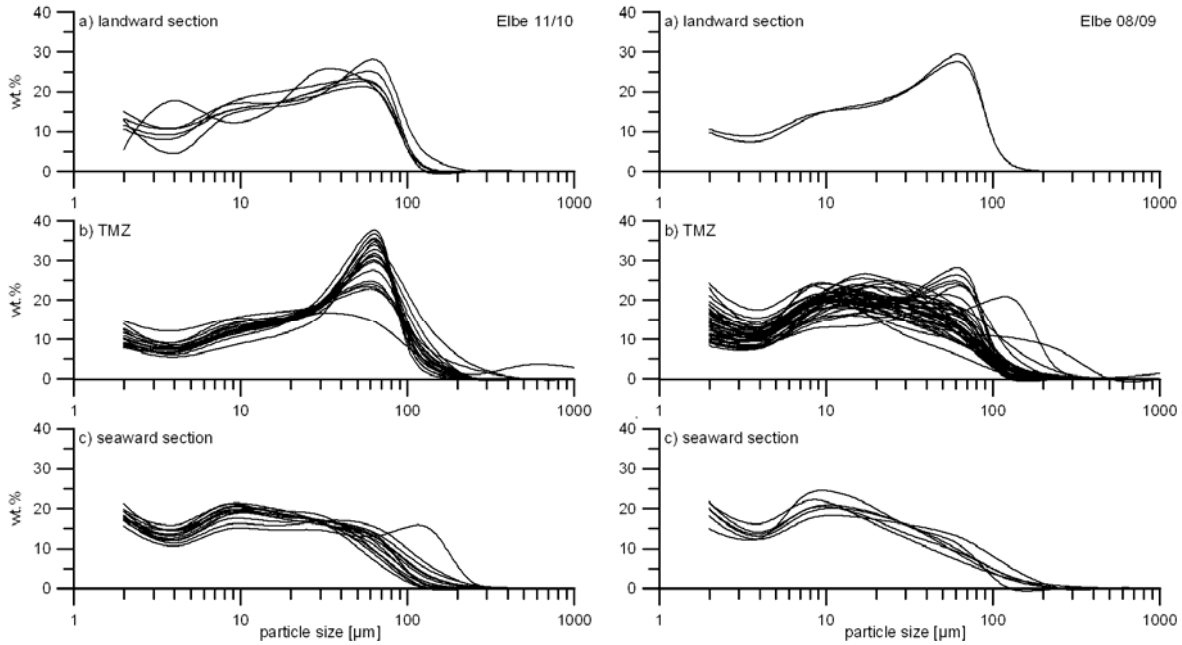

Figure 5.9: *Primary particle size distribution for (a) the landward section, (b) TMZ and (c) seaward section of the Elbe 11/10 survey (left) and the Elbe 08/09 survey (right). The data are based on samples from 4 m (Weser) and 5 m (Elbe) water depth as well as 1 m above bed in both estuaries; corresponding to the water sampling depth.*

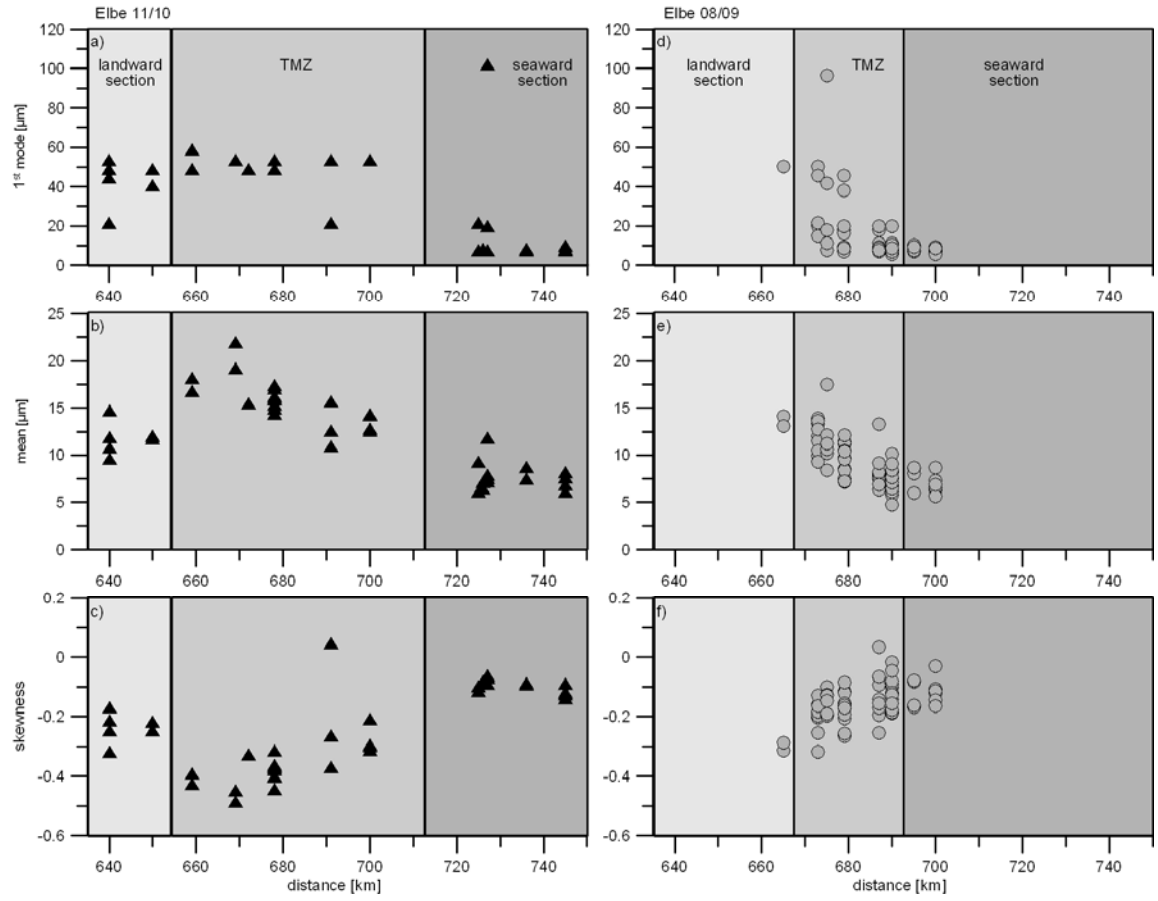

Figure 5.10: *Primary particle mode, mean and skewness vs. distance (km) for the Elbe 08/09 (a-c) and Elbe 11/10 survey (d-f). The statistical data base on Folk and Ward (1957).*

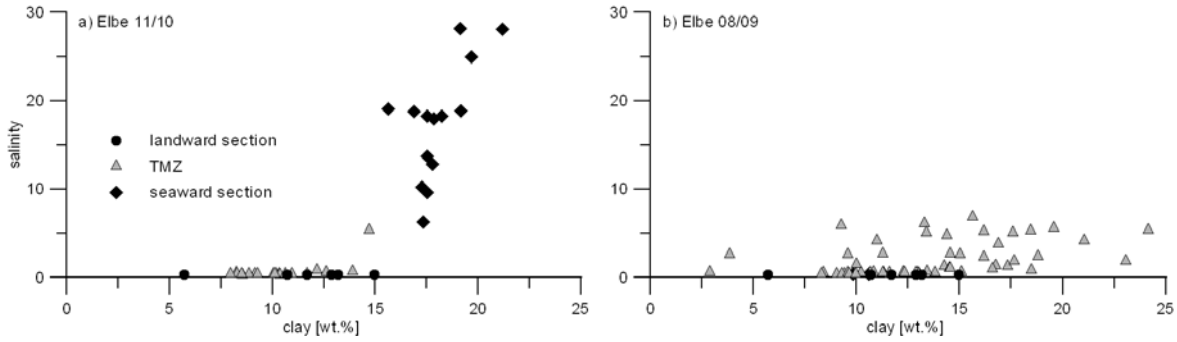

Figure 5.11: *Primary particle clay content vs. salinity for the landward section, TMZ and seaward section for (a) the Elbe 11/10 and (b) the Elbe 08/09 survey.*

A downstream decrease in particle mode and mean size is also present during the summer survey on the Elbe (08/09), but regional differences in PSDs are not as clear as during the winter survey (fig. 5.9 & fig. 5.10). A correlation between clay content and salinity does not exist (fig. 5.11). Further, an individual PSD in the TMZ, which differs to the PSD outside the TMZ, as observed during the winter survey is not present in summer. In fact, the TMZ comprises PSDs with a mode of approximately 50 µm (characteristic for the landward section) and PSDS with a mode of nearly 10 µm (characteristic for the seaward section). Modes larger than 40 µm are only present in the TMZ when the current velocity is larger than 0.6 m/s (fig. 5.12). Particularly, larger modes are more frequent near bed than at mid-depth (fig. 5.13). Such depth and current related differences are neither observed outside of the TMZ nor during the other surveys in Elbe and Weser estuaries.

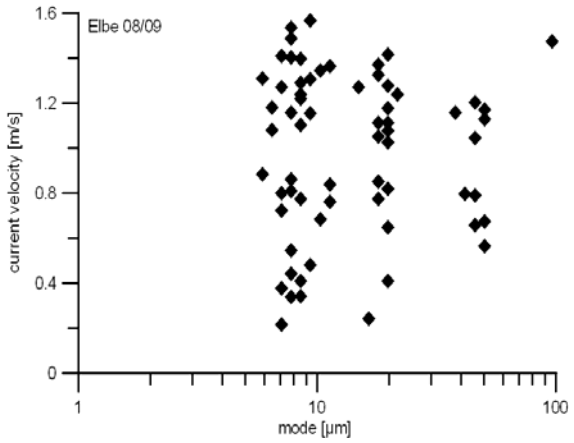

Figure 5.12: *Primary particle mode vs. current velocity for the Elbe 08/09 survey.*

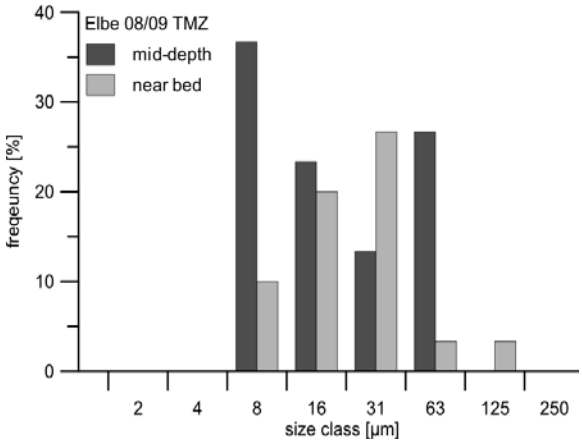

Figure 5.13: *Frequency distribution of the primary particle mode of samples from mid-depth and near bed in the TMZ (Elbe 08/09 survey).*

The PPSD for the Weser TMZ, where sampling mainly took place, is similar to those from the seaward section of the Elbe estuary. Seasonal differences are small. In winter fine to coarse sands are with less than 0.5 wt.% present.

A correlation between PPSD and ISPSD size does not exist in the Elbe estuary neither in the Weser estuary as shown in figure 5.14.

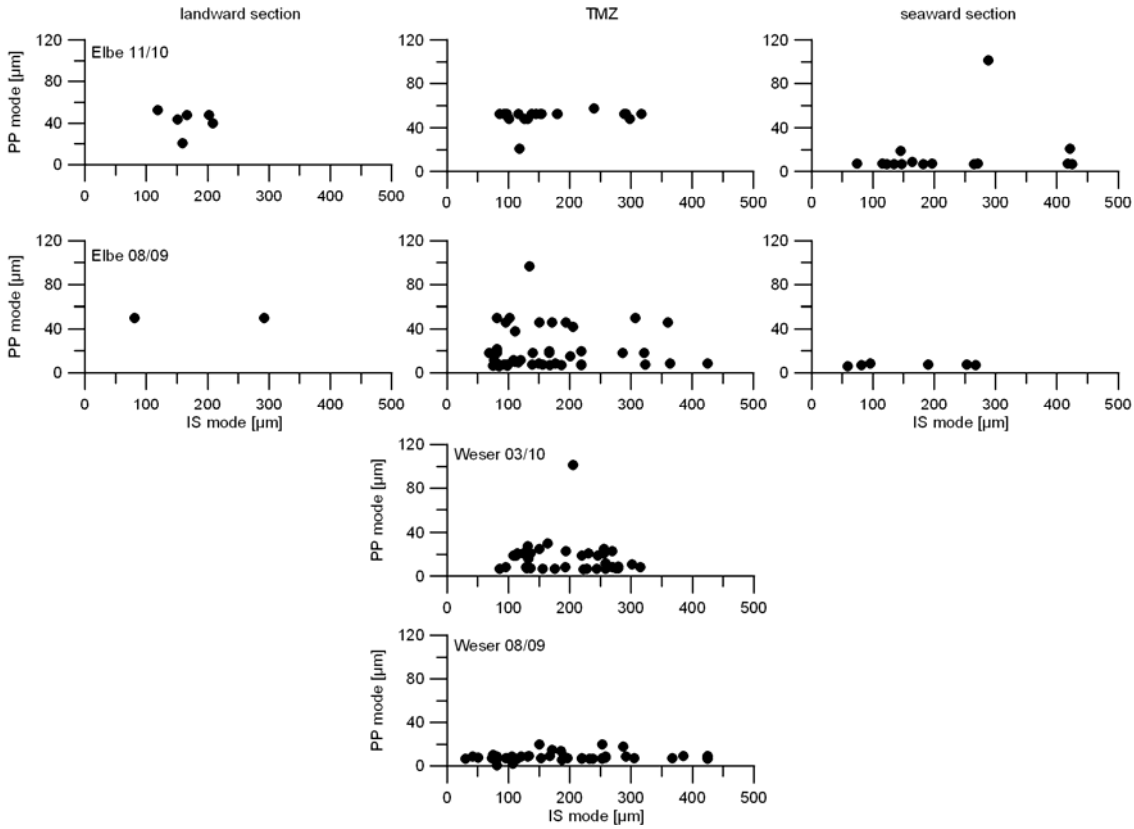

Figure 5.14: *Primary particle mode vs. in-situ mode for the four surveys on the Elbe estuary (differentiated into landward section, TMZ and seaward section) and on the Weser estuary in the TMZ.*

5.5: Discussion

The large particle modes found in-situ at the study sites in the Weser and Elbe estuaries indicate that the organic and inorganic suspended matter mostly appear in a flocculated state. The inorganic particles of around 8 µm which are known to act as the substrate for organic matter and hence promote flocculation (Chang et al 2007) are transported mainly from the seaside into the Elbe and Weser estuaries (BfG 2008). In the case of the Weser estuary, the primary particles can also originate from the TMZ. Here, deposits of fine

cohesive sediments, amongst fluid mud, with comparable PPSDs are well known (Papenmeier et al. 2011, Schrottke et al. 2006). A riverine origin of the ‘substrate size’ is in case of the Elbe estuary unlikely due to potential clay and marl layers on the steep riverbanks which cannot describe the amount of SPM and are known as quite erosion resistant (BfG 2008).

In the study of the Elbe estuary, the PPSD and hence the amount of this 'substrate size’ depends on the sampling location and the extension of the TMZ which is linked to the freshwater discharge. Generally, the upstream fining of the PPSD indicates that the fine inorganic fraction is transported from the seaward site into the estuary. However, the substrate size of approximately 8 µm, which acts as substrate for organic matter and hence necessary for flocculation, is present along the whole area surveyed in this study. Under low freshwater events, especially in summer, these fine-grained, inorganic particles are able to be transported up to the Hamburg Harbour or further (BfG 2008). Data of this study indicate that generally different PPSDs exist in the TMZ (unimodal with modes of almost 70 µm), the landward (slightly polymodal with modes of almost 70 µm) and seaward sections (slightly polymodal with modes around 10 µm). Nevertheless, a distinct extension of the TMZ is necessary to develop an individual PPSD which differs to the ones in the seaward and landward sections. In this study, the distance between the seaward and the landward section is too small in summer (< 15 km) to develop an individual PPSD within the TMZ like it has been observed for the TMZ in winter (fig. 5.9). Instead, the TMZ is in summer mostly influenced by PPSDs found in the seaward section. Larger particles (~70 µm) are not associated with particles found in the landward section but rather with re-suspended river bed sediments because they occur only near the riverbed when current velocities are high (> 0.6 m/s). This observation coincides with the re-suspension of larger particles under high hydrodynamic forcings in the York River, Virginia, USA (Fugate & Friedrichs 2003).

Kranck (1981) describes a linear relationship between PPSD and ISPSD for SPM found in the Miramichi estuary, when the total concentration is high (> 20 mg/l). The author assumes that only at these SSCs, a complete flocculation of both primary particle and organic matter and a stable density of the flocculated material exist so that PPSD and ISPSD can vary simultaneously. A relationship between PPSD and ISPSD has not been

observed in this study neither in the Elbe estuary nor in the Weser estuary although the SSC is mostly higher. The observation of a missing relationship between PPSD and ISPSD coincides with studies in the Elbe estuary by Eisma et al. (1991). A relation between the frequency of distinct an ISPSD in both current velocity and SSC indicates particle collision as control mechanism for the in-situ particle size.

Particles with modes > 125 µm (macroflocs) exist when current velocity and shear stress is low (Bale & Morris 1991). The fragile macroflocs can comprise of 50% or more of the total amount of flocs when current velocities are < 0.3 m/s around slack water. Disaggregation of the macroflocs with beginning ebb or flood flow (current speeds > 0.5 m/s) is indicated by a decreasing frequency of macroflocs and a simultaneous increased frequency of particles within the size spectrum of 63 to 125 µm. Particles of this size spectrum represent the more stable microflocs. Even at peak ebb or flood current they do not disaggregate into particles with modes < 33 µm. Eisma (1986) reports that in nature microflocs are relatively resistant to further breakage. A disaggregation into single inorganic grains is only possible by chemical or physical treatment (Eisma 1986).

The tidal signal in in-situ floc size is weaker in the Elbe and Weser estuaries during summer. Generally, the trend of decreasing particle size at increasing current velocity is present in summer, but macroflocs still exist at maximum current velocities whereas in winter macroflocs are completely disaggregated at peak current flow. From studies in the Ems estuary (Eisma 1986, Eisma et al. 1991) it is known that high biological activity in spring and summer lead to strong inter-particle bindings because bacterial polysaccharides, algae and higher plants act as a glue. Hence, the organic and inorganic aggregates of macrofloc size are more resistant against break-up caused by shear stress.

Weak regional differences in the Elbe ISPSD, described by an increased frequency of particles with modes of 500 µm or greater in the TMZ and the seaward section, are related to 2-4 times higher SSCs than measured in the landward section. An increased amount of macroflocs by the SSC induced particle collision is well known from diverse works (Chen et al. 1994, Eisma 1986, Kranck 1981, Manning et al. 2006, Mikkelsen et al. 2007, Whitehouse et al. 2000). A similar relationship between SSC and maximum floc size exist also within the TMZ of the Weser estuary. However, from earlier studies within the

Weser estuary it is known that this theory does not apply for the entire Weser estuary because the mean in-situ particle size is slightly larger in the freshwater section (144 µm) than in the TMZ (133 µm) although SSC is 2-6 times lower (Papenmeier et al. 2009, Papenmeier et al. 2010). Based on that, other parameters, rather than increased particle collision, must have a stronger impact on the ISPSD. It is assumed that biological effects are responsible for the varying PSD in the Weser estuary. Salt flocculation as known for particles < 1 µm (Sholkovitz 1976, Sholkovitz et al. 1978) is not present, as shown by the missing relation between salinity and floc size in the Weser and Elbe estuaries. Therefore, the required sharp contact of salt and freshwater is missing in the partially to well mixed Weser and Elbe estuaries.

5.6: Conclusion

The use of a LISST device enables the measurement of undisturbed ISPSDs in the Elbe and Weser estuaries which are prone to physical disruption. In combination with the analysis of primary particle sizes extracted from water samples, it is possible to identify control mechanisms of the ISPSD and PPSD on different temporal and spatial scales and to describe their interaction. In both estuaries inorganic and organic SPM is mostly in a flocculated state. Increased amounts of fine inorganic particles near the river mouth indicate that the substrate for the organic matter which is needed for flocculation is mainly transported from the seaside into the estuaries. In the case of the Weser estuary, PPSDs are in the size range of fine cohesive sediment accumulations found in the TMZ, which suggest the re-suspension of river bed sediments. PPSDs with modes of > 40 µm, found in the Elbe estuary only near the riverbed at high current velocities (> 0.6 m/s) originate from the re-suspension processes. However, it is assumed that these particles are in suspension as single grains and not incorporated in the aggregates.

In the Elbe estuary, when the freshwater discharge in winter is high and the extension of the TMZ is large, individual PPSDs exist each in the TMZ and the landward and seaward section close to it. Missing individual PPSDs within the TMZ in summer show that a certain distance (> 15 km) between the seaward and landward section is needed to obtain an

individual sorting within the TMZ. A quantification of regional changes of the PPSD in the Weser estuary is not possible due to the lack of data.

Regional differences in the PPSD have no influence on the ISPSD. The in-situ size is controlled primarily by the particle collision frequency powered by tidal forces and increased SSCs. The ISPSD increases with decreasing current velocity and increasing SSC. Macroflocs (> 125 µm), well known from slack water conditions, break-up successively into smaller microflocs (< 125 µm) with a start in the current flow. Smallest microflocs are present during highest current velocities. But these microflocs are strong enough, to withstand further breakage into their inorganic constituents. Temperature induced biological activity can strengthen the floc stability and hence weaken the tidal signal in summer. Salt induced flocculation does not exist during our surveys because the partially to well mixed Weser and Elbe estuaries do not have the necessary sharp contact between the fresh and salt water bodies.

Although flocs aggregate and disaggregate over a tidal cycle they presumably do not change their PPSD. According to these observations it can be suggested that primary particles are not extracted from or added to the floc. This assumption supports the theory early described that microflocs are in nature resistant to disaggregation into their inorganic constituents. To get reliable PPSD for different in-situ size classes sampling and analysis of single flocs would be necessary, but this is almost impossible due to the fragility of the flocs.

Acknowledgements

The authors would like to thank the captain and crew of the '*RV Littorina*' for their excellent job and inexhaustible patience during the acquisition of the data-sets for this study. The lab assistance of A. Trumpf and all trainees is also gratefully acknowledged. Furthermore, we wish to thank our colleagues for fruitful discussions and S.Peters for linguistic corrections. This study was funded by the Cluster of Excellence 'The Future Ocean' in Kiel.

Chapter 6: Sedimentological and rheological properties of the water–solid bed interface in the Weser and Ems estuaries, North Sea, Germany: Implications for fluid mud classification

Svenja Papenmeier[1], Kerstin Schrottke[2], Alexander Bartholomä[3], Burghard W. Flemming[4]

[1] Corresponding author: Institute of Geosciences & Cluster of Excellence „The Future Ocean“, at Kiel University, Otto-Hahn Platz 1, 24118 Kiel, Germany, sp@gpi.uni-kiel.de

[2] Institute of Geosciences & Cluster of Excellence „The Future Ocean“, at Kiel University, Otto-Hahn Platz 1, 24118 Kiel, Germany, ks@gpi.uni-kiel.de,

[3] Senckenberg Institute, Dept. of Marine Research, Suedstrand 40, 26382 Wilhelmshaven, Germany, abartholomae@senckenberg.de

[4] Senckenberg Institute, Dept. of Marine Research, Suedstrand 40, 26382 Wilhelmshaven, Germany, Burghard.Flemming@senckenberg.de

Accepted in December 2011 in the Journal of Coastal Research.

Abstract

Fine, cohesive sediment suspensions are a common feature of estuarine environments. Generally, multilayer models are used to describe the vertical distribution of such sediments. Such conceptional models normally distinguish at least high suspended sediment concentrations (SSCs) as a topmost layer and a consolidated bed layer, often including an intermediate, fluid mud layer. Rheological and in particular sedimentological properties are rarely included in these models. New data from two different estuaries provide new insights that can contribute toward the classification of near bed cohesive sediments.

The water–solid bed interfaces within the turbidity maximum zones of the Weser and Ems estuaries were sampled with 2–4-m-long cores. At 10-cm intervals, values of SSC,

viscosity, particulate organic matter, mud : sand ratio, temperature, salinity, and grain size distributions were determined. By normalizing these parameters to SSC and performing a cluster analysis, sediment suspensions of, 20 g/L SSC, fluid mud with up to 500 g/L SSC, and an underlying cohesive/consolidated bed can each clearly be distinguished. However, changes in flow behaviour and sedimentological characteristics represented by a shift in the cluster grouping support a subdivision of the fluid mud into a low-viscosity (I) (20–200 g/L SSC) and a high-viscosity (II) (200–500 g/L SSC) layer. Furthermore, by normalizing SSC measurements, site-specific differences were observed in the rheological behaviour of the fluid mud which might be caused by differences in grain-size composition. This suggests that the widely accepted 3-layer model of vertical SSC profiles should be extended by two layers of fluid mud identified in this study.

ADDITIONAL INDEX WORDS: *cohesive sediments, Rumohr-type gravity corer, viscosity, grain size, cluster analysis*

6.1: Introduction

High suspended sediment concentrations (SSCs) of fine, cohesive material are characteristic for tidal estuaries, especially in the turbidity maximum zones (TMZs). The amount and spatial distribution of this suspended particulate matter (SPM) depend on river runoff, tidal forcing, and marine and fluvial sediment supply. Generally, SSCs in microtidal estuaries reach values around 0.1–0.2 mg/L, as opposed to macrotidal estuaries, where SSCs typically reach values of 1–10 g/L (Brown et al., 2006).

Vertical distributions of SSC and SPM density in the water column and the underlying bed are often described using two- or three-layer models (e.g., Nichols, 1984). Two-layer models represent particle-by-particle settling from dilute suspensions onto a previously settled mud bed under zero horizontal and vertical flow. In those cases, density profiles indicate a discontinuity at the water–bed interface (Nichols, 1984). Three-layer models are more frequently used in higher energetic environments where an additional intermediate layer consisting of a denser suspension is distinguished (Nichols, 1984). The

classification and terminology of the constituent layers vary in the literature. The upper layer in the three-layer models is often termed low to highly concentrated suspension (Winterwerp and van Kesteren, 2004) or mobile suspension (Ross, Lin, and Mehta, 1987; Ross and Mehta, 1989; Uncles, Stephens, and Harris, 2006). In this fluid-supported layer, particles settle freely in SSCs of a few milligrams to grams per litre (Ross, Lin, and Mehta, 1987). The concentrated suspensions behave like a Newtonian fluid (Wurpts, 2005). Initially, as SSC increases with water depth, the settling velocity increases because of Brownian motion (Uncles, Stephens, and Law, 2006). This condition changes at higher SSCs, where settling velocities are slowed because of the effects of hindered settling (Dankers and Winterwerp, 2007).

The onset of hindered settling is often associated with the appearance of a lutocline (Kineke and Sternberg, 1995; Mehta, 1991; Nichols, 1984; Ross and Mehta, 1989; Ross, Lin, and Mehta, 1987; Smith and Kirby, 1989). Lutoclines represent the upper boundary of the intermediate layer or the so-called fluid mud. The SSC values at which lutoclines occur, as described in the literature, are summarized in Table 6.1. A widely reported and generally accepted SSC value is 10 g/L (Kineke and Sternberg, 1995; Kirby, 1988; Manning, Langston, and Jonas, 2010; Ross and Mehta, 1989; Wells and Coleman, 1981). In general, fluid mud is a mixture of water, clay, silt, and particulate organic matter (POM) (McAnally et al., 2007). In more energetic environments, very fine and fine sands are sometimes additional constituents (McAnally et al., 2007). At higher fluid mud concentrations, downward settling of particles is inhibited by upward escaping fluid and the progressive development of a particle-supported framework structure (Kineke and Sternberg, 1995; Nichols, 1984). In addition, the flow behaviour becomes non-Newtonian (Manning, Langston, and Jonas, 2010; McAnally et al., 2007). However, vertical and horizontal particle movement is still possible (Kirby, 1988; Mehta, 1991). The lower fluid-mud boundary is generally specified by the level at which the horizontal flow velocity becomes zero (Mehta, 1991; Ross and Mehta, 1989). In the literature, SSC values at this boundary vary between some hundreds of grams per litre (cf. Table 6.1).

In most studies, the description of suspended sediments is based on a rather limited number of parameters, such as SSC, SPM density, and current velocity. However,

Table 6.1: *Source literature for upper and lower fluid mud boundary SSC by different authors.*

Author(s)	Upper fluid mud boundary [g/l]	Lower fluid mud boundary [g/l]
Inglis and Allen (1957)*	10	480
Krone (1962)*	10	170
Sylvester and Ware (1976)	4	400
Wells (1983)*	50	480
Nichols (1984)	3	320
Faas (1984)	10	480
Kendrick and Derbyshire (1985)*	200	400
Winterwerp and van Kesteren (2004)	10	several 100

additional properties have been shown to be important (e.g., Faas, 1984). Among those are properties reflecting the shear behaviour of the fluid flow, such as the relationships among SSC, shear rate, and shear stress, as observed in laboratory-generated mud (e.g., Wright and Krone, 1989). The few field studies on natural fluid mud show that viscosity increases exponentially with increasing SSC (Faas, 1984; Granboulan et al., 1989). In situ measurements by Wells and Coleman (1981) in fluid mud on the continental shelf between the Amazon and the Orinoco rivers yielded values of 0.002–21.0 pascal-seconds (Pa·s) Again, fluid mud viscosities of up to 15 Pa·s, measured with a viscosimeter, are known from the Gironde estuary, France, where maximum SSC values reach 600 g/L (Granboulan et al., 1989). There, higher values are exclusively linked to brackish and marine sites with higher amounts of suspended silt and sand, such as in freshwater environments with clay-dominated fluid mud. Changes in the flow behaviour of fluid mud from the NE continental shelf of Brazil are also linked to increasing SSC (Faas, 1984). Fluid mud of lower concentration (< 300 g/L SSC) behaves pseudoplastic, whereas at higher concentrations, a viscosity ‘‘notch’’ appears. At that point, the flow behaviour is dependent on the shear rate. Initially, at low shear rates, fluid mud flow behaviour is pseudoplastic, being related to the rapid breakdown of loose, flocculent particle structures (Faas, 1981). With increasing shear rates, the flow changes to dilatants behaviour, where individual clay particles orientate themselves into a parallel alignment with closer packing, thereby, causing a temporary shear thickening (Faas, 1981). At greater shear rates, the fabric structure breaks down and pseudoplastic behaviour is reestablished (Faas, 1981). The SSC boundary, at which flow behaviour changes, seems to be dependent on the nature of the estuarine environment. Thus, in fluid mud of the NE continental shelf of Brazil, this boundary occurs at around 300 g/L SSC (Faas, 1984).

Generally, freshly formed fluid mud is weakly consolidated, and as long as its behaviour is pseudoplastic, it can be eroded throughout the range of shear stresses and shear rates that realistically occur in estuarine environments.

Particle size and composition can strongly influence shear behaviour and settling velocity. Mean particle sizes in fluid mud vary substantially, ranging from < 10 φ (Wells and Coleman, 1981) to 7.9–6 φ (Nichols, 1984) and 6.6–4.3 φ (Mitchell et al., 2002). The settling velocity of particles increases with size, especially for particle aggregates formed during slack water (Kranck, 1981; Mitchell et al., 2002). Sand within the matrix increases the bounding potential between clay particles (Manning, Langston and Jonas, 2010) and enhances the compaction and densification of the material (Whitehouse et al., 2000). A sand : mud ratio of 50 wt% can raise the erosional shear stress by a factor of two (Mitchener and Torfs, 1996). In addition, the type of clay controls the cohesiveness of the suspension. Kaolinite is the least cohesive and smectite and montmorillonite are highly cohesive, whereas illite occupies an intermediate position (Mehta, 1989).

Particulate organic matter also plays an essential role in the development of fluid mud, by promoting particle flocculation (Kranck, 1981). Internal friction, and hence the flow behaviour of fluid mud, changes with varying organic content (de Jonge and van den Bergs, 1987). On the one hand, microbial slimes act as lubricants (Wurpts, 2005; Wurpts and Torn, 2005), whereas, on the other hand, POM has a stabilizing effect when polymers produced by biological processes are absorbed onto particle surfaces to form bridges between the particles (van Leussen, 1999). The POM content and composition are controlled by environmental conditions. Light limitation, caused by high turbidity, reduces primary production and, thereby, the amount of organic matter (Herman and Heip, 1999). Changes in temperature, salinity, and nutrients can result in a turnover of species and their distribution (Herman and Heip, 1999). The POM content in fluid mud is highest in quiescent environments (e.g., Lake Okeechobee, Florida: 40 wt%;Mehta, 1991), whereas values are generally lower in estuaries, deltas, and along high energy coasts (e.g., the continental shelf between the Amazon and Orinoco rivers, where POM contents range from 1.5– 2.2 wt%; Wells and Coleman, 1981).

To date, it has been difficult to compare fluid mud properties retrieved from different estuarine systems or other coastal regions because a standardised definition is lacking. Furthermore, fluid mud is often described by only one parameter and is based on single-point measurements. In this study, simultaneous samples were recovered for analyses of SSC, viscosity, mud : sand ratio, grain sizes, POM, temperature, and salinity at closely spaced, vertical intervals across the water–solid bed interface at a number of different sites of two estuaries. On this basis, more parameters than merely SSC and sediment density were available. These were grouped by means of a hierarchical cluster analysis into statistically significant categories, which served to promote a multilayer classification of near-bed, fine, cohesive sediments.

6.2: Regional settings

The upper mesotidal to lower macrotidal, coastal plain estuaries of the Weser and Ems rivers are located along the southern North Sea coast of Germany (Figures 6.1 a–c). The tidally influenced parts, which extend from the open North Sea to the weir at Bremen, Germany, in the case of the Weser estuary and up to Herbrum, Germany, in the case of the Ems estuary, are about 120 and 100 km long, respectively (Table 6.2). Both estuaries are channel-like along the upper river section and funnel-shaped along the lower section. Both river geometries are strongly anthropogenically influenced by repeated deepening, ongoing maintenance, and constructional works in and along the navigation channels. The sustained navigable depth in the channel-like section of the Weser estuary is currently 9 m at low springs (Schrottke et al., 2006) and 5.7 m in the Ems estuary (Schuchardt et al., 2007). As a consequence of the man-induced changes in river geometry during the past decades, the tidal range has substantially increased in both estuaries (Table 6.2). Today the mean tidal range in the Weser estuary varies from 3.6 m at Bremerhaven, Germany, to 4 m at Bremen, Germany (Grabemann and Krause, 2001). In the Ems estuary, it currently amounts to 3.8 m (Jürges and Winkel, 2003).

Both estuaries are characterised by semidiurnal tides but differ in tidal dominance, river runoff, sediment budget, and spatial distribution of fluid mud, despite their geographical

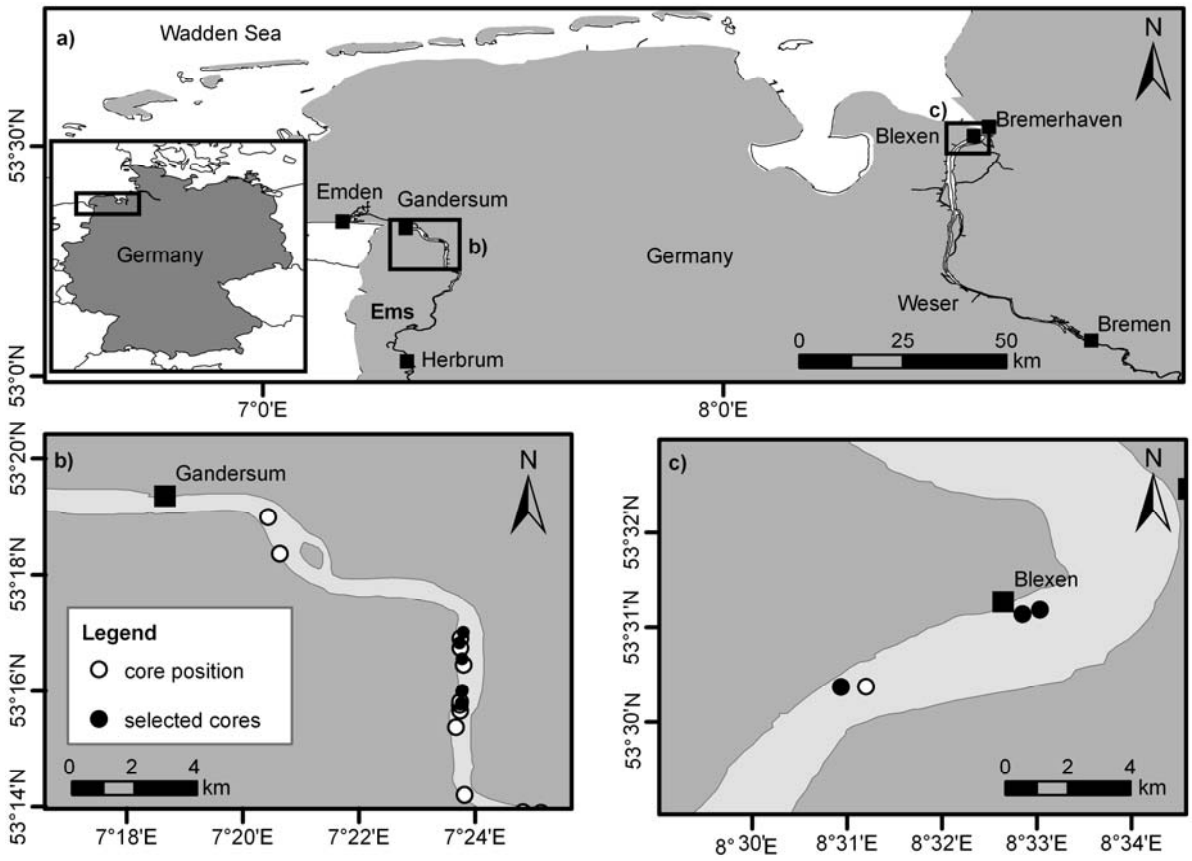

Figure 6.1: *Location of the study areas along the German North Sea coast (a). Detailed charts of the study areas within the Ems (b) and Weser (c) estuaries showing sample positions. Black circles highlight the cores which were used for SSC-normalization in Figure 6.3.*

proximity (Table 6.2). The long-term, mean, annual, freshwater discharge amounts to 326 m^3/s in the Weser estuary and 80 m^3/s in the Ems estuary (NLWKN, 2009). Average current velocities in the Weser estuary range from 1 to 1.3 m/s; maximum values of 2.6 m/s are achieved during the ebb-tidal phase (BfG, 1992). Average current velocities in the Ems estuary are considerably lower, rather site-specific, and variable in dependence on freshwater discharge (Spingat and Oumeraci, 2000). Thus, maximum current velocities around 1 m/s occur near Herbrum, Germany, only during periods of high freshwater discharge (Spingat and Oumeraci, 2000). Overall, the current velocity decreases slightly downstream because of the widening of the channel cross-section (Spingat and Oumeraci, 2000). Both the Weser and Ems estuaries are partially mixed and exhibit well-developed TMZs extending to the low-salinity reaches located around Blexen, Germany, in the case of the Weser estuary, and around Gandersum, Germany, in the case of the Ems estuary (Figures 6.1 a–c). The TMZ of the Weser estuary extends 15–20 km (Grabemann and Krause, 2001), whereas that of the Ems estuary extends for more than

60 km (van de Kreeke, Day, and Mulder, 1997). Values of SSC in the water column of the TMZs differ markedly between the estuaries. Thus, in the fairway of the Weser TMZ, the SSC ranges between 0.03 and 1.5 g/L (Grabemann and Krause, 2001), with average values of 0.13 g/L (Schuchardt, Haseloop and Schirmer, 1993). The Ems TMZ, by contrast, has experienced a dramatic increase in SSC during the past few years (de Jonge, 1983). Whereas a maximum value of 0.4 g/L in the water column was measured in 1988 (de Jonge, 1988), the SSC has risen by more than 1 g/L in only 12 years (Spingat and Oumeraci, 2000), reaching values up to 1.6 g/L SSC in 2005 (Wurpts and Torn, 2005).

The riverbed morphology of the Weser TMZ reveals a complex bathymetry comprising stretches of smooth bed, subaqueous dunes of varying size and shape, as well as dredged areas riddled with large dredge scours (Schrottke et al., 2006). Bottom sediments are mainly characterised by mud and fine- to coarse grained sands, whereas the mud content locally reaches 98% (Schrottke et al., 2006). Mud deposits are in variable states of consolidation, ranging from very fluid to highly compacted (Schrottke et al., 2006). Organic-rich sediments, such as peat, outcrop at some locations, in particular near the riverbanks (Schrottke et al., 2006). Outside of the Weser TMZ, bottom sediments in the fairway generally consist of fine to medium sand with clay and silt contents < 1% and POM contents < 0.1% (Grabemann and Krause, 1989, 2001). In the case of the Ems estuary, most of the information on morphology and sediment composition is limited to the lower estuarine section, where 85% of the area is covered by tidal flats (de Jonge, 1988). Surface sediments are mainly composed of very fine to fine sand containing abundant peat debris. The clay content varies between 0.3 and 3.5%, increasing toward the shores (de Jonge, 1988).

Fluid mud deposits are regularly observed in both estuaries during slack-water, but they vary with respect to spatial distribution and thickness (Schrottke et al., 2007). In general, fluid mud coverage and thickness is small in the Weser estuary, compared with the Ems estuary, where deposits occur throughout the TMZ and reach thicknesses of up to 6 m (Schrottke et al., 2007).

Table 6.2: *Environmental data from the German Weser and Ems estuaries.*

	Weser	**Ems**
estuary type:	coastal plain	coastal plain
length:		
total	477 km (*1)	370 km (*1)
tidal influenced part	~120 km (Intschede - Wadden Sea)	~100 km (Herbrum - Wadden Sea)
shape:		
upper estuary	channel-like (Bremen – Bremerhaven)	channel-like (Herbrum – Pogum)
lower estuary	funnel-shaped, double channel (Bremerhaven – Wadden Sea)	funnel-shaped (Pogum – Wadden Sea)
Navigation depth: channel like section at low-springs	9 m (*2)	5.7 m (*3)
tide:	semidiurnal ebb-dominated	semidiurnal flood-dominated
range changes	0.13 m (1882) – 4 m (1990) (*4)	2.9 m (1981) – 3.7 m (1998) (*6)
mean range	~4 m (Bremen; macrotidal) (*5) ~3.6 m (Bremerhaven; mesotidal) (*5)	3.8 m (mesotidal) (*6)
freshwater discharge measured at…:	…Intschede	… Versen
Mean (MQ)	326 m^3/s (*7)	80 m^3/s (*7)
Low mean (MLQ)	117 m^3/s (*7)	16 m^3/s (*7)
High mean (MHQ)	1,230 m^3/s (*7)	373 m^3/s (*7)
currents:		
mean velocity	1-1.3 m/s (*4)	location specific
maximum velocity	2.6 m/s (*4)	1 m/s (*8)
TMZ:	partially mixed	partially mixed
length	15-20 km (*5)	> 60 km (*9)
location	around Blexen	around Gandersum
SSC in TMZ:		
range	0.03 – 1.5 g/l (*10)	up to 1.6 g/l (*12)
mean	0.13 g/l (*11)	0.9 g/l (*12)
bed morphology:	*TMZ:* smoothed bed, dredged areas with dredge scours, subaqueous dunes (*2)	*lower Ems:* tidal flats (*13)
bottom material:	*TMZ:* mud (up to 98% of total sediment), fine-coarse sand (*2) *outside TMZ:* fine & medium sand (silt & clay < 1%, organic matter < 0.1%) (*5,10)	*lower Ems:* very fine-fine sand clay (0.3 – 3.5%) (*13) partly peat
fluid mud:		
distribution	extensive areas in the central section of the TMZ; patchy, in dune troughs throughout the whole TMZ	as layer in the whole TMZ
thickness	cm –metres (*2)	up to several metres (*14)

(*1) Seedorf and Meyer (1992), (*2) Schrottke *et al.* (2006), (*3) Schuchardt *et al.* (2007), (*4) BfG (1992), (*5) Grabemann and Krause (2001), (*6) Jürges and Winkel (2003), (*7) NLWKN (2008), (*8) Spingat and Oumeraci (2000), (*9) van de Kreeke *et al.* (1997), (*10) Grabemann and Krause (1989), (*11) Schuchardt, Haseloop and Schirmer (1993), (*12) Wurpts and Torn (2005), (*13) de Jonge (1988), (*14) Schrottke *et al.* (2007)

6.3: Methods and data base

This study is based on samplings using a Rumohr-type gravity corer. The mechanism is described in detail in Meischner and Rumohr (1974). Specially designed, transparent Perspex core barrels 2–4 m in length and 8 cm in diameter were used for rapid sediment sampling at vertical intervals of 10 cm (Schrottke et al., 2006). The core barrels were fitted with 2-cm diameter holes spaced at 10-cm intervals for sampling. Before deployment, the holes were sealed by tape and consecutively numbered from top to bottom. Depending on the flow regime, weights of 25 to 50 kg were used for gentle, vertical penetration of the core barrel through the near-bed suspensions and into the riverbed. After recovery, the core was immediately sampled from top downward to avoid sediment settling and consolidation. Depending on sediment density and viscosity, samples were transferred into bottles or bowls by means of polyethylene hoses or syringes. In the case where consecutive core sections had consistently low SSC values, only one large subsample was taken (Schrottke et al., 2006). Immediately on core retrieval, the temperature and salinity of the samples with SSC values below 500 g/L were measured using a multimeter of the type 'Cond 340i' by WTW (Weilheim, Germany). In the laboratory, subsamples were analysed for SSC, POM content, viscosity, and grain-size distribution. The SSC values were recorded as dry weight per unit sample volume. Depending on the sample consistency, an aliquot was prepared for vacuum filtration using a glass fibre filter (pore diameter 1.2 µm) or by taking 2 ml of consolidated sediment. In a next step, the aliquot was dried for about 12 hours at 60°C. After weighing, the dried samples were analysed for POM content by weight-loss on ignition, leaving only the clastic mineral components (Dean, 1974). This was done by combustion in a muffle furnace at 550°C for 2 hours and 6 hours, respectively.

A rotational rheometer of the Haake 'Rotovisco® RV20' (Berlin, Germany) equipped with a M5 Searle measuring system was deployed for viscosity measurements. To reduce the risk of wall slippage and to minimize sample and structure disturbance during tool insertion and measurement, a four-bladed vane tool (diameter = 36.0 mm, height = 20.0 mm) was used. Assuming a linear shear rate in the gap between the vane tool and the cup, the cup diameter (diameter = 39.0 mm) was selected to be slightly larger than the chosen vane. Approximately 24 ml of sample, just enough to cover the

vane tool, was used. Before the measuring procedure, the samples were left to adjust to a temperature of about 20°C and were then thoroughly shaken for complete dispersal. A controlled shear rate (CSR) test was carried out for the determination of viscosities (Mezger, 2000). For that test, the vane tool was rotated by an electrical motor with a shear rate of 0.548 s^{-1}. To determine flow behaviour, the shear stress was measured for shear rates between 0.07 and 30 s^{-1}. Reproducibility measurements were only carried out above 0.14 Pa·s and 20 g/L SSC, respectively.

Grain-size analyses were performed using an autonomous settling tube of the 'MacroGranometer™' (Neckargemuend, Germany) type (height = 1.8 m; diameter = 0.2 m) to analyse grain sizes in a range between 5 and 22 φ (Brezina, 1979, 1986). Grain-size classes from 10.75 to 4 φ were analysed by the x-ray–based SediGraph particle analyser (types '5100™' and '5120™'; Micromeritics Instrument, Norcross, Georgia). Both methods include grain characteristics such as particle shape and density as well as fluid density and viscosity (Flemming and Thum, 1978). An undisturbed, individual, particle-settling process was assumed throughout a turbid-free liquid (Syvitski, Asprey, and Clastenburg, 1991). Before analysis, the samples were desalinated and separated in mud and sand fractions by wet sieving. POM was removed by treatment with 35% hydrogen peroxide. The sand fraction was additionally treated with 25% hydrochloric acid for the destruction of the carbonate fraction. A representative split of 0.5–1.0 g was used for analysis in the settling tube. For SediGraph measurements, 4–6 g of the sample was transferred into a 60–80-ml sodium pyrophosphate (0.05%) sedimentation liquid. Any remaining aggregates were dispersed by ultrasonic treatment in a bath where sample material is simultaneously heated up to a measuring temperature of 36.5°C.

The data sets were based on five surveys carried out with the research vessel Senckenberg during the periods 27–28 September 2005 (Ems, neap tide 25 July), 20–27 September 2006 (Ems, neap tide 22 September), 13–14 March 2007 (Weser, neap tide 12 March), 13–20 June 2007 (Ems, spring tide 15 June), and 17 July 2007 (Weser, neap tide 14 July). Samplings represent different sites within the TMZs of the Weser and the Ems estuaries (Figures 6.1 b and c). Altogether, 26 cores with a total amount of 445 subsamples were analysed.

A hierarchic cluster analysis was used to group similar sedimentological and rheological properties. Squared Euclidean distances among SSC, viscosity, POM, and mud : sand wt% free statistical software 'R' (Version 2.13.0). Grain-size parameters were not considered in the cluster analysis because, in some cases, not enough material was available for grain-size measurements.

One important requirement for comparison of down-core trends is normalization. Core-to-core comparisons concerning sedimentological and rheological parameters were normalized to a single parameter, as shown schematically in Figure 6.2. Normalization took place by, e.g., sorting parameter B based on parameter A, keeping the descending order of each sampled core section. Parameter similarities, which would not occur without this procedure (Figure 6.2 a), are highlighted after data processing (Figure 6.2 b). It is important to note that processed data no longer indicate the actual retrieval depth but still reflect the sequence number.

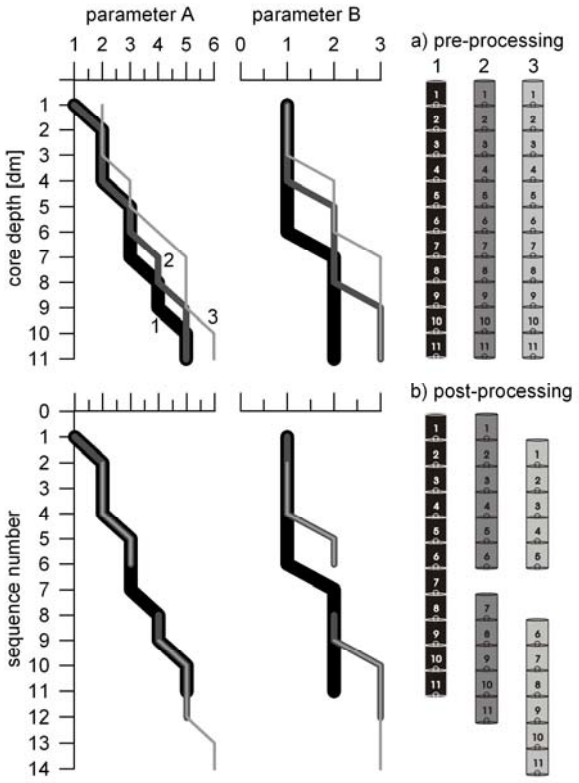

Figure 6.2: *Data processing scheme for normalized parameter comparison: a) Pre-processing: Parameters A and B of cores 1-3 plotted over depth. No obvious similarities can be identified. b) Post-processing: core data normalized to parameter A. Similarities with parameter B are now apparent.*

6.4: Results

The SSC-normalized, depth-related variations of viscosity, POM, and mud : sand wt% ratio are reflected in comparative plots as shown in Figures 6.3 a–e. The data predominately reflect a down core increasing SSC, viscosity, and sand wt% as well as decreasing POM and mud wt% (Figure 6.3). The affiliation toward the clusters is represented by different symbols in Figure 6.3. In all, four clusters with different sedimentological and rheological characteristics were identified with the cluster analysis. Upper and lower limits, as well as median values and upper and lower quartiles, are represented by the box plots in Figure 6.4.

Cluster one represents less-concentrated, suspended-sediment samples (Figure 6.4 a). These predominately consist of very poorly sorted, polymodal mud ranging from clay to medium sized silt particles with a prominent peak at 6.5 φ. Samples with SSC > 100 g/L in parts represent small amounts of well to very well sorted, unimodal, very fine sand fractions with a peak at 3.3 φ. Up to 20 wt% of the sample material was of organic origin. Whereas the POM contents (wt%) do not correlate with SSC, the absolute POM concentration (g/L) shows a positive linear correlation, as expressed in Figure 6.5. With increasing SSC, the viscosity also increases (Figure 6.6) but in an exponential manner (Weser estuary: viscosity = exp(0.013 × SSC) × 0.094, R^2 = 0.8, n = 33; Ems estuary: viscosity = exp(0.020 × SSC) × 0.091, R^2 = 0.8, n = 155). The degree of dispersion for SSC, viscosity, POM, and mud : sand ratio is quite low, which can be seen by the lower and upper quartiles shown in Figure 6.4. When log-scaling, the upper SSC-normalized core section reveals a jump in SSC around 10 g/L within cluster one (Figure 6.3 a).

The part of the core section dominated by cluster one coincides with a sudden increase in SSC at 200 g/L, which is underestimated by SSC normalization but is more prominent when data are not SSC normalized, as shown by the example in Figure 6.7. Below the cluster-one core section follows a section (200–500 g/L SSC) where cluster types one to three exist simultaneously. This section is characterized by very high viscosities (Figure 6.3 c). The data reveal that the material from the Weser estuary is quite different from that from the Ems estuary in viscosity relative to SSC (Figure 6.3 c). Weser estuary samples are less viscous at corresponding higher SSC values than corresponding samples

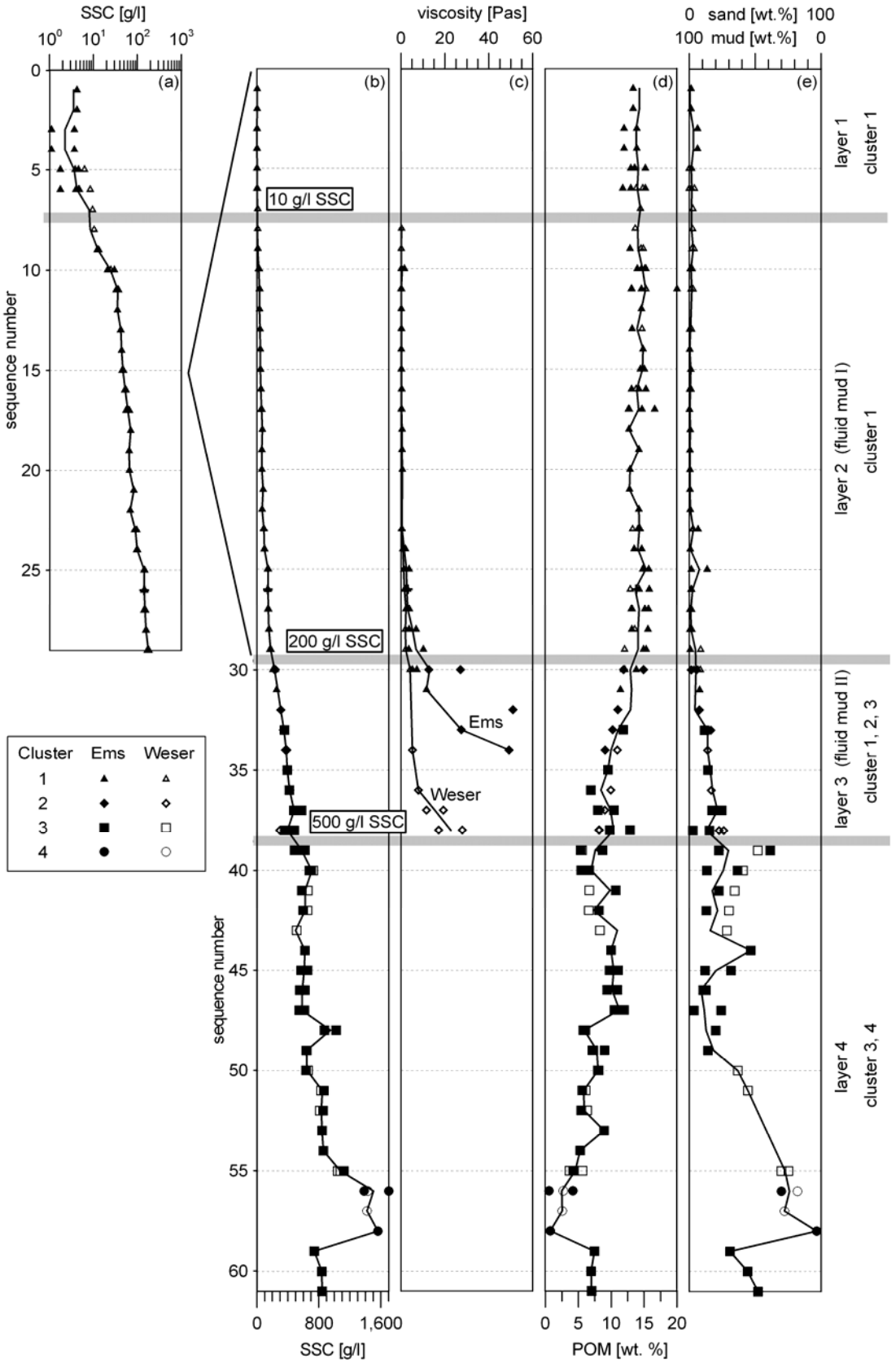

Figure 6.3: *Normalized mean down-core trends in SSC (a, b), viscosity measured at a shear rate of 0.548 s^{-1} (c), POM (d) and mud-sand content (e) based on samples from nine cores from the Weser and Ems estuaries. Left box displays SSC values of sequence numbers < 30 on a logarithmic scale. The three thick horizontal lines highlight marked changes in the boundaries of the layers 1-4. The symbols represent the cluster affiliation.*

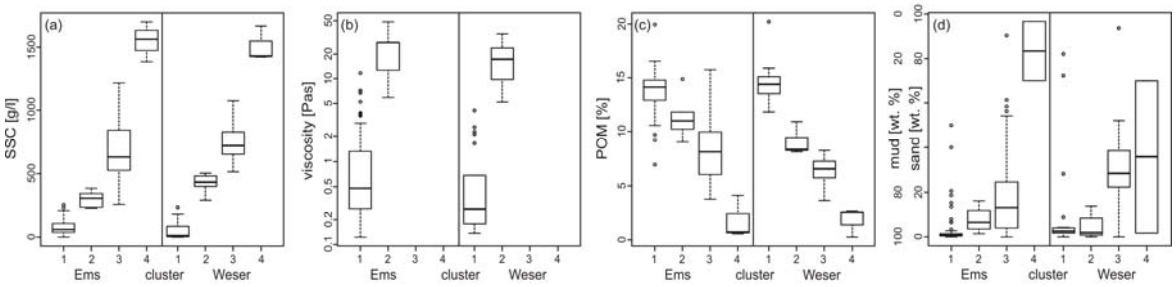

Figure 6.4: *Boxplots representing the upper- and lower limits as well as median values and upper and lower quartiles of SSC (a), viscosity measured at a shear rate of 0.548 s^{-1} (b), POM (c) and mud-sand ratio (d) for cluster 1-4 of Weser and Ems.*

from the Ems estuary, as expressed by the different exponential fits shown in Figure 6.6. Although POM and mud : sand ratios are relatively constant in the section dominated by cluster one (< 200 g/L SSC), both parameters decrease with increasing SSC in the section between 200 and 500 g/L SSC. The change in mud : sand ratio is also reflected in the grain-size distribution (Figure 6.8). Thus, the mud fraction around 6.5 φ (medium silt) is slightly diminished, whereas the coarse silt fraction (5–6 φ) is enriched. At the same time, the sand fraction has a second subordinate peak around 2.1 φ, at least in the case of the Ems estuary samples. This secondary peak is not present in the sand fractions of the Weser estuary.

Samples with SSCs > 500 g/L are dominated by clusters three and four. Typical for these clusters are the missing viscosity data. Rheological measurements were no longer

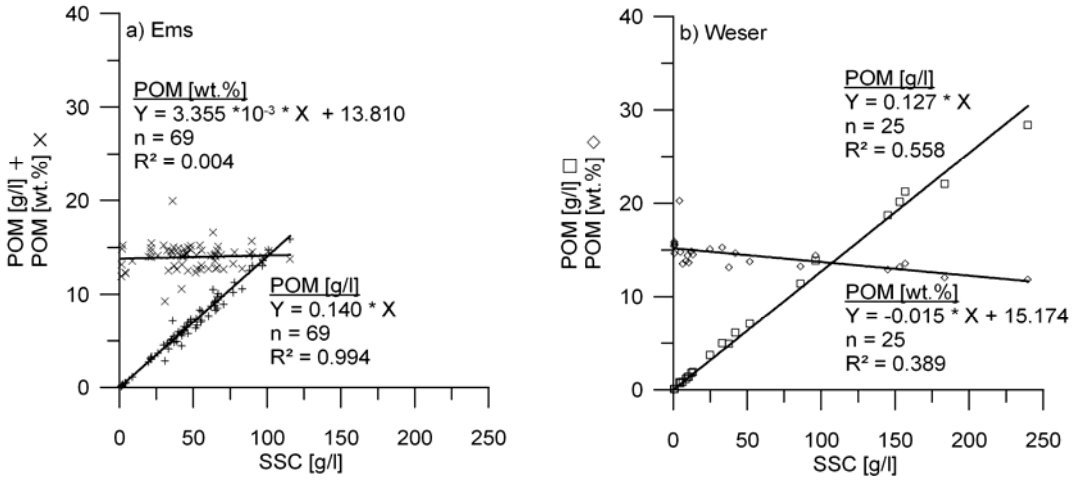

Figure 6.5: *Correlations between POM and SSC for samples of cluster one of the Ems (a) and the Weser (b).*

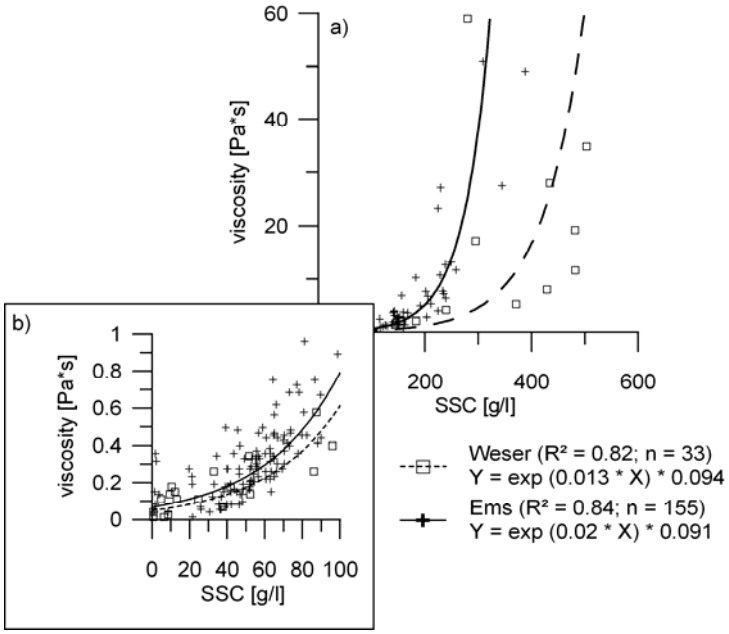

Figure 6.6: *Correlations between viscosity (measured at a shear rate of 0.548 s^{-1}) and SSC, based on 33 samples from 4 cores in the case of the Weser, and 155 samples from 23 cores in the case of the Ems. a) Entire data set; b) Blow-up.*

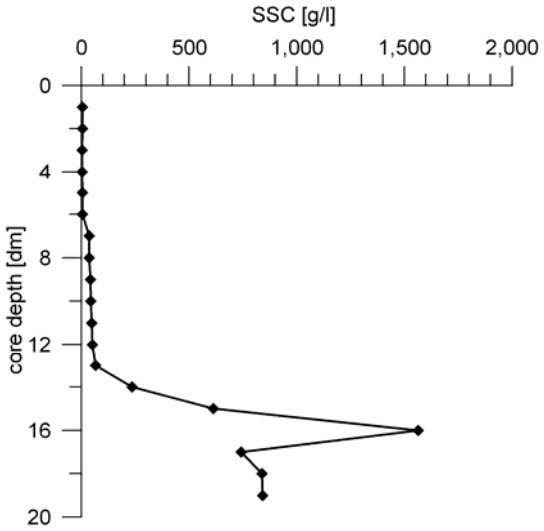

Figure 6.7: *Down-core trend of SSC of a selected core with a rapid increase in concentration at 200 g/l.*

possible on the semisolid samples because friction, caused by high SSCs and sand contents, exceeded the maximum torque of the rheometer. Mud : sand ratios are highly variable in these samples, varying from 80 : 20 to 50 : 50 wt% with increasing SSC. Samples from the lowest part of this core section could even be completely composed of

sand. In that case, POM was almost absent. In general, the contribution of finer silt sizes to the mud fractions from this layer increases up to 8%. Fine sand (2.1 φ) is also well represented. A third-intermediate population peaks at 2.6 φ. The POM and mud : sand ratio are highly variable.

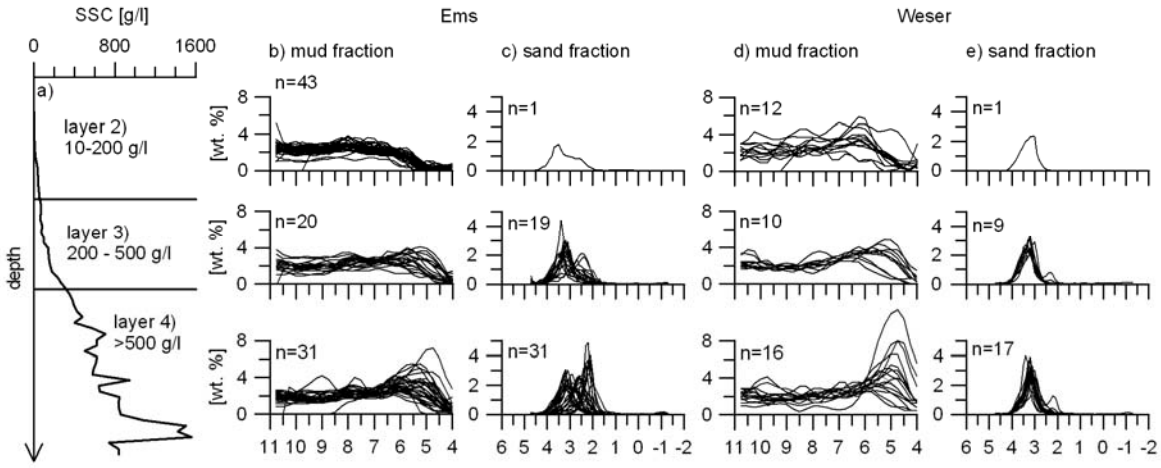

Figure 6.8: *Depth- and SSC-related classification of estuarine near-bed cohesive sediments (a) and corresponding grain-size distributions of the mud (b, d) and sand fractions (c, e) of samples from eleven cores from the Weser and the Ems estuaries. The SSC curve represents mean SSC-values of samples from the Weser and Ems.*

Salinity, temperature, and flow behaviour were not considered so far. Sample temperatures range between 9.5°C and 24.1°C, although there are no systematic depth-related changes recognisable. Temperature differences between the cores reflect seasonal changes. Tide- and lunar-induced temperature variations are not obvious. Salinities ranged between 1 and 7 with no site-specific differences. Generally, salinity decreases downcore. Stratification of near-bed water masses is indicated at some locations. Neither tidal and lunar phases nor seasonal variations are evident in the salinity data.

The flow behaviour is selectively shown in Figure 6.9 for two samples from the Ems estuary, one having an SSC of 99 g/L, the other of 258 g/L. The low-SSC sample shows pseudoplastic behaviour (shear-thinning) for all shear rates, whereas the high-SSC sample indicates different flow behaviours when subjected to changing shear rates. In the latter case, pseudoplastic flow changes to dilatant (shear-thickening) flow at shear rates between 0.22–0.71 s^{-1} and 0.91–3.29 s^{-1}.

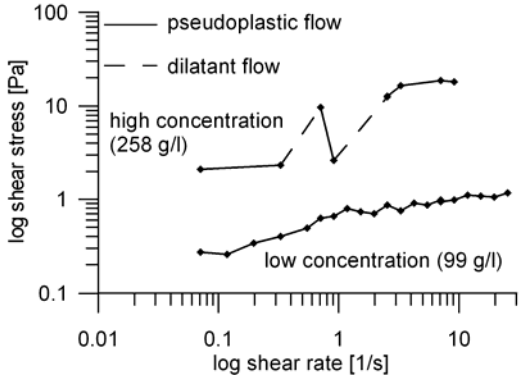

Figure 6.9: *Comparison of flow behaviour of samples having different SSC values of 99 g/l (lower curve) and 258 g/l (upper curve).*

6.5: Discussion

The vertical distribution of SSC varies by up to four orders of magnitude between the top and bottom of cores from the Weser and the Ems estuaries. This is in accordance with the three layer models often applied to high-energy environments (e.g., Nichols, 1984). However, after SSC normalization and consideration of different sedimentological and rheological properties, down-core trends indicate at least four layers as also identified in the cluster analysis.

The first layer (< 20 g/L SSC) (Figure 6.3) is comparable to the highly concentrated, Newtonian sediment suspension defined in three-layered models (e.g., Winterwerp and van Kesteren, 2004). High organic contents and a lack of silt- and sand-sized particles suggest flocculation processes associated with accelerated settling velocities and enhanced settling rates, particularly under slack-water conditions as also observed by Dankers and Winterwerp (2007). The relatively large variance in SSC within this layer is probably related to variable environmental conditions where stress history and flow regime have a significant influence on the process of hindered settling. Under turbulent conditions SSC has to be higher before floc settling changes from free to hindered settling rates. The interface between layers one and two (Figure 6.3) represents the upper fluid–mud boundary, which is characterised by a rapid change in concentration between 5 and

20 g/L SSC. With the occurrence of steep concentration gradients, the development of a strong shear-flow zone is reported (Mehta, 1991). Whether this also applies to the upper fluid–mud boundary in the Weser and Ems estuaries cannot be currently verified because no reliable viscosity data exist for SSCs below 20 g/L. In the present study, samples with more than 20 g/L SSC were defined as fluid mud when they indicated the appropriate flow behaviour during sampling and where viscosity measurements were possible.

The lower fluid mud boundary is set to 500 g/L SSC because samples with higher SSCs are not applicable for viscosity measurements, which fits well with results of other studies (see Table 6.1), where this boundary is commonly defined by the concentration at which the shear flow becomes zero (Mehta, 1991; Ross and Mehta, 1989). In addition, the grouping in the cluster analysis changes at this concentration level. The POM contents and mud : sand ratio show high standard deviations and at least one new grain-size population with a peak around 2.1 φ in the case of the Ems estuary samples.

However, the results of the cluster analysis, the flow behaviour, and the SSC normalisation suggest that two types of fluid mud exists, comprising layers two and three (Figure 6.3). Layer two identified in this study represents low-viscosity, fluid mud (I) with the exclusive characteristics represented by cluster one samples, whereas layer three represents high viscosity, fluid mud (II) comprising samples of clusters one, two, and three. Furthermore, measurements of shear stress at different shear rates show that the flow behaviour changes with increasing SSC. Thus, the less-concentrated, pseudoplastic, fluid mud sample with 99 g/L SSC (Figure 6.9), representing layer two, consist of fluid-supported particle assemblages, the loose flocculent particle structure of which will already be broken down by low shear rates, as also reported by Faas (1981). In contrast, the more-concentrated, fluid mud sample with 258 g/L SSC (Figure 6.9), representing layer three, seems to be a more grain-supported assemblage, where the shear rate defines the flow behaviour. The anomalous point in this plot can be explained by a viscosity notch, sensu Faas (1981). At low shear rates, the particle structure is broken down, as observed in the case of the less-concentrated sample, but particles subsequently reorient themselves to a parallel alignment with closer packing (Faas, 1981). This causes temporary shear thickening, until the particle structure again breaks down at higher shear rates. However, merely two flow behaviour measurements are not sufficient

to accurately determine the precise SSC value at which the flow behaviour of the fluid mud actually changes.

Looking at the viscosity in relation to SSC, a steep increase is apparent around 200 g/L SSC (Figure 6.6). It can be assumed that this increase in viscosity is related to the development of the space-filling concentration at which the suspended sediment begins to build up a network structure, as mentioned by van Maren et al. (2009), thereby, causing the change in flow behaviour. These observations are underpinned by rheological investigations on fluid mud carried out on the NE continental shelf of Brazil by Faas (1984). In that study, the changing particle structure is the cause for a change in flow behaviour. However, with a concentration of approximately 100 g/L, the space-filling concentration on the Brazil shelf is clearly higher than that in the Weser and Ems estuaries. A comparison of the two German estuaries reflects highly site-specific viscosity differences. Similar observations are made in the Gironde estuary in France by Granboulan et al. (1989), where viscosity differences at similar SSC values are induced by different sedimentological compositions. Although differences in the grain-size compositions of the suspended sediments from the Weser and Ems estuaries do exist, it cannot be finally ascertained whether grain size is the decisive parameter because the differences are very small. Possible additional factors, which have not been investigated in this study, may be the type of clay that controls the cohesiveness of the material (Mehta, 1989) or the type of POM, which may also influence the internal friction (de Jonge and van den Bergs, 1987).

Normalization of SSC measurements and cluster analysis not only reveal the relationship between viscosity and SSC but also a significant SSC dependence on grain size. Because aggregates containing larger particles, such as silt or fine sand, settle out first (Krone, 1993), a gravitationally induced down core coarsening takes place. An increase in grain-size composition with increasing SSC was also reported in the findings of Kranck et al. (1993). The shifts in grain size, as observed between 5–20 g/L SSC (interface between layers one and two) and 200 g/L SSC (interface between layers two and three), are related to the lutocline and the space-filling concentration, respectively, where the denser particle-supported framework structure promotes the incorporation of coarser material. This fits with the findings of Manning, Langston, and Jonas (2010), who observed that silt- and sand-sized particles increase the bounding potential of clay and the internal friction.

Also, in layer three (200–500 g/L), an increase in internal friction by increased sand content and grain size is responsible for viscosity changes. Particularly at the boundary of layers two and three, this effect is very obvious because a mud : sand ratio up to 50 : 50 cause excessive grain-to-grain friction and, thereby, prevent viscous behaviour. From Mitchener and Torfs (1996), it is known that a mud : sand ratio of 50 wt% can raise the erosional shear stress by a factor of two. In addition, internal friction will increase when the effect of lubrication diminishes with decreasing POM content, as shown by Wurpts (2005). Compaction, as a possible cause, can be excluded because samples were remoulded before measurements.

In the present case, it would appear that the low-viscosity fluid mud (I) and the high-viscosity fluid mud (II) have different sources. The composition of fluid mud (I) suggests that the material in that layer originates from the uppermost parts of the highly concentrated suspension of layer one, which has the characteristics defining cluster one. By contrast, fluid mud (II), which is characterized by three different clusters, can be generated in two different ways. On the one hand, it could be generated by consolidation of fluid mud (I), on the other, by the resuspension of the upper part of layer four. It can be assumed that the upper part of layer four is still susceptible to erosion, whereas the lower part of layer four represents the consolidated permanent bed, containing silt lenses or even extensive layers of coarser material. It is suggested these structures are generated by different flow regimes related to the neap-spring tidal cycle or seasonal events, such as increased freshwater discharge.

6.6: Conclusion

The deployment of a specially adapted Rumohr-type gravity corer enabled the simultaneous sampling of suspended sediment, fluid mud, and the underlying bed of consolidated mud at a higher vertical resolution (10 cm intervals) than in previous studies on fluid mud. On this basis, the comparison between SSC-normalized sedimentological and rheological parameters, supported by a cluster analysis, shows that the conventional three-layer model, as often used to describe vertical, cohesive sediment distributions in high-energy environments, such as estuaries, is evidently incomplete. The present study

shows that a low-viscosity and a high-viscosity layer can be distinguished within the fluid mud, provided that in situ measurements are sufficiently resolved vertically. The most important findings of this study can be summarized as follows:

- Layer one: Sediment suspensions < 20 g/L SSC of cluster one samples are linked to flocculation processes leading to enhanced, but free-settling, particles in a Newtonian fluid.

- Layer two: Low-viscosity fluid mud (I) of 20–200 g/L SSC, is composed of the same cluster of layer one but with fluid supported particle assemblages that show pseudoplastic flow behaviour caused by the onset of hindered settling.

- Layer three: High-viscosity fluid mud (II) of 200–500 g/L SSC occurs where the space-filling concentration is exceeded and the particle framework structure is grain supported. The flow behaviour changes between pseudoplastic and dilatant in dependence on the shear rate. The grouping into clusters one to three indicates the transition from low viscosity fluid mud to a cohesive or consolidated mud bed.

- Layer four: Cohesive or consolidated bed > 500 g/L SSC, with characteristics of cluster three and four, evolves from the consolidation of fluid mud containing silt and fine sand, the latter also occurring in the form of layers or lenses representing different flow regimes.

- Fluid mud (II) is suggested to represent recurrent, cohesive sediment accumulations, which frequently have to be dredged in harbours and shipping channels to maintain safe navigation depths. Therefore, new approaches to model fluid mud dynamics in greater detail would also serve to optimize dredging activities. Such models should include the two fluid mud layers as outlined in this study.

Acknowledgements

The authors would like to thank the captain and crew of the research vessel Senckenberg for their excellent work and inexhaustible patience during the acquisition of the data sets for this study.

The assistance of N. Mahnken, A. Raschke, C. Schollenberger, and all their trainees in the laboratories of the Senckenberg Institute, Wilhelmshaven, is also gratefully acknowledged. Furthermore, we wish to thank the working group ‘‘Marine Engineering Geology’’ at the University of Bremen for fruitful discussions and for providing the rotational rheometer. We also thank the reviewers for their helpful critiques and contributions. This study was funded by the Deutsche Forschungsgemeinschaft as part of the Research Centre for Marine Environmental Sciences (MARUM), the Senckenberg Institute who provided the ship time, and the Cluster of Excellence ‘The Future Ocean’ in Kiel.

Chapter 7: The use of acoustic interfaces for the quantification of the fluid mud boundary in the Weser and Elbe estuaries (Germany)

Abstract

Standard hydroacoustic devices often have in environments with high suspended sediment concentrations (SSCs) problems detecting the bottom depth correctly. In these cases large SSC-gradients (lutoclines) generate an acoustic reflector within the water column. So far, it is assumed that the strength of the acoustic interface reflects the density gradient at these interfaces.

In this study a relation between the amplitude of the acoustic interface (measured with the low frequency channel of a parametric sediment echo sounder, 'SES-2000® standard' by Innomar Technology GmbH (Warnemünde, Germany) and the SSC-gradient (sampled with a Rumohr-type gravity corer) is used to quantify the acoustic interfaces observed in the turbidity maximum zones of the Weser and Elbe estuaries. They are detectable when the SSC-gradient is > 23 g/l over a distance of 10 cm. The Rumohr-type gravity core samples indicate that the interfaces within the water column coincide with the upper boundary of so called fluid mud accumulations. Interfacial mixing at the fluid mud boundary can be shown by decreasing SSC-gradient with progressing tidal currents but significant changes in SSC-gradient do not occur until one hour after slack water in areas of smooth bed morphology. In areas where fluid mud accumulations of several metres were observed, consolidation of incomplete resuspended accumulations generates additional acoustic reflectors within the fluid mud layer. It is suggested that these reflectors represent the recurring, consolidated mud accumulations which reduce the navigable depth and lead to regular, cost intensive dredging activities.

Keywords: *sediment echo sounder, acoustic interfaces, amplitude, SSC, fluid mud, interfacial mixing*

7.1: Introduction

In hydrodynamic environments with high Suspended Sediment Concentrations (SSCs) it has been observed that standard depth measurements (e.g. echo sounding, density or nuclear density probes) 'will generally not correlate with one another, or perhaps not even give a consistent reading from one time to the next when the same type of instrument or technique is used.' (USACE 2002). In these cases, so called fluid mud accumulations are often present. Generally, they are described as a network of water, clay, silt and Particulate Organic Matter (POM) and can reach SSCs of up to 500 g/l (Papenmeier et al. 2011, chapter 6). The water-fluid mud boundary (around 20 g/l) is associated with a lutocline (Papenmeier et al. 2011, chapter 6) which can cause an acoustical impedance.

In estuarine environments, the appearance of lutoclines associated with fluid mud and the strength of the related acoustic reflector is changing over a tidal cycle (Becker 2011, Schrottke et al. 2006). In the Weser estuary for example, lutoclines were mainly found in the dune troughs of the Turbidity Maximum Zone (TMZ) from 1.2 hours before slack water until 2.3 hours after slack water. Before slack water, the surface of the lutoclines is flat or slightly inclined against current direction and corresponds to a relatively weak acoustic reflector. Around slack water, the reflectors become more flat and stronger than before. With increasing current velocity the strength of the acoustic interface is again reduced and the slope inclines in current direction (Becker 2011). In estuarine environments with extremely high SSCs, for example the Ems estuary (here: mean SSC is up to 1.6 g/l; Wurpts & Torn 2005), lutoclines can also be present during the whole tidal cycle (Held pers. communication). Here, the surface geometry of the lutoclines responds to the tidal forcing. Internal waves are present for nearly the whole tidal cycle except at high water slack. Maximum wave heights of up to 1.3 m were observed shortly after the maximum ebb current (Held pers. communication).

The acoustic strength of the reflector is interpreted to reflect the density gradient between the fluid mud layer and the water column above (Becker 2011). For the Weser estuary, SSCs of 0.3-0.5 g/l within in the layer above and a maximum SSC of 27-70 g/l SSC within the layer below the lutoclines have been reported (Becker 2011). How large the

SSC-gradient directly at the lutocline is and if a correlation between the acoustic strength and the SSC-gradient does exist has so far not been described. Moreover, possible changes of material properties at the lutocline such as grain size, which also influence the acoustic reflection characteristic of suspended sediments, are not known (USACE 2002).

The quantification of the relation between the acoustic strength and the SSC-gradient can give useful information about the accumulation and resuspension processes of fine cohesive sediments and can therefore improve expensive dredging activities in navigation channels and harbours. In this study, parametric sediment echo sounder records and Rumohr-type gravity core samples are used to describe the relation between the amplitude and the SSC-gradient at the acoustic interfaces within the water column as well as to describe their temporal and spatial distribution within the Weser and Elbe estuaries.

7.2: Regional settings

Physical settings and hydrodynamic parameters of the Weser and Elbe estuaries have been described in detail in chapter 5 and 6. The basic differences between the Weser and Elbe estuaries exist in the freshwater discharge (Weser: mean 326 m^3/s, Elbe: mean 713 m^3/s), the tidal dominance (Weser: ebb-dominated, Elbe: flood-dominated), depth of the navigation channel (Weser: 9m Elbe: 14.4 m at low-springs) and the SSC (Weser: 0.03 – 1.5 g/l, Elbe: 10-30 times the freshwater value of 0.035 g/l). The SSC increases and decreases, especially in the well developed TMZ (Weser: around Blexen, Elbe: between Glückstadt and Cuxhaven), as a function of the semi-diurnal tidal cycle modified by the spring-neap-cycle (Grabemann et al. 1995). Increased SSCs of up to some hundred grams per litre, associated with fluid mud accumulations, have been described in the Weser TMZ (Papenmeier et al. 2011, Schrottke et al. 2006) and in the harbour basin of Brunsbüttel (Elbe) (Nasner & Westermeier 2006, Nasner et al. 2007). In case of the Weser estuary fluid mud accumulations are preferentially found in subaqueous dune troughs of the TMZ whereas the fluid mud thickness, distribution and consolidation state varies within one tidal cycle (Becker 2011). Tidal induced sand dunes, often asymmetrical and superimposed by smaller ones, are the most prominent features in the strongly anthropogenically influenced navigation channels of the Weser and Elbe estuaries. In the

Weser estuary, the dunes are on average 2-3 m high and 50 m long with possible maximum heights of up to 6 m and maximum length of up to 150 m (Schrottke et al., 2006), while in comparison the dune dimensions in the Elbe estuary are on average 1.8 m high and 49 m long (maximum 100 m) (Zorndt et al. 2011). Especially pronounced are the dunes in the Weser estuary in the section south of the 'mud shoal'. The latter section is characterized by a smooth riverbed of muddy sediments and is located in the centre of the TMZ between km 55 and 58 and (BfG 2008, Schrottke et al 2006, Wellershaus 1981).

7.3: Methods

Hydroacoustic data and Rumohr-type gravity cores were taken during three cruises with the '*RV Littorina*' in the Weser estuary (03/2009, 08/2009, 03/2010) and two in the Elbe estuary (03/2009 & 08/2009). The data was recorded on the radar reference line as long as the narrow navigation channel was not restricted by commercial shipping vessels. The summer surveys took place during quite normal fresh water discharge conditions whereas high discharge events took place during the winter surveys (tab. 7.1). Spring tide took place on the 11th of March and 6th of August 2009 (Weser); neap tide conditions were present on the 7th of March 2010 (Weser) and on the 13th of August 2009 (Elbe).

Table 7.1: *Mean freshwater discharge (Q) during the survey and long time mean (1990-2010) for the survey time span at Intschede (Source: Wasser- und Schifffahrtsamt Verden) and Neu Darchau (Source: Wasser- und Schifffahrtsdirektion Nord), respectively.*

	Mean Q [m³/s]	
	survey	long time
Elbe 03/09	1697	1129
Elbe 08/09	396	402
Elbe 11/10	1504	774
Weser 03/09	641	564
Weser 08/09	117	152
Weser 03/10	650	558

The low-frequency channel (12 kHz) of a parametric sediment echo sounder ('SES-2000® standard') was used to identify the sediment surface and interfaces of acoustic impedance within the water column (see section 4.1.3). Owing to the parametric

acoustical effect has the low frequency the same narrow beam like the primary frequencies (resulting in a small footprint), short pulses and has no significant side lobes (Wunderlich et al. 2005) which improves the signal to noise ratio and results in a high vertical and lateral resolution (~6 cm, Schrottke & Bartholomä 2008). To take different gain settings as well as geometrical and physical attenuation into account, the amplitude is normalized on these factors (see section 4.1.3).

The acoustic interfaces within the water column and the water-solid bed interfaces were sampled with a special adapted light weight Rumohr-type gravity corer. Holes in 10 cm steps enabled a high vertical sampling resolution (see section 4.2.1 & 6.3). The core was mounted in a special constructed steel frame to enable sampling even at current velocities up to 1.5 m/s (details see section 4.2.1). Directly after core recovery samples were taken for temperature, salinity (see section 4.2.1), SSC, POM (see section 4.3.1) and grain size measurements (see section 4.3.2). Grain size classification is attached to the scale of Friedman and Sanders (1978) and statistical grain size data is based on Folk and Ward (1957). The SSC-gradients at the acoustic interfaces are calculated by the difference of the SSC value sampled directly above and below this interface with the Rumohr-type gravity corer. The SSCs and the underlying sediments were classified after Papenmeier et al. (2011) (chapter 6): sediment suspension (< 20 g/l), low viscous fluid mud I (20 - 200 g/l), high viscous fluid mud II (200 – 500 g/l) and cohesive or consolidated bed (> 500 g/l). Information about current velocity, magnitude and direction were obtained from a 1,200 kHz Zedhead-ADCP (RDI-Teledyne^{TM}, Poway, California) with a cell size of 50 cm (see section 4.1.2).

7.4: Results

7.4.1: Temporal and spatial occurrence of acoustical interfaces

Acoustical interfaces within the water column were recorded with the low frequency channel of the SES during all five surveys on the Weser and Elbe estuaries. At times more than one interface was observed in the lower water column (fig. 7.1). In the Weser estuary interfaces have generally been observed between km 49 (seaward reach of the ripple section) and km 76 (north of the Container Terminal, CT) (figure 7.2 a) but the

distribution depends on the location of the TMZ which is mainly related to the freshwater discharge. In figure 7.3 a & b the distribution of the interfaces during the surveys in March and August 2009 is shown. Here, they occur principally landward of Blexen, whereas in August 2009 when the fresh water discharge is low (Q = 117 m³/s) their presence reached up the seaward part of the ripple section. In the ripple section acoustic reflectors are found only within the ripple troughs (fig. 7.4). In March 2010 (fig. 7.3 c) the reflectors were observed exclusively in front of the CT where the water depth is kept by regular dredging activities always larger than 14 metres below NHN for the big container ships.

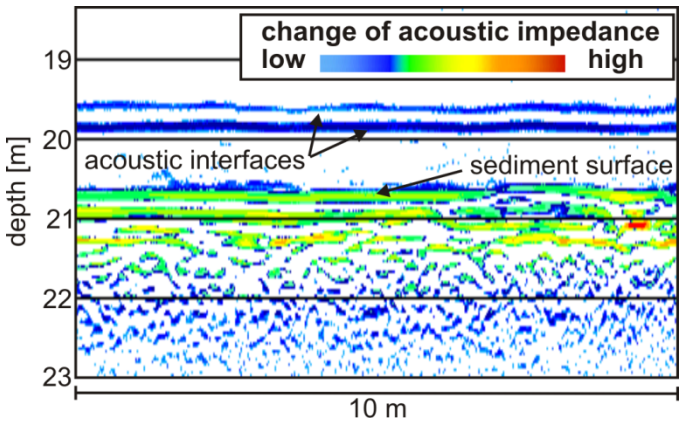

Figure 7.1: *Sediment echo sounder data (low frequency channel) with two acoustical interfaces in the lower water column.*

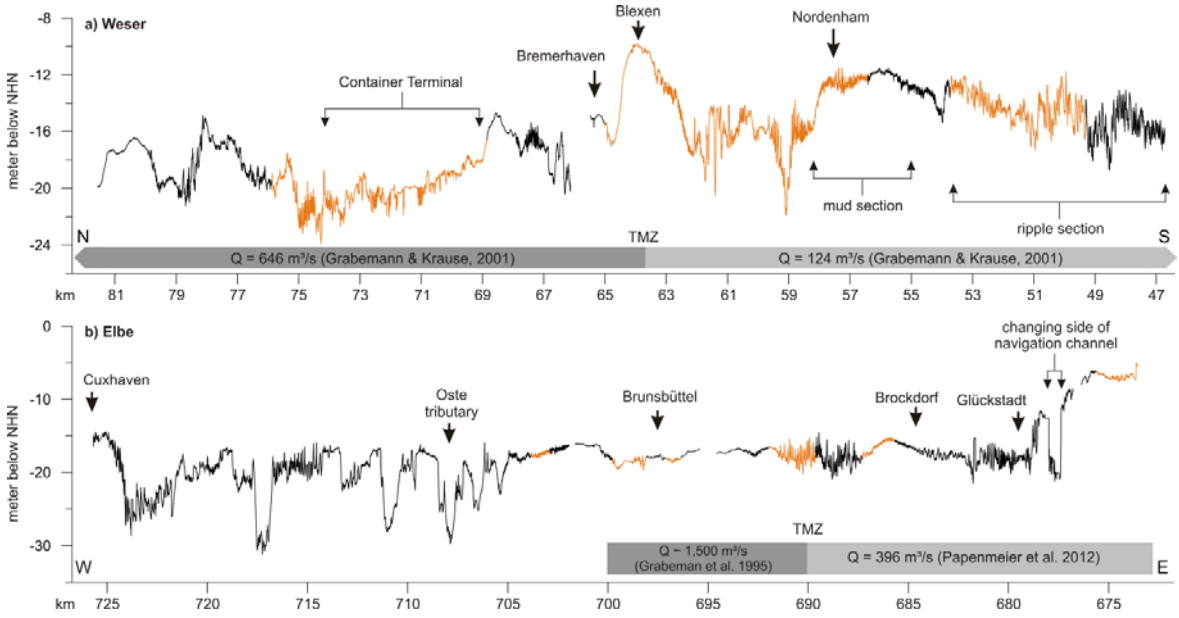

Figure 7.2: *Longitudinal bathymetric profile of the study sites a) Weser estuary and b) Elbe estuary with the spatial occurrence of acoustical interfaces (orange).*

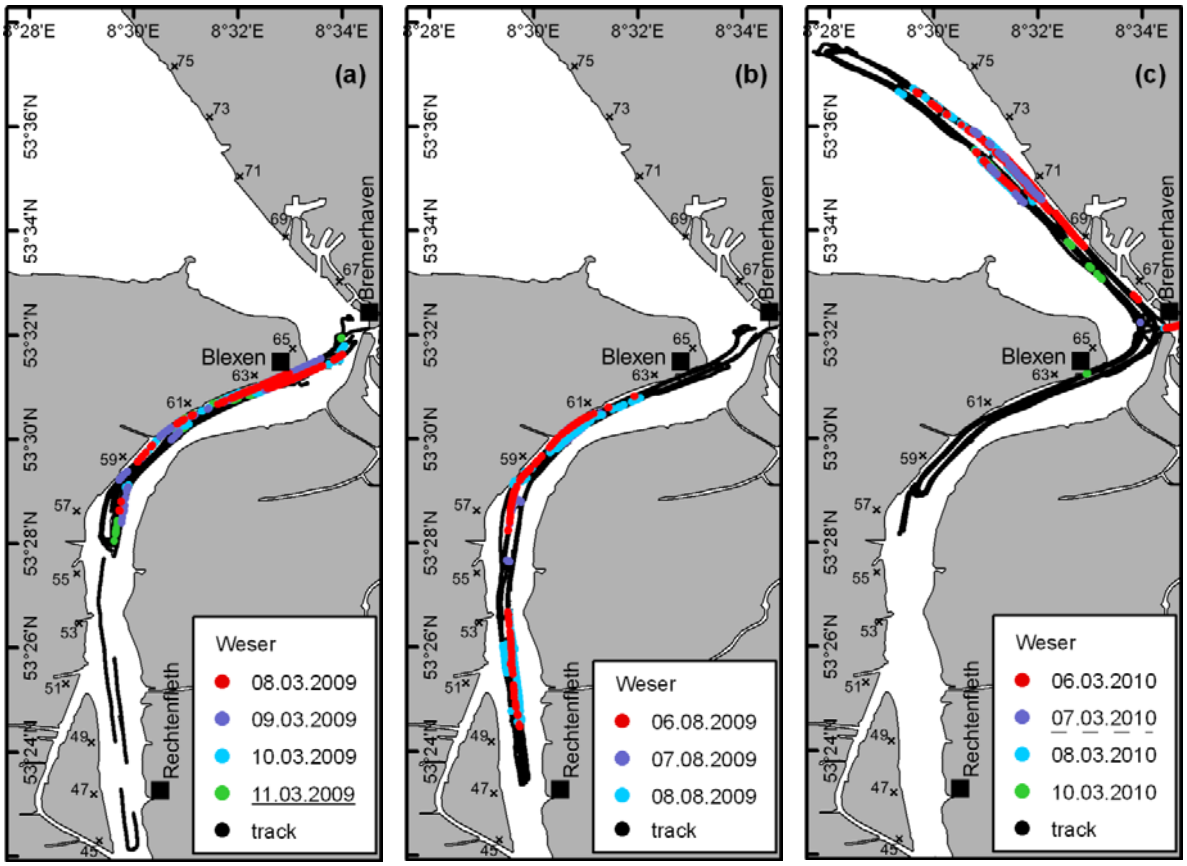

Figure 7.3: *Driven transects (black) and spatial distribution of the acoustic interfaces (coloured) for the surveys a) Weser 03/2009 (11.03.2009 spring tide), b) Weser 08/2009 and c) Weser 03/ 2010 (07.03.2010 neap tide).*

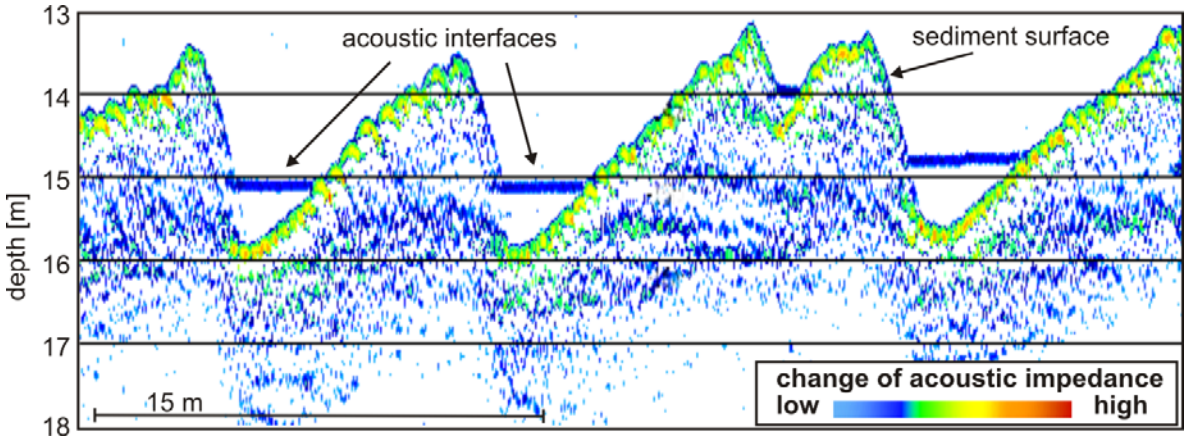

Figure 7.4: *Longitudinal profile within the ripple section of the Weser estuary recorded with the parametric sediment echo sounder (low frequency channel). Acoustical interfaces within the water column are only present in the dune troughs.*

In the Elbe estuary the occurrence of the interfaces is more infrequent than in the Weser estuary but also always related to the location of the TMZ (fig. 7.2 a). In March 2009 when the freshwater discharge is high (Q = 1697 m³/s) interfaces have been observed occasionally between Brunsbüttel and the Oste tributary (fig. 7.5 a). During a low freshwater discharge (Q = 396 m³/s, August 2009) interfaces occur in the dune section around km 690 and landward of Glückstadt (fig. 7.5 b).

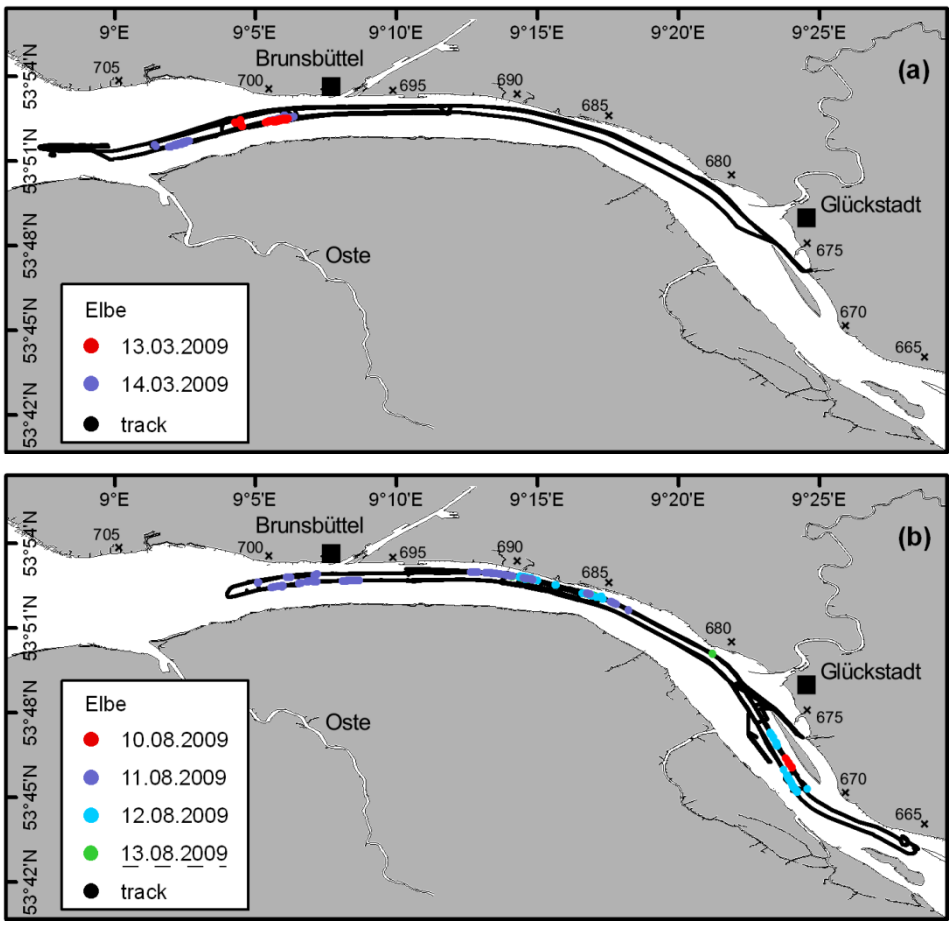

Figure 7.5: *Driven transects (black) and spatial distribution of the acoustic interfaces (coloured) for the surveys a) Elbe 03/2009 and b) Elbe 08/2009 (13.08.2009 neap tide).*

The height above river bed can be in the Weser estuary up to 3.1 m (south of Blexen) and 4.5 m (CT), respectively (fig 7.3 & fig. 7.6 a-c) whereas in the Elbe estuary the maximum height is 1.8 m which is noticeably less than in the Weser estuary (fig. 7.4 & fig. 7.6 d-e). The vertical scattering in figure 7.5 is related mainly to morphological changes. In the ripple section of the Weser estuary in particular, the distance from the interface to the river bed varies remarkably over a few meters depending on, whether the measurement was done within a ripple trough or at its slopes (fig. 7.4).

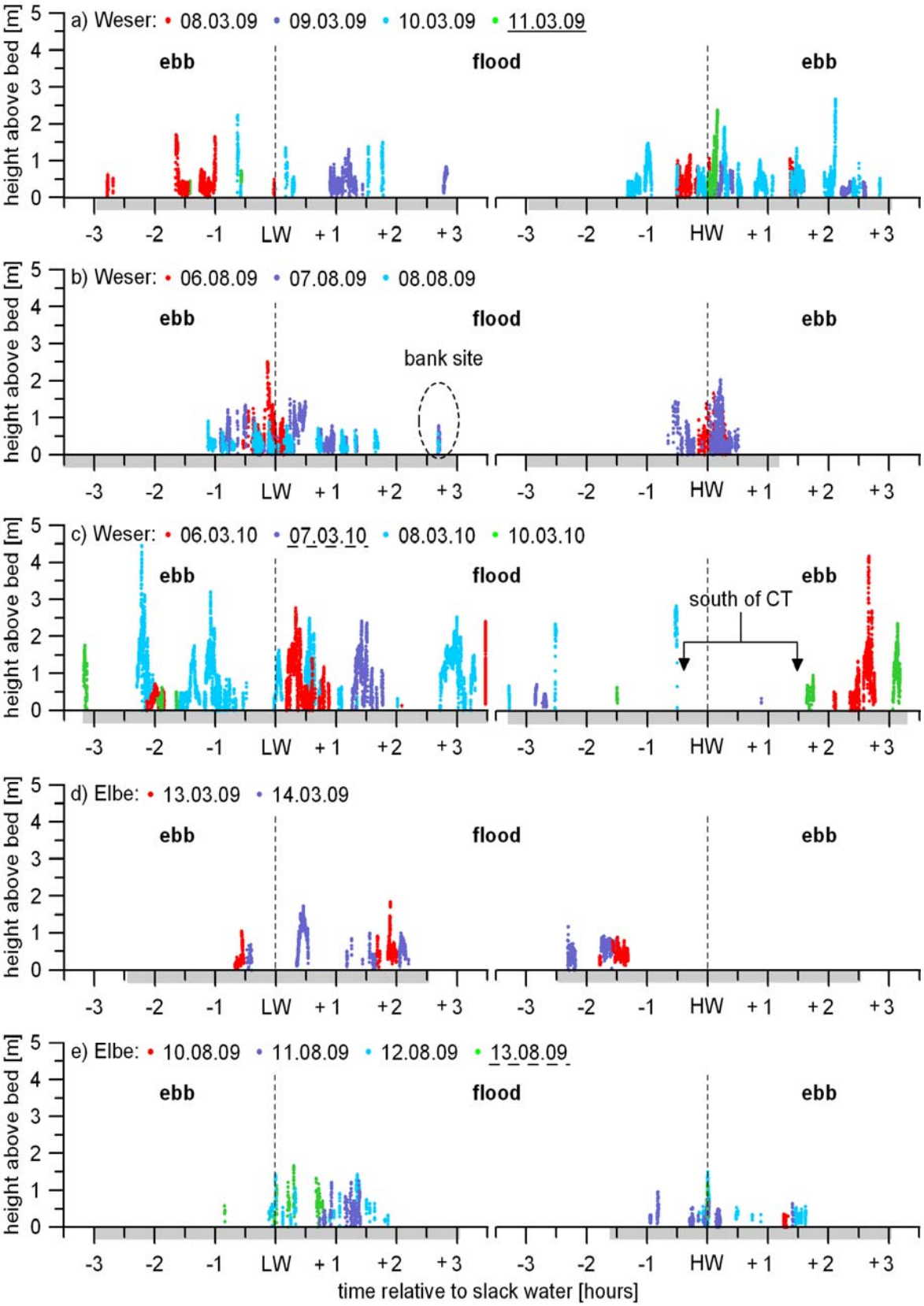

Figure 7.6 a-e): *Occurrence and distance of the acoustic interfaces towards the river bed relative to slack water recorded with the low frequency channel of a parametric sediment echo sounder during the surveys a) Weser 03/2009 (11.03.2009 spring tide., b) Weser 08/2009, c) Weser 03/2010 (07.03.2010 neap tide), d) Elbe 03/2009 and e) Elbe 08/2009 (13.08.2009 neap tide).*

In figure 7.6 b it can be seen that in August 2009 landwards of Blexen (Weser) the scattering caused by the morphology is superimposed by a tidal induced signal. Around low water in particular the height above the bed increases towards slack water and decreases with the begin of tidal current. Apart from that, the temporal occurrence of the acoustic reflectors is highly variable (figure 7.6). In the Elbe estuary for example, interfaces are most frequently observed during the entire flood phase independent of the seasonal controlled freshwater discharge. In the Weser estuary, in contrast, interfaces occur at nearly each tidal phase when the freshwater discharge is high (March 2009 & 2010) but are restricted under low freshwater discharge events (August 2009) to the slack water phase plus / minus one hour. The interfaces observed three hours after slack water during low discharge (fig. 7.6 b) are restricted to the bank sites.

Generally, the distance between the reflector and the river bed is in case of the Elbe estuary higher during ebb current than during flood current and vice versa in the Weser estuary. Maximum heights above bed have been measured during spring tide (figure 7.6).

7.4.2: Interface characteristics

The acoustic interfaces were sampled with 11 Rumohr-type gravity cores at current velocities between 0.2 and 1.1 m/s representing the slack water condition as well as ebb and flood current. Additional 16 cores were sampled when no acoustical interfaces were present. The Rumohr-type gravity cores comprise of the following sedimentological units: sediment suspensions, fluid mud I & II as well as cohesive consolidated and non-cohesive bed sediments. Their sedimentological characteristics such as the grain size composition correspond to the classification of Papenmeier et al. (2011) and do not change with varying current velocities.

In figure 7.7 the SSC-difference between the samples above and below the acoustic interface is plotted versus the normalized amplitude of the interface. The interfaces are basically linked to a lutocline with an abrupt SSC change and can be divided into three clusters. The first one (triangles) describes the interfaces within the water column with a minimum distance of 35 cm towards the sediment surface. In cases where two or more

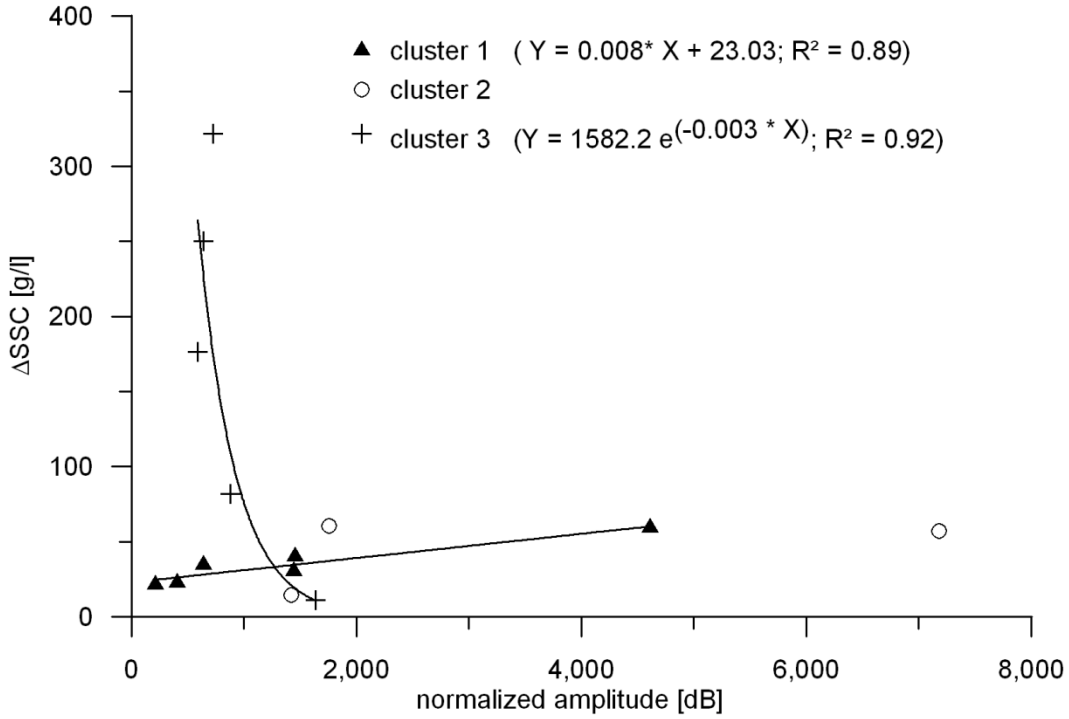

Figure 7.7: *Correlations between SSC-difference (of Rumohr-type gravity core samples taken above and below the acoustic interface) and the normalized amplitude of the interface represent three clusters. 1) Acoustic interfaces with distance > 0.35 m towards the river bed 2) Second and third interfaces 3) Acoustic interfaces with distance < 0.35 m towards the river bed.*

interfaces exist, the upper most interface belongs to the first cluster. The relation between the SSC difference and the normalized amplitude increases in a linear manner ($\Delta SSC = 8.1 * 10^{-3} A_N + 23.03$; R^2 = 0.89). Samples above the interfaces have SSCs of 0.2 - 1.5 g/l (sediment suspensions) and samples below the interfaces indicate SSCs of 22 - 60 g/l (low viscous fluid mud). SSC differences of 22 – 59 g/l, as typical for cluster one, have also been observed in some cores 10-60 cm above river bed but an acoustical interface in the SES data does not exist. The second cluster (circles) represents samples of the second or third interfaces when more than one layer was present. The SSC-gradient at the interface varies between 14 and 60 g/l. In total the Rumohr-type gravity core samples below and above the interface are higher concentrated (42 – 132 g/l) than cluster one and can be described as low viscous fluid mud. The three data points do not so far show any relationship. Near bed interfaces, with less than 35 cm distance towards the sediment surface, belong to the third cluster (crosses). Here, the normalized amplitude is exponentially decreasing with an increasing SSC-difference ($\Delta SSC = 1582.2\, e^{-0.003\, A_N}$; R^2 = 0.92). The sampled interfaces represent not only the transition between sediment

suspensions and high viscous fluid mud but also between low and high viscous fluid mud. The SSC differences at the interface vary between 11 – 322 g/l.

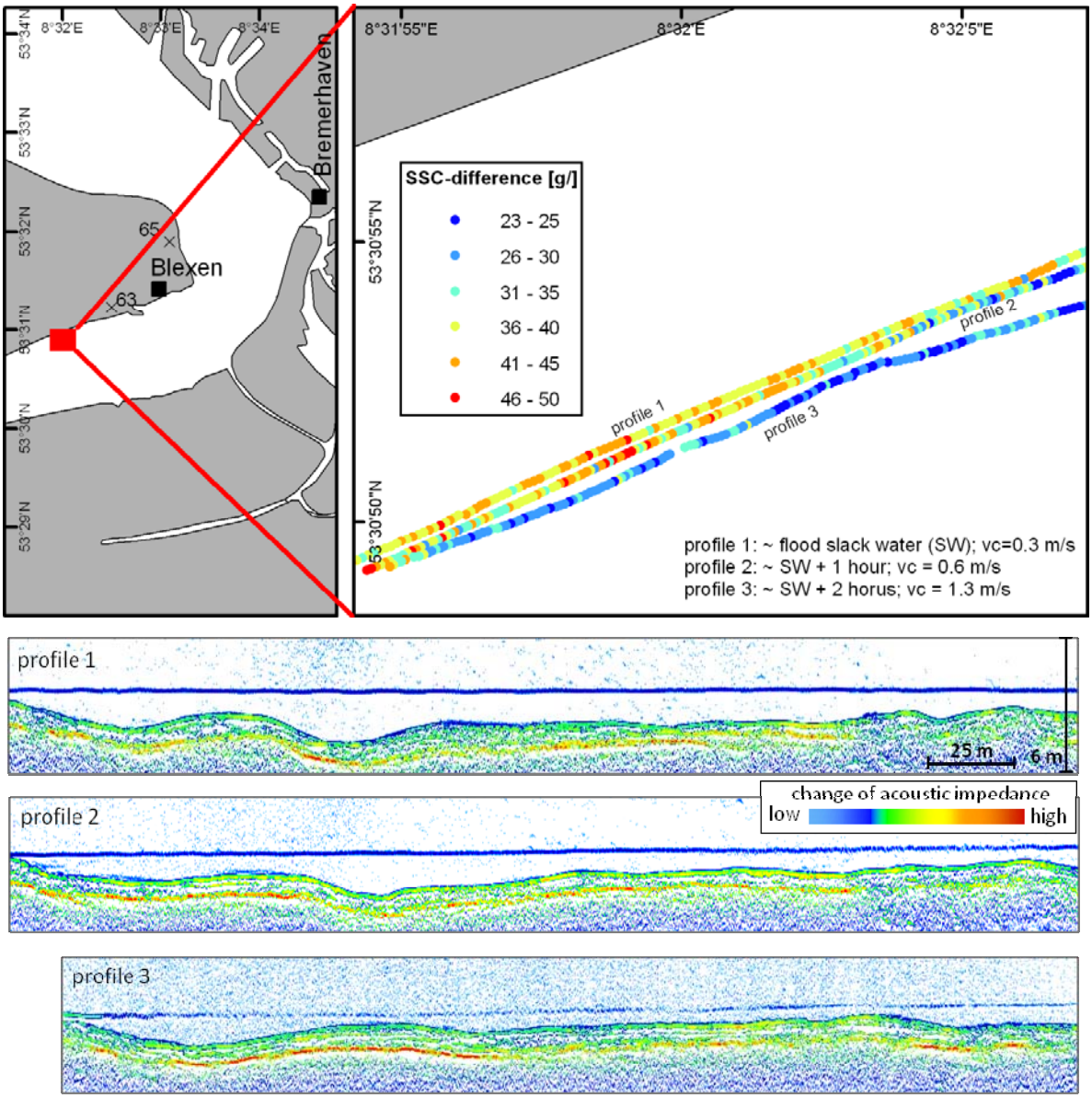

Figure 7.8 top: *SSC-differences at the acoustic interface (height above bed > 0.35 m) and* ***bottom:*** *longitudinal sediment echo sounder profiles (low frequency) for different current velocities (vc) during ebb tide recorded in the Weser estuary at the 11th of March 2009 (spring tide).*

Areas of distinct SSC-gradients do not exist. In fact, the acoustic strength and the related SSC-differences seem to be dependent on the tidal progress. In figure 7.8, variations in acoustic strength and the SSC-gradient of cluster type one interfaces (height above bed > 0.35 m) is shown for progressing current velocity. At slack water condition (profile 1) the interface is characterised by a strong reflector with SSC-differences between 28 and 49 g/l (mean 39 g/l). One hour after slack water at current velocities of 0.6 m/s (profile 2)

the acoustic interface at the north-eastern end of the transect starts to weaken and the SSC-gradient is slightly smaller decreased (mean ΔSSC = 23-35 g/l). Apart from that both parameters are very comparable to slack water condition. Significant changes are present two hours after slack water (profile 3) at current velocities of 1.3 m/s. Here, the reflector strength is very weak and SSC-gradients range between 23-37 g/l (mean 27 g/l) while the water column above the reflector is characterised by a relative high back scatter (fig. 7.8 bottom).

7.5: Interpretation and discussion

The interfaces observed in the water column and near bed of the Weser and Elbe estuaries are related to changes in acoustical impedances which are typically caused by strong density gradients (USACE 2002). In this study the density gradients originated from SSC differences as shown by the Rumohr-type gravity core samples. The comparison of the SSC values from the Rumohr-type gravity cores and the normalized amplitude of the interfaces has shown that a minimum SSC-difference of 23 g/l over a maximum distance of 10 cm has to be present to generate an acoustic interface within the low frequency channel of the SES. Missing acoustic reflectors in the SES data despite appropriated SSC-gradients in the Rumohr-type gravity core samples are related to the river bed morphology and the approximate distance of 5 m between the SES and Rumohr-type gravity corer. This distance can be of relevance when sampling takes place in a dune trough and the SES ensonificates the dune slope or crest.

The strength of the acoustic reflectors within the water column is related to the SSC gradient at the interface as assumed by Becker (2011) but behaves differently for near bed interfaces (distance to the river bed < 0.35 m) as well as interfaces within the water column (distance to the river bed > 0.35 m). In case of cluster 1, where the acoustic amplitude is increasing positive linear with the SSC-gradient, the interfaces represent the boundary between high SSCs and fluid mud (I) (classified after Papenmeier et al. 2011, chapter 6). This coincides with previous works (e.g. Granboulan et al. 1989, Schrottke et al. 2006, Vantorre 2001, Wurpts & Torn 2005) which associate acoustic interfaces with the lutocline at the upper fluid mud boundary. This boundary is generated by an

enhanced settling of suspended particulate matter (SPM) which leads to the onset of hindered settling and the development of a space-filling network (Winterwerp 2002). The concentration where the space-filling network starts to develop, the so called gelling concentration, was computed by Winterwerp (2002) with a 1DV POINT MODEL and sated for distances of > 0.35 m towards the sediment bed between SSCs of 10 and 40 g/l. This coincides with the observed strong SSC-gradients between < 1.5 and 22 - 60 g/l SSC and confirms the assumption of Papenmeier et al. (2011) who described the upper fluid mud boundary at around 20 g/l SSC.

The second cluster, linked to situations where more than one interface is present, represents strong SSC-gradients within the fluid mud but does not match with the fluid mud (I) and (II) boundary. Such multiple interfaces were mainly found in front of the CT where at least one acoustic interface was observed over the whole tidal cycle. The single interfaces might be linked to special discharge events, tidal or lunar cycles where large amounts of fluid mud have been generated or the shear stress was too low to resuspend the accumulations completely between two slack water events. Dewatering and internal rearrangement of the remaining accumulations leads to a densification of the fluid mud (McAnally 2007) and generates density gradients which are imaged through the acoustic interfaces.

As mentioned earlier, the near bed interfaces differ in their exponential SSC-gradient – amplitude relation completely from those interfaces which are located within the water column. A satisfying explanation for the increasing amplitude with decreasing SSC-gradient has so far not been found but one hypothesis might be that larger density gradients are necessary to generate an acoustical impedance when a certain consolidation sate is exceeded. The fluid mud (II) accumulations, located below the cluster 3 interfaces, are partly consolidated and are no longer in a suspended state (Papenmeier et al. 2011). It might be possible that the SSC-gradient is e.g. in case of overlying fluid mud (I) in relative terms too small to generate an acoustic impedance.

Interfacial mixing, which is essential for suspended sediment transport processes (Wolanski et al. 1989), can be described on the basis of the changing SSC-gradients and acoustic reflector strength with progressing tidal current. Very constant SSC-gradients

and acoustic reflectors at the upper fluid mud boundary during slack water and up to one hour later (current velocity < 0.6 m/s) indicate that during this time period no vertical mixing exists. Becker (2011) describes that the upper fluid mud boundary is stable while the tidal current is characterized by velocity shear and the entrainment phase starts with turbulent flow. For the ripple section in the Weser estuary turbulent entrainment was described for current velocities > 0.42 m/s (Becker 2011) but in areas of smooth morphology much higher values have been observed. The example of the 'Blexer curve' shows that tidal induced reduction in reflector strength and SSC-gradient indeed exit at current velocities of 0.6 m/s but significant changes occur later than one hour after slack water (current velocity > 0.6 m/s).

7.6: Conclusion

The acoustic interfaces recorded in the Weser and Elbe estuaries with the low frequency channel of a parametric sediment echo sounder are induced by strong SSC changes over a short vertical distance. Interfaces within the water column have on the basis of Rumohr-type gravity core samples doubtlessly been identified as the lutocline at the upper fluid mud boundary. They occur when at least a SSC-gradient of 23 g/l over a distance of 10 cm is present and have been observed for nearly the entire reach of the Weser TMZ but are less often present in the Elbe TMZ. Interfacial mixing at the interfaces within the water column with progressing tide can be quantified on basis of the reflector strength. The reflector correlates in a linear manner with the SSC-gradient at the interface which has so far not been quantified in literature. Significant changes in the SSC-gradient and hence interfacial mixing have been observed in areas of smooth bed morphology later than one hour after slack water. In cases of fluid mud accumulations of several metres thickness one ebb or flood phase is not sufficient for complete resuspension. Interfaces within the fluid mud indicate the consolidation of the fluid mud accumulations. This state causes the reduction of the navigation depth and leads to regular, cost intensive dredging activities.

Acknowledgement

The author would like to thank the captain and crew of the *'RV Littorina'* for their excellent job and their inexhaustible patience during the acquisition of the data sets. This study was funded by Cluster of Excellence 'Future Ocean' in Kiel.

Chapter 8: Consequences of water injection dredging on estuarine suspended sediment dynamics and river bed structures: A case study in the subaqueous dune reaches of the German Weser estuary

The next chapter describes the influence of water injection dredging within the Weser estuary on the river bed form geometry, their sediment characteristics as well as on the suspended sediment dynamics. The content is based mainly on the following publications:

- Schrottke, K., Bartholomä, A. and **Papenmeier, S.** (2008). Effects of dredging on the sediment dynamics in the tidal estuary Weser (German North Sea coast). Proceeding of Seventh International Conference on Tidal Environments. 25-27 September, 2008 Qingdao, China
- **Papenmeier, S.**, Schrottke, K., Bartholomä and A., Steege, V. (2010). Wirkungskontrolle von Wasserinjetkionsbaggerungen auf subaquatischen Dünenfeldern in der Unterweser auf der Basis von hydroakustischen, optischen und laseroptischen Messungen. Deutsche Gesellschaft für Limnologie (DGL), Erweiterte Zusammenfassungen der Jahrestagung 2009 (Oldenburg), Hardegsen, 6 S.
- **Papenmeier, S.**, Schrottke, K. and Bartholomä, A. (2011). Total volume concentration and size distribution of suspended matter at sites affected by water injection dredging of subaqueous dunes in the German Weser Estuary. Coastline Reports Vol 2010-16: 71-76.
- Schrottke, K., Bartholomä, A. and **Papenmeier, S.** (2011). Auswirkungen von WI-Baggerungen subaquatischer Dünen auf die Sedimentcharakteristik und -dynamik der Gewässersohle in der Tideweser. In: Umweltauswirkungen von Wasserinjektionsbaggerungen. WSV-Workshop, 21./22. Juni 2010, Bremerhaven. BfG, Koblenz, 42-52.

Abstract

In environments of high sediment dynamics (e.g. estuarine navigation channels), Water Injection Dredging (WID) has gained in the last few decades increased importance. High dumping costs are redundant due to the active sediment transport by the natural current. The sediment mobilization and transport in sandy environments as well as the dredging effect on the suspended sediment dynamics is still not fully understood. To investigate the impact of WID in a high spatial and temporal resolution, hydroacoustic data, Suspended Sediment Concentrations (SSCs) as well as in-situ particle sizes were measured

in June 2008 at two dredging sites in the navigation channel of the Weser estuary. One reflects the brackwater and the other the tidal freshwater reach. At each site subaqueous dune crests which reduce the navigational depth were eroded by injecting huge amounts of water in the upper sediment layer and were transported by hydrodynamics.

At both sites dune crests were removed precisely while the internal sediment structure was disturbed in the upper decimetres. The eroded sediments of preferentially sand sized particles were accumulated on the dune slopes or in the adjacent troughs. The mobilization has not generated bed loads or suspended sediment loads of exceptional SSCs in the current lee site of the dredging site. Furthermore, differences in in-situ particle size distribution within the water column have not been observed. Hydroacoustic interferences in the current lee site of the dredging vessel were predominately related to turbulences and air bubbles within the water column. Overall, it can be concluded that WID does not seem to have a significant impact on suspended sediment dynamics and the spatial redistribution of the removed sediments is very small.

8.1: Introduction

Dredging activities are necessary in all frequently used estuarine navigation channels and in most of the adjacent harbours. Through sediment movement by tidal currents subaqueous bedforms are formed frequently in navigation channels, affecting the safe ship access. Dredging activities are not a permanent success due to the invariably regeneration of bed forms thus high efficient low cost dredging techniques are of great interest. Since the mid eighties the world wide operation of Water Injection Dredging (WID) has increased (Meyer-Nehls 2000). The sediments are resuspended by huge amounts (8,000-12,000 m^3/h) of water which is pumped from the river surface through a framework of water jets, lowered on or near the riverbed, and injected with relatively low pressure (0.8-1 bar) into the sediment surface (Meyer-Nehls 2000, Nasner 1992, Stengel 2006). Near bed a sediment-water mixtures of partly substantially higher density than the surrounding water (in case of resuspended mud accumulations) is created and transported by hydrodynamics (Meyer-Nehls 2000) or due to natural density flux (Netzband et al. 1999). The transport direction depends on the tidal flow direction and

the morphology. Pumping capacity and the injecting water pressure vary between Water Injection (WI) devices and can be adapted to the bed characteristics. Initially, WID have been developed for the remobilization of fine cohesive sediments (Aster 1993, Spencer et al. 2006, Woltering 1996) but in the last few years the efficiency of WID also been proven for sandy sediments (Clausner 1993, Nasner 1992, Stengel 2006). Costs of this hydrodynamic dredging technique have decreased compared to the conventional techniques because the sediment is no longer removed out of the river system and dumped on- or offshore. For example, in the Weser estuary costs have been reduced to more than 60% within one year (Kerner & Jacobi 2006). The disadvantage of the WID technique, which is also known for other dredging techniques, is that the coarsening of sediments can be caused by different mobility rates of the grain sizes (Meyer-Nehls 2000).

Only few studies deal with the spatial and temporal expansion of the WID induced Suspended Sediment Concentrations (SSCs) and its characteristics, especially in sandy environments. Studies from the Hamburg and Ems harbour (Germany) have shown, that differing concentration from the background signal could not be detected from further than 100 m (Meyer-Nehls 2000) and 200 m (Aster 1993), respectively. In the Hamburg harbour the vertical intrusion did not exceed 1-2 m in height (Meyer-Nehls 2000). General SSC expansions of some meters to some hundreds of meters haven been described by Meyer-Nehls (2000). WID induced changes in In-Situ Particle-Size Distribution (ISPSD) of the SSC are so far not known. Changes in ISPSD in a backhoe dredging plume have been described by Mikkelsen & Pejrup (2000) in the Øresund (between Denmark and Sweden) with negligible tidal influence. In-situ size spectra changes from fine-grained, poorly sorted to coarser-grained, better sorted with increasing distance to the dredging device. Because grain size distribution in primary particles did not change, changes in the in situ spectra are related to flocculation.

8.2: Motivation and objectives

The WID technique which has been used since 2004 in the Weser estuary for maintenance work should also be used for a planed deepening of the Weser navigation

channel. Due to the influence of WID on the natural sediment dynamic and the water ecology is not satisfying known, the multidisciplinary monitoring campaign 'Wirkungskontrolle Wasserinjektion' was done in the Weser estuary in June 2008 (BfG 2011). The objective of this study, which is part of the monitoring campaign, is the investigation of WID effects on the sub-bottom sediment characteristics as well as the suspended sediment dynamics recorded with temporal and spatial high resolution hydroacoustical and optical measurements.

8.3: Study area

The 477 km long Weser river discharges north of Bremerhaven into the southern North Sea of Germany (Seedorfer & Meyer 1992). The Lower Weser, the section between Bremen and Bremerhaven (approximate length of 65 km) is mesotidal to macrotidal influenced (fig. 8.1) and comprises a brackwater zone as well as a tidal fresh water region (Schuchardt et al. 1993) which differs in their hydrological parameters.

The brackwater zone is located approximately between Bremerhaven and km 40 - 70, depending on tidal phase and meteorological conditions. The water column is well mixed due to strong tidal currents of an average velocity of 1-1.3 m/s (Grabemann & Krause 2001). Through the mixing of fresh- and saltwater sediment loads in the brackwater zone, the SSC can reach values of up to 126 mg/l (Schuchardt et al. 1993). In the low salinity reach of the brackwater zone around Blexen a 15-20 km long Turbidity Maximum Zone (TMZ) is present. Here, the SSC can even reach values of 30 to 1,500 mg/l (Grabemann & Krause 1989, 2001). The distribution of SSC changes with the tidal situation. During ebb and flood currents the SSC is relatively high and suspended particulate matter (SPM) are distributed through the water column (Grabemann & Krause 2001). As soon as current intensity is too low to keep the sediments in suspensions, they start to settle down forming aggregates of organic and inorganic material. Aggregates of larger than 100 µm have been described by Wellershaus (1981) and in chapter 5.

The tidal fresh water reach is located between the upper most border of the tide, a tidal weir in Bremen, and the border of the brackwater zone. The mean current velocity is with 1 m/s slightly lower than in the brackwater zone (Schuchardt et al. 1993). The amounts of SPM are controlled by the input from the hinterland. Generally, in the tidal fresh water reach, outside of the brackwater zone, the SSC is lower than 0.05 g/l (Grabemann & Krause 2001). Schuchardt et al. (1993) describe for the tidal fresh water reach an average SSC of 0.042 g/l. Intratidal variations are not as pronounced as in the brackwater zone.

Between km 20 and 60 the bed morphology of the navigation channel is characterised by a subaqueous dune reach with dunes of up to 6 m in height and a length of up to 150 m (Schrottke et al 2006). The dunes are mostly two- or three-dimensional, lateral orientated to the navigation channel and asymmetrical in the direction of the ebb tide (Schrottke et al. 2006). The sediments in the dune reach consist mainly of middle to coarse sand with a low amount of fine grained sediments (Stengel 2006) and can restrict without dredging the navigation depth.

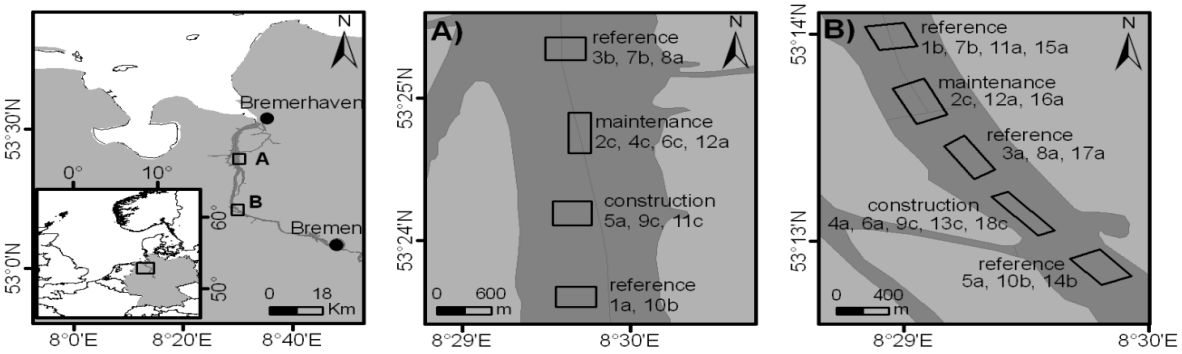

Figure 8.1: *Left: Overview map of northern Europe with Germany (grey) and overview map of the study site A (brackwater area) and B (freshwater area) in the Weser estuary. Study site A) and B) with the different study section and the LISST profiles.*

8.4: Material and methods

Measurements derived from two study sites in the subaqueous dune reach in the Weser navigation channel: One in the brackwater reach by river km 50 at 10th of June 2008 (denoted A) and another in the freshwater reach by river km 31 at 24th of June 2008 (denoted B). The latter is located in a river curve. Additional measurements were done one day before and after dredging activity. Both study sites were subdivided in 4-

5 smaller study sections and treated differently by the WI device (fig. 8.1). Within the 'construction section', the deepening of the Weser navigation channel towards 14 m below mean level was simulated. Within the 'maintenance section' the dune crests were removed up to the present maintained depth. The other sections are located up- and downstream of the dredging sites and were not processed by the WI device and were used as reference sections. All subsections exhibited comparable hydrodynamic and sedimentological conditions. Measurements were done over one tidal cycle during neap tide at a river discharge of 180 m^3/s (Water and Shipping Authority Bremen, 2009, pers. comm.). The dredging activities were carried out by the WID vessel *'Akke'* during ebb and flood phase. While drifting with the tidal current water was injected via a 10 m wide sledge into the sediment surface.

A parametric Sediment Echo Sounder ('SES-2000® standard', Innomar Technology GmbH, Warnemünde, Germany), using a primary (about 100 kHz) and secondary (here 12 kHz) frequency, enabled the comparison of sub-bottom structures and dune geometry before and after dredging. The penetration depth is here up to 5 m with a vertical resolution of about 6 cm (Schrottke & Bartholomä 2008). For a detailed technical description see also section 4.1.3. Extensive investigations of the bed surface characteristics were done with a dual-frequency Side Scan Sonar (SSS) of type 'Sportscan® 881' (Imagenex, Port Coquitlan, Cananda). The device was operated with 330 kHz, 60 metre range and a gain on 8 dB. For more information see section 4.1.4. The ground-truthing was done with a Van-Veen-grab sampler. Grain size analyses were done with a SediGraph ('5120™', Micromeritics Instruments, Norcross, Georgia) and a settling tube of the type 'MacroGranometer™' (Neckargemuend, Germany), respectively (details can be read in section 4.3.2). Current velocity and direction as well as average backscatter intensity of SPM in a profiling mode were measured with an 1,200-kHz direct-reading broadband Acoustic Doppler Current Profiler (ADCP) (RD Instruments®, Poway, California). Details can be gathered from section 4.1.2.

In-Situ Particle Size Distributions (ISPSDs) were detected by the laser diffraction principle with a Laser In-Situ Scattering and Transmissometry system ('LISST-100X') of type C by Sequoia® Scientific Inc (Bellevue, Washington). The PSD is measured in 32 logarithmically spaced size classes in the range of 2.5-500 µm (8.6 - 1 Phi). The size distribution is

presented as volume concentration (VC) in each of the size classes and the sum of VC results in the total volume concentration (TVC) (Agrawal & Pottsmith 2000). The optical transmission (τ) is measured by a photodiode. To increase the upper threshold concentration, a 50% path reduction module was installed to reduce the optical path length and thus the sample volume. A full technical description of the LISST is done by Agrawal & Pottsmith (2000), Agrawal et al. (2008) and in section 4.1.1. The LISST measurements were done in a number of vertical profiles while the research vessel drifted freely with the current. Maximum measurement depth was approximately one metre above ground, to avoid misalignment of optics by ground contact. Simultaneously, vertical profiles of SSCs were recorded with an Optical BackScatter (OBS) sensor 'ViSolid® 700 IQ' (WTW, Weilheim, Germany) which is described in detail in section 4.1.5. The data, given as SiO_2 equivalent concentration data, were calibrated with SSCs of filtered and dry weighted water samples. These were collected with a horizontal Hydro-Bios GmbH (Kiel, Germany) water sampler at near surface and near bed (see section 4.2.2). The LISST and OBS profiles were numbered consecutively for each study site. The index indicates if the measurement was done in the current luv site (a) of the WI device in the current lee site (b) or at the dredging station (c).

The hydroacoustic and optical devices were generally operated from the working vessel *'Scanner'* (Senckenberg Institute Wilhelmshaven). Transverse and cross-sectional profiles were taken before, during and after dredging. The vessel was able to drive up to a few metres of the dredging vessel *'Akke'*. On the days where the *'Akke'* was operating, the optical measurements and water sampling was done from the working vessel *'Rüstersiel'* (Water- and shipping authority Wilhelmshaven). The measurements started approximately 60 meters behind the current lee side of the dredging vessel. With ongoing measurement time the working vessel drifted with the tidal flow.

8.5: Results

8.5.1: River bed

The river bed in the maintenance and construction areas of study site A and B were dominated before dredging by up to 4 m high ebb orientated subaqueous dunes of well

sorted middle sands, often superimposed by smaller ripples (fig. 8.2 a). The sub-bottom data indicated the typical internal cross-bedding of subaqueous dunes (fig. 8.3 a). The dune crests, limiting the navigational depth, were successively removed with the WI device (fig. 8.2 b & c, fig. 8.3 a & b). The progress can be seen in the sonar data by means of the sledge location (fig. 8.2 b & c white arrow, fig. 8.3 b). After dredging the dune crests are removed at each study site at the exact demanded navigation depth. In the case of figure 8.2 d (construction area of study site B) the upper two metres of the dunes were removed. The dredged sediments were accumulated on the dune slopes and in the adjacent dune troughs (fig. 8.2 d). The acoustic backscatter in the dredged area is decreased while the un-dredged area is characterised by high acoustical backscatter

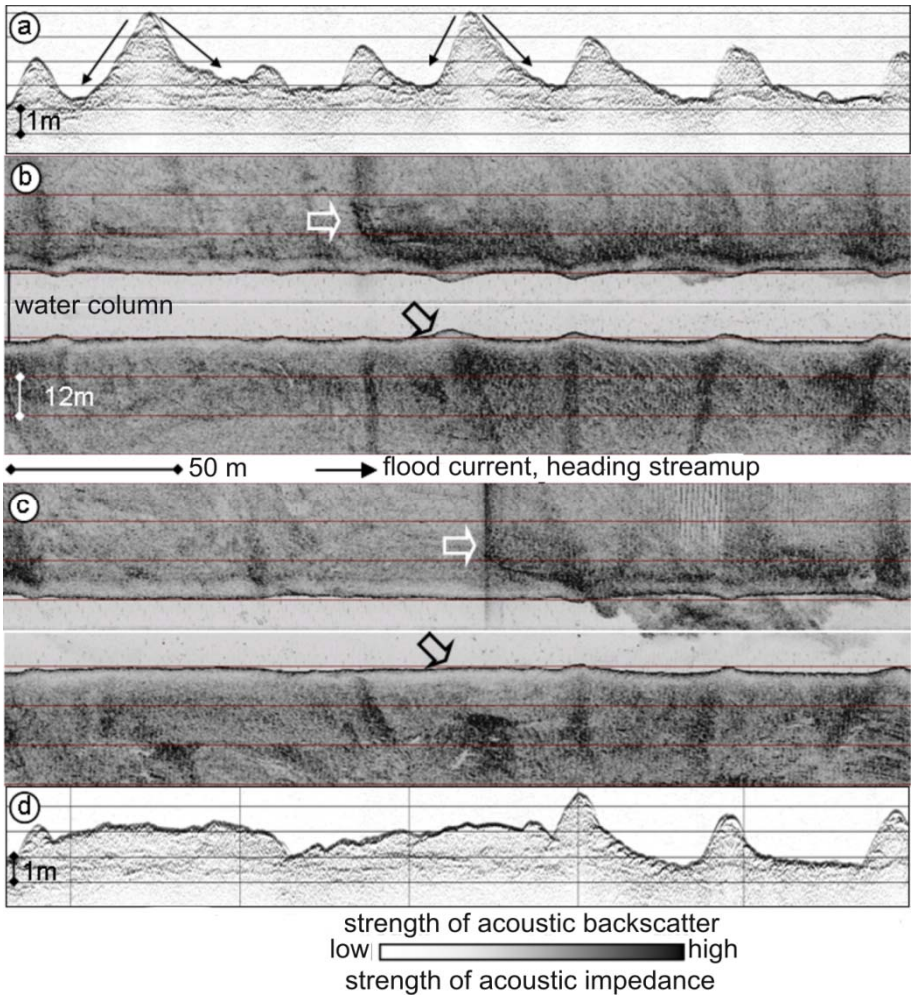

Figure 8.2: *Sediment Echo Sounder (SES) and Side-Scan Sonar (SSS) profiles of the construction area in the freshwater reach. a) SES profile before dredging (arrows highlight the direction of possible sediment transport), b)+c) SSS records during dredging (white arrow: position of the water injection sledge, black arrow different dredging progress), d) SES profile after dredging.*

induced by small bed forms like ripples (fig. 8.2 b, fig. 8.3 c) which are not anymore present after dredging. Sediment samples taken before and after dredging do not show a significant shift in grain size as shown by figure 8.4 (construction area of study site B). The internal cross-bedding within the river bed does not exist anymore in the upper decimetres (fig. 8.3 a). The new accumulated sediments indicate no internal structures but smaller untreated ripples and small dunes are still visible below the newly accumulated sediments (fig 8.2 d). Adjacent dunes do not show changes in their internal structures.

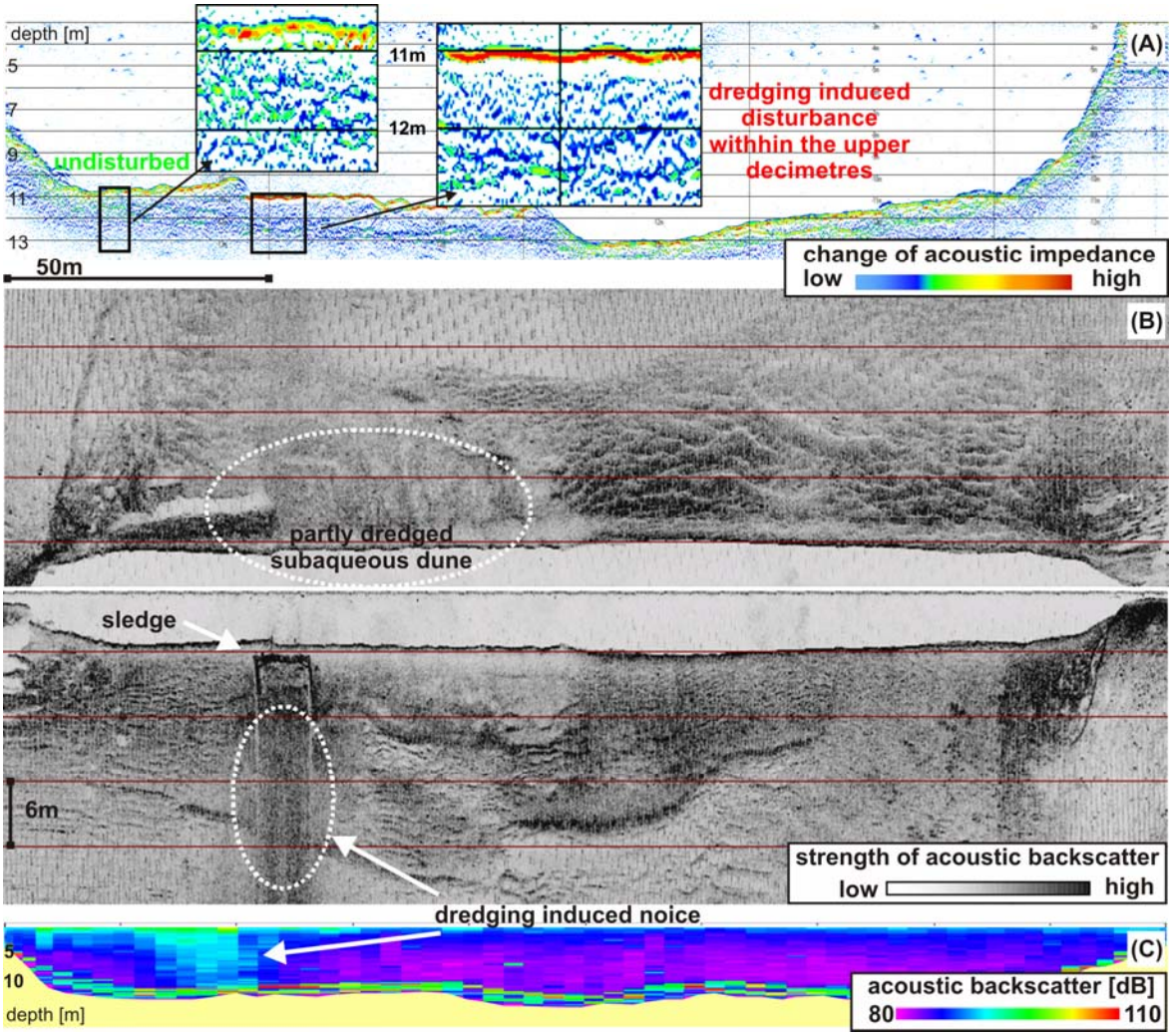

Figure 8.3: *Cross section through the construction area within the freshwater reach (modified after Schrottke et al. 2011). A) Sediment echo sounder profile with undisturbed dune beside a removed crest. B) Side-scan sonar profile with shadow of WI-sledge and partly dredged dune crest. C) ADCP profile with increased backscatter in the vicinity of the WI-device.*

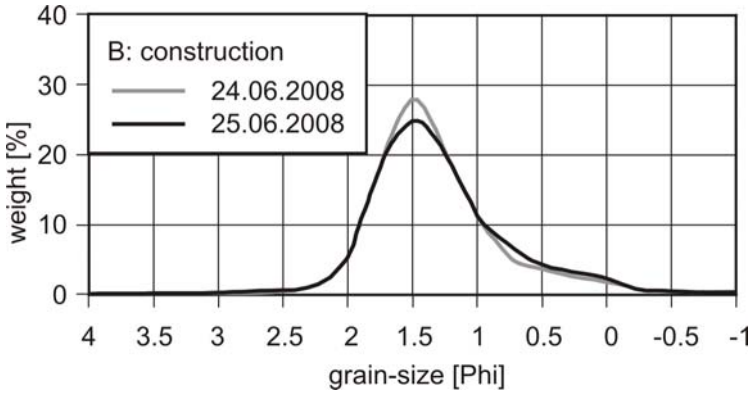

Figure 8.4: *Mean particle size distribution of sediment samples taken in the construction area within the freshwater reach before dredging (24.06.2008) and afterwards (25.06.2008) (modified after Schrottke et al. 2011).*

8.5.2: Water column

Increased acoustical signals have been observed in the current lee side of the dredging device when water was injected into the sediment (fig. 8.3 a, fig. 8.5). The river bed signal in the SSS data is directly behind the sledge superimposed by high acoustical backscatter (figure 8.2 b & c, fig. 8.3 b). The sideward extension is here limited on the width of the sledge (10 m) (fig. 8.3 b). In the ADCP data, increased backscatter extends up to 50 metres in the lateral direction (fig. 8.3 c, fig. 8.5 c) whereas the lateral expansion in this case is stronger at the inner side of the river curve than at the outer side (fig. 8.5).

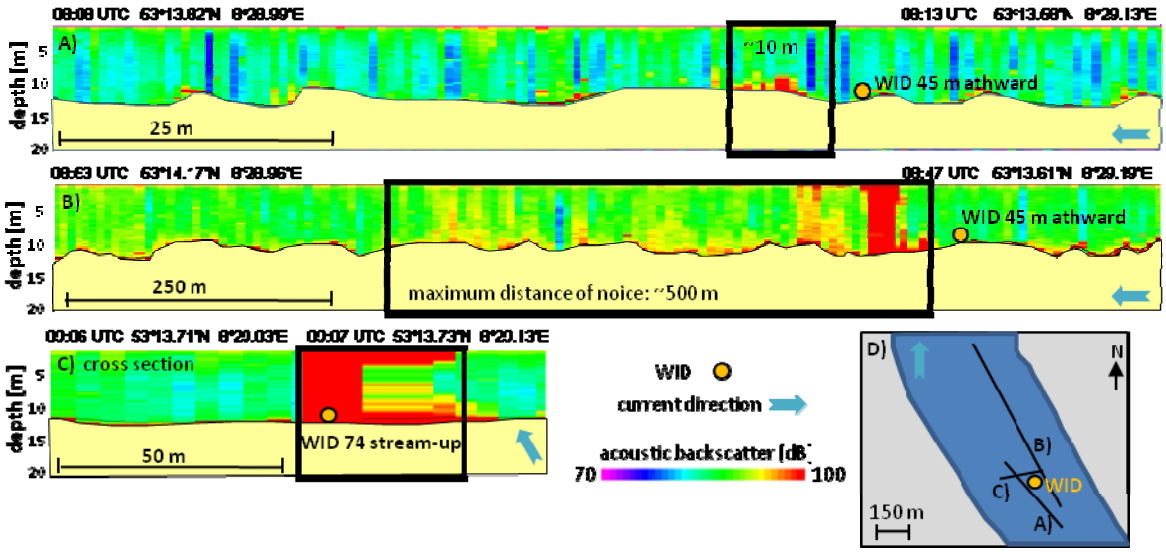

Figure 8.5: *Profiles of acoustic backscatter within the water column of the freshwater maintenance area measured with an ADCP during ebb current. A) and B) longitudinal profiles, C) cross section and D) sketch of profile locations.*

An increased acoustical signal is present through nearly the whole water column directly behind the sledge (fig. 8.3 c & fig. 8.5) but with increasing distance in current direction decreases the signal and is more and more limited to the near bed water column. At a maximum distance of 250 m for the SSS and 500 m for the ADCP the signal does not differ to the natural background signal.

The natural background signal varies between 22 and 320 mg/l in the brackwater section and between 26 and 128 mg/l in the freshwater section (tab. 8.1). The SSCs, measured with the OBS sensor, increased in both sections with increasing current velocity (fig. 8.6). Around slack water the SPM settled down in the brackwater section and thus enriched near bed. This phenomenon was not observed in the freshwater section. Considering a minimum distance of 60 m between sampling and dredging device, SSC changes have not been measured during water injection as shown exemplary in figure 8.6 (profiles 2).

Table 8.1: *Measured parameter at the brackwater (A) and freshwater (B) site.*

Study site	A				B			
	Mean particle size [Phi]	TVC [µl/l]	τ	SSC water sample [mg/l]	Mean particle size [Phi]	TVC [µl/l]	τ	SSC water sample [mg/l]
min	4.85	29.89	0.06	22	3.34	103.65	0.20	26
max	1.97	1598.35	0.58	320	1.85	469.39	0.41	128
mean	2.91	650.22	0.22	113	2.75	239.16	0.34	47
Samples τ < 0.3			80%				15%	

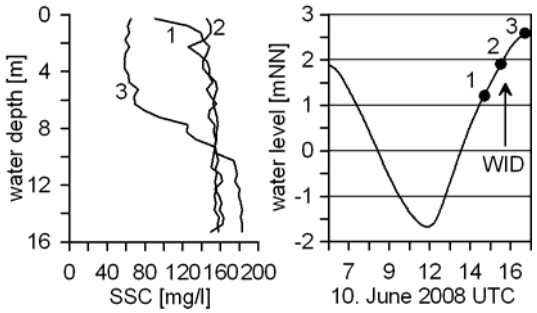

Figure 8.6 a: *Vertical Suspended Sediment Concentration (SSC) profiles measured in the brackwater site during flood phase. Water Injection Dredging (WID) took place in the vicinity of profile 2.*

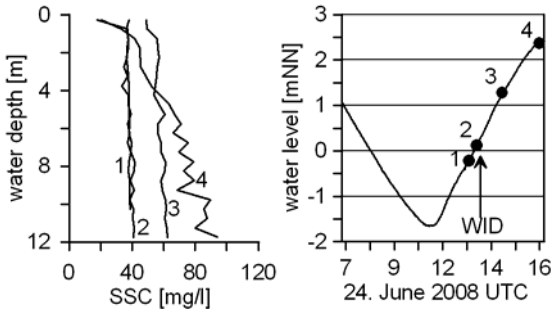

Figure 8.6 b: *Vertical Suspended Sediment Concentration (SSC) profiles measured in the freshwater site during flood phase. Water Injection Dredging (WID) took place in the vicinity of profile 2.*

TVC and τ, measured with the LISST simultaneously to the OBS data, correlate at both study sites in an exponential manner (fig 8.7). Overall, τ did not exceed 0.6, more often it decreased below 0.3, as found for 80 % and 15 % of all measurements, carried out at site A and B, respectively (tab. 8.1). Depth-related changes of the PSD and VC at site A are displayed in figure 8.9. The PSD changed within seconds from unimodal curves to ones with rising tails at the coarse end of the size spectra as shown in figure 8.8. Mean particle

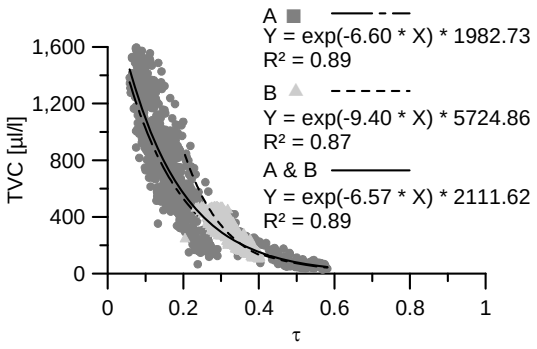

Figure 8.7: *Correlation of optical transmission τ and Total Volume Concentration (TVC) for study site A (brackwater) and B (freshwater).*

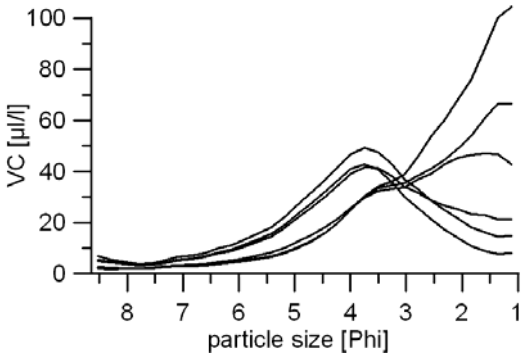

Figure 8.8: *Particle size distribution showing the variance in particle-size distribution obtained around 1.5 m water depth and a position without water injection dredging influence within 10 seconds*

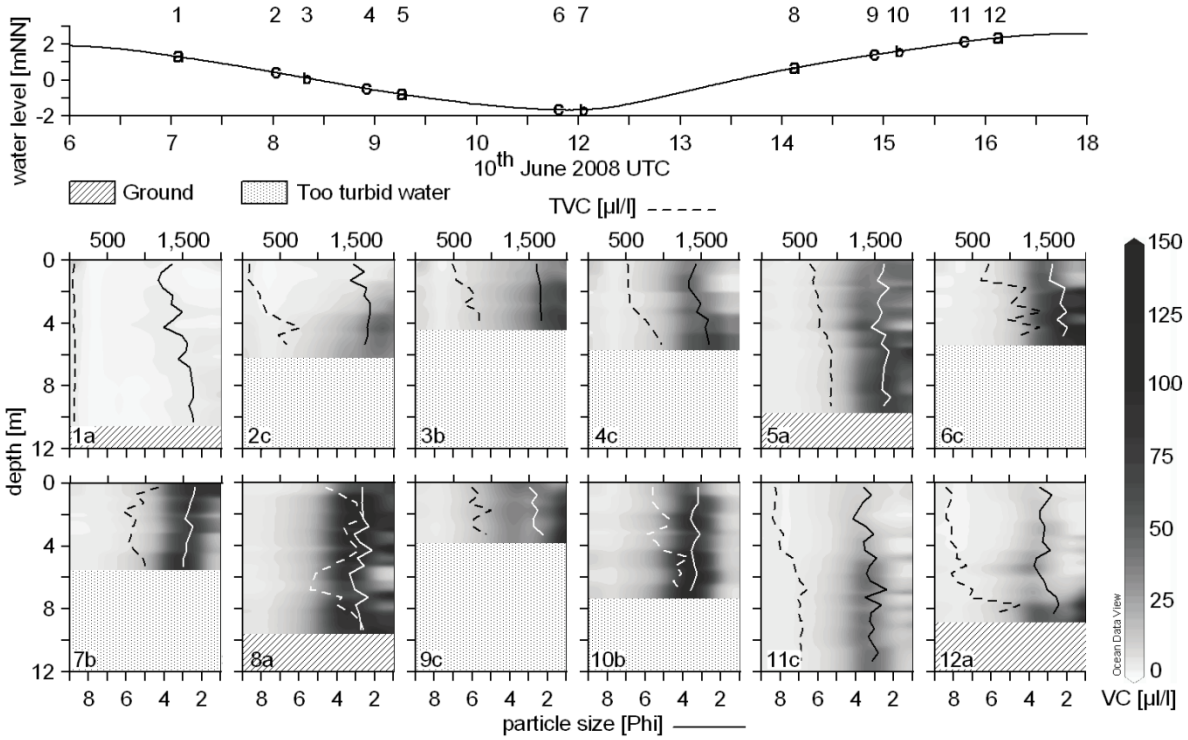

Figure 8.9: *Particle size distributions recorded by the LISST plotted over the depth for study site A (brackwater) at 10th of June 2008. The solid curve presents the mean particle size and the dashed line the Total Volume Concentration (TVC). Areas where no LISST data are present due to reaching the ground are hatched and data lack due to overload is dotted.*

sizes range here from 2.0 to 4.9 Phi (tab. 8.1). A downward particle coarsening from ~3.1 Phi (surface) to ~2.8 Phi (near bed) as well as a slight increase of VC for the size spectra > 8 Phi was observed. A distinct development in mean particle size between the profiles is not obvious. In contrast to the OBS data the LISST announced several times too high water turbidity before reaching the ground at the dredging (b) and current lee (c) sampling sites. An exception was station 11c (fig 8.9) which was measured at the end of the flood phase where SSC data was lower than at the other stations. The decreased transmission does not correlate with specific changes of the TVC or particle sizes For example the LISST measured down to the ground at station 8a with a TVC around 1,300 µl/l whereas at station 7b the LISST stopped measuring at a TVC of 1,000 µl/l though both stations have similar particle sizes (fig 8.9). At site B, the mean particle-size range of 1.9 to 3.3 Phi (tab. 8.1) was slightly smaller, but again with no depth-related changes (fig. 8.10). Mean particle size only varied among the subsections.

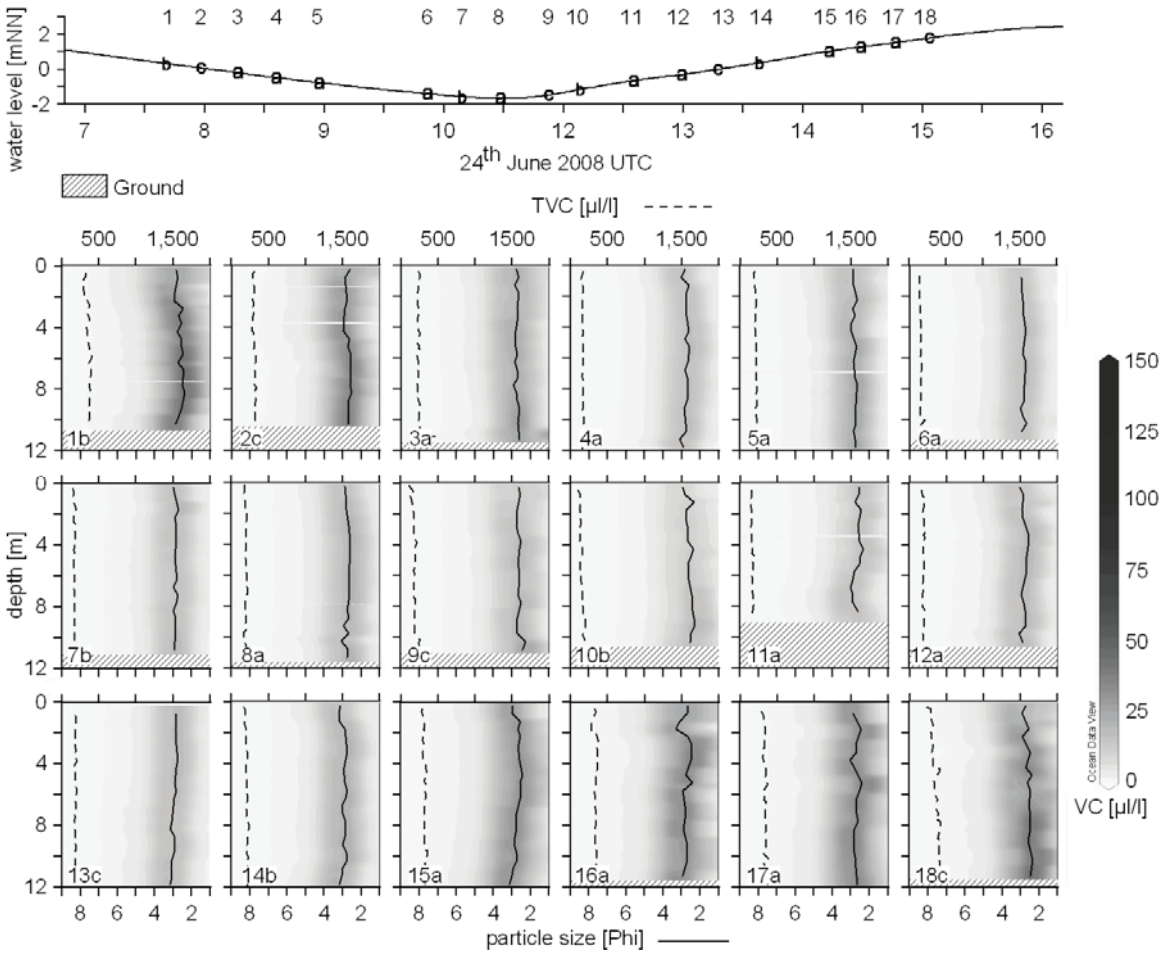

Figure 8.10: *Particle size distribution recorded by the LISST plotted over the depth for study site B (freshwater) on 24th of June 2008. The solid curve presents the mean particle size and the dashed line the Total Volume Concentration (TVC). Areas where no LISST data are present due to reaching the ground.*

8.6: Interpretation and discussion

The comparison of the SSS and SES data before and after dredging have shown that the WID vessel was able to remove the subaqueous dune crests at the demanded height with a given tolerance of 50 cm. This result corresponds with the data of accompanying studies taken by the associated project partners (refer to BfG 2011) as well as by relevant literature (e.g. Meyer-Nehls 2000). While water is injected into the riverbed, the internal sediment structures (mostly cross bedding) are disturbed within the upper decimetres. Changes in dune geometry are induced by the accumulation of mobilized sediments (mainly well sorted middle sands) on the dune slopes and in the adjacent troughs. Small bed forms like ripples which have been observed before dredging but not afterwards were covered by the remobilized sediments. The sub-bottom data indicate that these structures still exist below the freshly accumulated sediments. The expansion of newly accumulated sediments can be limited on the basis of the SSS data on several tens of metres preferentially in the direction of the current flow. These distances have also been shown by Stengel (2006) by comparison of bathymetric profiles or by Piechotta (2011) on basis of SES data and elevation difference maps. The transition between areas influenced by the dredging device and unaffected areas can be very sharp.

The transport of the mobilized sediments is reported in literature generally as near bed suspension over a distance of some meters to kilometres which is mainly valid for fine cohesive sediments (Meyer-Nehls 2000). New knowledge concerning the uplift and the transport distance of coarser particles like middle sands as found in this study area can be derived by comparing the acoustical backscatter signals of the SSS, SES and ADCP with the SSC, transmission and PSD data. Clouds of increased acoustical backscatter have been observed in the current lee site of the WID vessel whereas the detected perturbed distance varies with the used frequency of the acoustical devices. Additionally, the LISST pronounced in relation with dredging activities in study area A too turbid water before reaching the ground while no indication of the WID impact is given at site B. However, the increased transmission and acoustical signals observed at study site A do not match with the significant increased TVCs or SSCs. Too turbid water with simultaneously relative low mass concentrations can only be explained by large aggregates with high organic contents (Williams et al. 2007). From literature it is well known that the cohesive suspended

sediments in the Weser estuary are generally in an aggregated state (e.g. Papenmeier et al. 2011 – chapter 5, Wellershaus 1981) but these also exist at dredging influenced sites. A dredging induced resuspension or generation of such aggregates is unlikely due to middle sands of the river bed being inappropriate for aggregation. Papenmeier et al. (2011 – chapter 5) have shown that aggregation in the Weser estuary preferentially takes place when sediments of silt size and organic matter are present. Additionally, missing significant changes in the grain size distribution indicate, that nearly no specific size classes are removed. ISPSDs in the range of the river sediment can be an indicator for mobilization and uplift of sandy particles. However, these PSDs have been observed only sporadically at all sites, including dredging influenced sites. Moreover nearly no sandy particles have been observed in the water samples.

A further factor which can generate increased signals in the hydroacoustic data are water turbulences and air bubbles (Blondel 1996). The presence of the latter one can explain why SSCs do not vary in the vicinity of the dredging device while the LISST announced too high turbidity. The device is not able to differentiate between particles and air bubbles (Mikkelsen & Pejrup 2000). If air bubbles are the main factor, the effect has also to be present at study site B which is not the case. It is more likely that an interruption of measurement at study site A is related to a very low transmission caused by a combination of big particles, air bubbles and the SSC. At study site B, the SSC is generally lower so that the combination of SSC, particle size and air bubbles seem not to exceed the operational turbidity threshold of the LISST. This is also valid for the dredging site 11c at study site A, where tidal controlled SSC had already decreased.

Significant influence of the dredging induced turbulences on the ISPSD within the water column has not been observed in this study as reported by Mikkelsen & Pejrup (2000) for a backhoe dredging plume in the Øresund between Denmark and Sweden. They described a break-up of the fragile in-situ particles in the vicinity of the device but with increasing distance particles flocculated again. It is possible that due to a higher SSC in the Weser estuary the dredging induced break up is compensated by an increased particle collision frequency within the turbulent water.

8.7: Conclusion

With the WID technique the selected sandy subaqueous dunes were removed very precisely within the given tolerance of 50 cm. This enables a reduction of the dredging volume and related expenses. The spatial expansion of sediment removal as well as accumulation and thus potential effects on the benthic fauna is restricted to the proximate dredging site. A significant transport of the sandy sediments beyond the dune slopes or adjacent troughs has not been observed and the internal sediment structures are only disturbed in the upper decimetres directly at the dredging site. Changes in the PSD as known from the literature were not measured after one dredging cycle.

Increased hydroacoustic signals in the current lee site of the dredging vessel have been identified in combination with water samples, an OBS sensor and an in-situ particle sizer as mainly as water turbulences and air bubbles. This signal is some hundred meters behind the dredging vessel in current flow direction superimposed by the tidal controlled SSCs. Bed loads or suspended sediment loads of exceptional SSCs do not occur in the current lee site of the dredging site. The generation of such loads is not possible in the investigated, sandy river sections due to very low amounts of fine cohesive sediments which are able to keep in suspension over longer distances.

Differences in sediment redistribution or suspended sediment processes have not been observed between the brackwater and freshwater section as well as between the maintenance and construction area. Overall, it can be concluded that WID does not seem to have a significant impact on suspended sediment dynamics and spatial redistribution of the removed sediments is very small.

Acknowledgements

We would like to express our thanks to the German Research Foundation (DFG) for supporting this study. It was carried out by the excellence cluster ‘Future Ocean’ and the Senckenberg Institute Wilhelmshaven and was furthermore affiliated with the research programme ‘Wirkungskontrolle Wasserinjektion’ The Water and Shipping Authority (WSA) of Bremerhaven and Bremen, the WSA Cuxhaven as well as the Federal Waterways Engineering and Research

Institute Hamburg (BAW) were the overall control for this programme. We would also like to express our gratitude to the WSA Wilhelmshaven for supplying ship and personal.

Chapter 9: Overall conclusion

The main aspect of this thesis was to provide enhanced knowledge of not only near bed fine cohesive sediment dynamics but also of fine cohesive sediment dynamics in the water column under 'natural'" circumstances and under the influence of WID. A multiple-methodological approach was able to show the complexity of fine cohesive sediment processes in estuarine environments and indicates the importance of consistent definitions (e.g. fluid mud characteristics) and the application of the state of the art techniques.

Suspended fine cohesive sediments are generally transported as very fragile flocs or aggregates which break-up easily when shear-stress is applied. In this study it was possible to show tidal induced aggregation and disaggregation by means of LISST measurements which provide fast and high data density without floc disruption (chapter 5). Supplementary investigations of PPSDs indicate that flocs are even at high current velocities strong enough to withstand the breakage into their inorganic constituent parts. The distribution of PPSD remains stable during the flocculation processes but vary at least in the Elbe estuary between the salt-, freshwater reach and the TMZ. ISPSD and PPSD in combination have not been studied in such detail before. However, knowledge about floc size and composition is important to estimate settling velocities of SPM. The experiences of ISPSD and PPSD acquired in this study should be applied in further studies on estuarine systems with e.g. different tidal dynamics, stratifications or SSCs. First investigations in the TMZ of the ebb-dominate Weser estuary show similar ISPSDs as observed in the TMZ of the flood-dominated Elbe estuary but different PPSDs. Appropriate data is still missing for the reaches outside of the TMZ. Special focus should also be done on very high concentrated estuarine systems such as the Ems estuary where the question arises as to at which extent high SSCs influence the flocculation behaviour. The first attempts of measuring ISPSD with the LISST system failed due to too high SSCs. Also earlier studies with e.g. camera systems as described in literature were labour-intensive and less than satisfactory. Future in-situ particle size investigations in high SSC environments will be a technical challenge.

Increased particle settling can lead to enhanced near bed fine cohesive sediment concentrations especially in the TMZs where the SSCs are generally high. The deployment of special adapted Rumohr-type gravity corer indicate that the widely accepted 3-layer models often used to describe vertical, cohesive sediment distribution (sediment suspension - fluid mud - cohesive bed) is evidently incomplete (chapter 6). Sedimentological and rheological investigations, statistically proven by a cluster analysis, have shown that between a low-viscosity layer (I) and high-viscosity layer (II) within the fluid mud can be distinguished. Furthermore, it was possible to define on basis of the combined sedimentological and rheological data the SSC-limits of both fluid mud types. This is a substantial progress compared with earlier studies which are mainly based on SSCs or density data. The differentiation of the two fluid mud types is not trivial because fluid mud (II) is suggested to represent recurrent, cohesive sediment accumulations which frequently have to be dredged in harbours and navigation channels whereas fluid mud (I) is more likely resuspended with a progressing tidal current. Apparently, the sedimentological characteristics of the identified units do not change with increasing or decreasing current velocity (chapter 7). Variations of rheological behaviour with changing current velocity have to be answered in future studies because the viscosity can exert a control over the resuspension and deposition of fine cohesive sediments.

Spatial fluid mud occurrence and temporal interfacial mixing have been shown for the Weser and Elbe estuaries on basis of acoustic interfaces (chapter 7). By means of the low frequency channel of a parametric echo sounder those interfaces can be clearly differentiated from the river bed reflector. So far, conventional echo sounders have problems to detect such accumulations adequately and detected the interface within the water column as the navigational depth which often caused confusion when the navigational depth is suddenly reduced by several metres. However, the Rumohr-type gravity core samples taken during this study reveal the interface undoubtedly as the upper boundary of fluid mud (I) which is referred as navigable. Up to now it was assumed that the strength of the reflector is related to the intensity of the SSC-gradient. Ground-truthing with the Rumohr-type gravity core samples taken at different current velocities reveal a correlation between the interface strength and SSC-gradient, which has so far not been quantified in literature. SSC-gradients at the upper fluid mud boundary

decreases with progressing tidal currents but significant variations in SSC-gradient do not occur in areas of smooth bed morphology until at least one hour after slack water. It will be never be possible to generalize the time and strength of resuspension because this process is dependent on several parameters such as the bed morphology, fluid mud thickness or consolidation time. However, the acoustic approach is a good way to quantify the resuspension and consolidation of fluid muds.

Dredging amounts and rates of fine cohesive sediment accumulations and sandy subaqueous dunes have increased during the past few decades in the navigation channels of the German estuaries. This study has shown that WID is at least in environments with sandy subaqueous dunes an effective dredging technique (chapter 8). The dune crests are removed exactly at the demanded height while the internal sediment structure is only destroyed in the upper decimetres. The removed sediments are accumulated on the dune slopes or in the adjacent troughs. In this manner, potential dredging effects on the benthic fauna are restricted to the proximate dredging site. Effects on the fine cohesive sediment dynamics such as increased SSCs or variations in floc size have not been observed although acoustic interferences suggest turbulences at the current lee-side of the dredging device. WID techniques have been revealed at least in sandy environments as good alternative compared to conventional techniques were sediments were expensively dumped or even completely removed from the river system. In focus of suspended cohesive sediment dynamics and recurring depth restricting accumulation it is worth to intensify research in muddy environments where the ability of sediment mobilization is larger than in sandy environments.

In summary the new knowledge about flocculation processes and floc composition, fluid mud characteristics, distribution and interfacial mixing as well as the effects of WID on the cohesive sediment dynamics present a new basis to make the complex estuarine system more comprehensible. Specific values of this study can validate and enhance future numerical modelling.

Acknowledgements

This PhD Thesis was carried out and financed by the working group ‘Sea-Level Rise and Coastal Erosion’ in the course of the Excellence Cluster ‘Future Ocean’ in Kiel (Germany). I would like to thank Prof. Dr. Kerstin Schrottke for taking on the supervision and Prof. Dr. Karl Stattegger for taking on the co-supervision.

I thank Dr. Alexander Bartholomä for insightful discussions throughout the last years and proof-reading of the manuscripts.

Furthermore, I would like to thank the project partners of the multidisciplinary monitoring campaign ‘Wirkungskontrolle Wasserinjektion’ for the excellent cooperation.

I thank Helmut Beese, Eric Steen, Angela Trumpf and the technical assistants of the Senckenberg Institute in Wilhelmshaven for dealing with all kinds of technical problems and for the lab assistance, respectively. Not to forget, many thanks go to all trainees for their assistance in the lab and during the surveys. Special thanks go to Stephie P. for the patient spell checking.

Besides, I would like to thank the master and crew of *‘RV Senckenberg’*, *‘RV Littorina’* and working vessel *‘Rüstersiel’*. Their excellent job, the inexhaustible patience and some spontaneous sampling device improvements lead to the great data basis of my thesis.

Many thanks goes to the working group ‘Experimentelle und Theoretische Petrologie’ at Kiel University for providing their furnace as well as to all others who provided this with word and deed.

Special thanks go to my colleagues for support and discussion and a very nice working atmosphere (including several fruitful after-work discussions).

Finally I would like to thank my family and friends supporting me permanently with word and deed. They helped me in the last years to relax, provided my physical well-being and prevent several nervous-breakdowns.

References

AGRAWAL, Y.C., MC CAVE, I.N., RILEY, J.B. (2007): Laser diffraction size analysis. In: Syvitski, J.P.M. (Ed.), Principles, methods, and application of particle size analysis. Cambridge University Press, Cambridge, 119-128.

AGRAWAL, Y.C., POTTSMITH, H.C. (2000): Instruments for particle size and settling velocity observations in sediment transport. Marine Geology 168: (1-4), 89-114.

AGRAWAL, Y.C., WHITMIRE, A., MIKKELSEN, O.A., POTTSMITH, H.C. (2008): Light scattering by random shaped particles and consequences on measuring suspended sediments by laser diffraction. Journal of Geophysical Research 113: (C04023).

ASTER, D. (1993): Der Einfluss von Wasseinjektionsbaggerung auf die Wassertrübung. Hansa 130: (3), 64-65.

BALE, A., MORRIS, A.W. (2007): In situ size measurements of suspended particles in estuarine and coastal waters using laser diffraction. In: Syvitski, J.P.M. (Ed.), Principles, methods, and apllication of particle size analysis. Cambridge University Press, Cambridge, 197-208.

BARNES, H.A., HUTTON, J.F., WALTERS, K. (1989): An introduction to rheology. Elsevier, Amsterdam, 199 p.

BARNES, H.A., NGUYEN, Q.D. (2001): Rotating vane rheometry - a review. Journal of Non-Newtonian Fluid Mechanics 98: (1), 1-14.

BECKER, M. (2011): Suspended sediment transport and fluid mud dynamics in tidal estuaries. PhD Thesis, University of Bremen, 176 p.

BfG (1992): Anpassung der Fahrrine der Außenweser an die künftig weltweit gültigen Anforderungen der Containerschiffe -SKN- 14 m Ausbau (UVU). Bundesanstalt für Gewässerkunde (BfG), Koblenz, 217 p.

BfG (2008): WSV-Sedimentmanagement Tideelbe - Strategien und Potenziale - eine Systemstudie. Ökologische Auswirkungen der Umlagerung von Wedeler Baggergut. Untersuchungen im Auftrag des Wasser- und Schifffahrtsamt Cuxhaven. Bundesanstalt für Gewässerkunde (BfG), Koblenz, 374 p.

BfG (2011): Umweltauswirkungen von Wasserinjektionsbaggerungen. WSV-Workshop am 21./22. Juni 2010 in Bremerhaven. Bundesanstalt für Gewässerkunde (BfG), Koblenz, 117 p.

BLONDEL (2009): The handbook of sidescan sonar. Springer, Berlin, 316 p.

BLOTT, S.J., PYE, K. (2006): Particle size distribution analysis of sand-sized particles by laser diffraction: an experimental investigation of instrument sensitivity and the effects of particle shape. Sedimentology 53: (3), 671-685.

BREKHOVSKIKH, L.M., LYSANOV, Y.P. (2003): Fundamentals of ocean acoustics. Springer, New York, 279 p.

BREZINA, J. (1979): Particle size and settling rate distributions of sand-sized materials. 2nd European Symposium on Particle Characterisation (PARTEC), 24-26 Sep. 1979, Nürnberg, 44 p.

BROWN, E., COLLING, A., PARK, D., PHILLIPS, J., ROTHERY, D., WRIGHT, J. (2006): Waves, tides and shallow-water processes. Butterworth-Heinemann, Oxford, 227 p.

CHANG, T.S., FLEMMING, B.W., BARTHOLOMÄ, A. (2007): Distinction between sortable silts and aggregated particles in muddy intertidal sediments of the East Frisian Wadden Sea, southern North Sea. Sedimentary Geology 202: (3), 453-463.

CHEN, S., EISMA, D., KALF, J. (1994): In situ distribution of suspended matter during the tidal cycle in the Elbe Estuary. Netherlands Journal of Sea Research 32: (1), 37-48.

CLAUSNER, J.E. (1993): Water injection dredging demonstration on the Upper Mississippi River. U.S. Army Corps of Engineers, Waterways Eperiment Station. Dredging Research DRP-3-10, 1-16.

COAKLEY, J.P., SYVITSKI, J.P.M. (2007): SediGraph technique. In: Syvitski, J.P.M. (Ed.), Principles, methods and application of particle size analysis. Cambridge University Press, Cambridge, 129-142.

DALRYMPLE, R.W., MACKAY, D.A., ICHASO, A.A., CHOI, K.S. (2012): Processes, morphodynamics, and facies of tide-dominated estuaries. In: Davis, R.A.Jr., Dalrymple, R.W. (Eds.), Principles of tidal sedimentology. Springer, Dordrecht, 79-107.

DANKERS, P.J.T., WINTERWERP, J.C. (2007): Hindered settling of mud flocs: Theory and validation. Continental Shelf Research 27: (14), 1893-1907.

DE JONGE, V. (1983): Relations between annual dredging activities, suspended matter concentrations, and the development of the tidal regime in the Ems Estuary. Canadian Journal of Fischeries and Aquatic Sciences 40, 289-300.

DE JONGE, V.N. (1988): The abiotic environment. In: Baretta, J., Ruardij, P. (Eds.), Tidal flat estuaries: simulation and analysis of the Ems estuary. Springer, Berlin, 14-27.

DE JONGE, V.N., VAN DEN BERGS, J. (1987): Experiments on the resuspension of estuarine sediments containing benthic diatoms. Estuarine, Coastal and Shelf Science 24, 725-740.

DEAN, W.E. (1974): Determination of carbonate and organic matter in calcareous sediments and sedimentary rocks by loss on ignition; comparison with other methods. Journal of Sedimentary Research 44: (1), 242-248.

DUINKER, J.C., HILLEBRAND, M.T.J., NOLTING, R.F., WELLERSHAUS, S. (1982): The river Elbe: Processes affecting the behaviour of metals and organochlorines during estuarine mixing. Netherlands Journal of Sea Research 15: (2), 141-169.

DYER, K.R., CORNELISSE, J., DEARNALEY, M.P., FENNESSY, M.J., JONES, S.E., KAPPENBERG, J., MC CAVE, I.N., PEJRUP, M., PULS, W., VAN LEUSSEN, W., WOLFSTEIN, K. (1996): A comparison of in situ techniques for estuarine floc settling velocity measurements. Journal of Sea Research 36: (1-2), 15-29.

EISMA, D. (1986): Flocculation and de-flocculation of suspended matter in estuaries. Netherlands Journal of Sea Research 20: (2-3), 183-199.

EISMA, D., BERNARD, P., CADÉE, G.C., ITTEKKOT, V., KALF, J., LAANE, R., MARTIN, J.M., MOOK, W.G., VAN PUT, A., SCHUHMACHER, T. (1991): Suspended-matter particle size in some west-European estuaries; part I: Particle-size distribution. Netherlands Journal of Sea Research 28: (3), 193-214.

EISMA, D., CHEN, S., LI, A. (1994): Tidal variations in suspended matter floc size in the Elbe river and Dollard estuaries. Aquatic Ecology 28: (3), 267-274.

EISMA, D., KALF, J., VEENHUIS, M. (1980): The formation of small particles and aggregates in the Rhine Estuary. Netherlands Journal of Sea Research 14: (2), 172-191.

FAAS, R. (1981): Rheological characteristics of Rappahannock Estuary muds, Southeastern Virginia, U.S.A. In: Nio, S.-D., Schüttenhelm, R.T.E., van Weering, T.C.E. (Eds.), Holocene marine sedimentation in the North Sea Basin. Blackwell Scientific Publications, Oxford, 505-515.

FAAS, R. (1984): Time and density-dependent properties of fluid mud suspensions, NE Brazilian Continental Shelf. Geo-Marine Letters 4: (3), 147-152.

FENNESSY, M.J., DYER, K.R., HUNTLEY, D.A. (1994): INSSEV: An instrument to measure the size and settling velocity of flocs in situ. Marine Geology 117: (1-4), 107-117.

FLEMMING, B., THUM, A.B. (1978): The settling tube - a hydraulic method for grain size analysis of sands. Kieler Meeresforschungen: (SI 4), 82-95.

FOLK, R.L., WARD, W.C. (1957): Brazos River bar: a study in the significance of grain size parameters. Journal of Sedimentary Petrology 27, 3-26.

FRIEDMAN, G.M., SANDERS, J.E. (1978): Principles of sedimentology. Freeman, New York, 792 p.

FUGATE, D.C., FRIEDRICHS, C.T. (2003): Controls on suspended aggregate size in partially mixed estuaries. Estuarine, Coastal and Shelf Science 58: (2), 389-404.

GIBBS, R.J. (1974): A settling tuby system for sand-size analysis. Journal of Sedimentary Petrology 44: (2), 583-588.

GORDON, R.L. (1996): Acoustic Doppler Current Profiler - principal and operation - a practical primer. RD Instruments, San Diego, 52 p.

GRABEMANN, I., KAPPENBERG, J., KRAUSE, G. (1995): Aperiodic variations of the turbidity maxima of two german coastal plain estuaries. Netherlands Journal of Aquatic Ecology 29: (3-4), 217-227.

GRABEMANN, I., KRAUSE, G. (1989): Transport proccesses of suspended matter derived from time series in a tidal estuary. Journal of Geophysical Research 94: (C10), 14373-14379.

GRABEMANN, I., KRAUSE, G. (2001): On different time scales of suspended matter dynamics in the Weser estuary. Estuaries and Coasts 24: (5), 688-698.

GRABEMANN, I., UNCLES, R.J., KRAUSE, G., STEPHENS, J.A. (1997): Behaviour of turbidity maxima in the Tamar (U.K.) and Weser (F.R.G.) Estuaries. Estuarine, Coastal and Shelf Science 45: (2), 235-246.

GRANBOULAN, J., FERAL, A., VILLEROT, M., JOUANNEAU, J.M. (1989): Study of the sedimentological and rheological properties of fluid mud in the fluvio-estuarine system of the Gironde estuary. Ocean and Shoreline Management 12: (1), 23-46.

GUERRERO, M., SZUPIANY, R.N., AMSLER, M. (2011): Comparison of acoustic backscattering techniques for suspended sediments investigation. Flow Measurement and Instrumentation 22: (5), 392-401.

HERMAN, P.M.J., HEIP, C.H.R. (1999): Biogeochemistry of the MAximum TURbidity Zone of Estuaries (MATURE): some conclusions. Journal of Marine Systems 22: (2-3), 89-104.

INGLIS, C.C., ALLEN, F.H. (1957): The regime of the Thames estuary as affected by currents, salinities, and river flow. Proc. Inst. Civ. Eng. 7, 827-868.

JAMES, A.E., WILLIAMS, D.J.A., WILLIAMS, P.R. (1987): Direct measurement of static yield properties of cohesive suspensions. Rheologica Acta 26: (5), 437-446.

JÜRGES, J., WINKEL, N. (2003): Ein Beitrag zur Tidedynamik der Unterems. Mitteilungsblatt der Bundesanstalt für Wasserbau 86, 29-31.

KAPPENBERG, J., GRABEMANN, I. (2001): Variability of the mixing zones and estuarine turbidity maxima in the Elbe and Weser Estuaries. Estuaries and Coasts 24: (5), 699-706.

KENDRICK, M.P., DERBYSHIRE, B.V. (1985): Monitoring of a near-bed turbid layer. Report SR44. Hydraulic Research, Wallingford, 20 p.

KERNER, M. (2007): Effects of deepening the Elbe Estuary on sediment regime and water quality. Estuarine, Coastal and Shelf Science 75: (4), 492-500.

KERNER, M., JACOBI, A. (2006): Ausbau- und Unterhaltungskosten für die deutschen Seehäfen. WWF, Frankfurt am Main, 23 p.

KINEKE, G.C., STERNBERG, R.W. (1995): Distribution of fluid muds on the Amazon continental shelf. Marine Geology 125: (3-4), 193-233.

KINEKE, G.C., STERNBERG, R.W., TROWBRIDGE, J.H., GEYER, W.R. (1996): Fluid-mud processes on the Amazon continental shelf. Continental Shelf Research 16: (5-6), 667-696.

KIRBY, R. (1988): High concentration suspension (fluid mud) layers in estuaries. In: Dronkers, J., van Leussen, W. (Eds.), Physical Processes in Estuaries. Springer, Berlin, 463-487.

KRANCK, K. (1981): Particulate matter grain-size characteristics and flocculation in a partially mixed estuary. Sedimentology 28, 107-114.

KRANCK, K., PETTICREW, E., MILLIGAN, T.G., DROPPO, I.G. (1993): In situ particle size distributions resulting from flocculation of suspended sediment. In: Mehta, A. (Ed.), Nearshore and estuarine cohesive sediment transport. American Geophysical Union, Waschington, 60-74.

KRONE, R. (1962): Flume sstudies of the transport of sediment in estuarial shoaling processes. Final Report. Hydr. and Eng. Res. Lab. University of California, Berkely, 118 p.

KRONE, R. (1993): Sedimentation revisited. In: Mehta, A. (Ed.), Nearshore and estuarine cohesive sediment transport. American Geophysical Union, Washington, 108-125.

KRULIS, M., ROHM, H. (2004): Adaption of a vane tool for the viscosity determination of flavoured yoghurt. European Food Research and Technology 218: (6), 598-601.

LURTON, X. (2002): An introduction to underwater acoustics: principles and applications. Springer, Berlin, 347 p.

MANNING, A.J., BASS, S.J. (2006): Variability in cohesive sediment settling fluxes: Observations under different estuarine tidal conditions. Marine Geology 235: (1-4), 177-192.

MANNING, A.J., BASS, S.J., DYER, K.R. (2006): Floc properties in the turbidity maximum of a mesotidal estuary during neap and spring tidal conditions. Marine Geology 235: (1-4), 193-211.

MANNING, A.J., LANGSTON, W.J., JONAS, P.J.C. (2010): A review of sediment dynamics in the Severn Estuary: Influence of flocculation. Marine Pollution Bulletin 61: (1-3), 37-51.

MCANALLY, W.H., FRIEDRICHS, C., HAMILTON, D., HAYTER, E., SHRESTHA, P., RODRIGUEZ, H., SHEREMET, A., MUD, A.T.A.T.C.O.M.O.F. (2007): Management of Fluid Mud in Estuaries, Bays, and Lakes. I: Present State of Understanding on Character and Behavior. Journal of Hydraulic Engineering 133: (1), 9-22.

MCCAVE, I.N., SYVITSKI, J.P.M. (2007): Principles and methods of geological particle size analysis. In: Syvitski, J.P.M. (Ed.), Principles, methods and application of particle size analysis. Cambridge University Press, Cambridge, 3-21.

MEHTA, A. (1991): Understanding fluid mud in a dynamic environment. Geo-Marine Letters 11: (3), 113-118.

MEHTA, A.J. (1989): On estuarine cohesive sediment suspension behavior. J. Geophys. Res. 94: (C10), 14303-14314.

MEISCHNER, D., RUMOHR, J. (1974): A light-weight, high-momentum gravity corer for subaqueous sediments. Senckenbergiana marit 6: (1), 105-117.

MEYER-NEHLS, R. (2000): Das Wasserinjektionsverfahren: Ergebnisse einer Literaturstudie sowie von Untersuchungen im Hamburger Hafen und in der Unterelbe. Ergebnisse aus dem Baggeruntersuchungsprogramm. Freie und Hansestadt Hamburg Wirtschaftsbehörde Strom- und Hafenbau, Hamburg, 111 p.

MEZGER, T. (2000): Das Rheologie-Handbuch: für Anwender von Rotations- und Oszillations-Rheometer. Vincentz, Hannover, 271 p.

MEZGER, T. (2011): The rheology handbook. Vincentz, Hannover, 432 p.

MIKES, D. (2011): A simple floc-growth function for natural flocs in estuaries. Mathematical Geosciences 43: (5), 593-606.

MIKKELSEN, O., PEJRUP, M. (2001): The use of a LISST-100 laser particle sizer for in-situ estimates of floc size, density and settling velocity. Geo-Marine Letters 20: (4), 187-195.

MIKKELSEN, O.A., HILL, P.S., MILLIGAN, T.G. (2006): Single-grain, microfloc and macrofloc volume variations observed with a LISST-100 and a digital floc camera. Journal of Sea Research 55: (2), 87-102.

MIKKELSEN, O.A., HILL, P.S., MILLIGAN, T.G. (2007): Seasonal and spatial variation of floc size, settling velocity, and density on the inner Adriatic Shelf (Italy). Continental Shelf Research 27: (3-4), 417-430.

MIKKELSEN, O.A., HILL, P.S., MILLIGAN, T.G., CHANT, R.J. (2005): In situ particle size distributions and volume concentrations from a LISST-100 laser particle sizer and a digital floc camera. Continental Shelf Research 25: (16), 1959-1978.

MIKKELSEN, O.A., PEJRUP, M. (2000): In situ particle size spectra and density of particle aggregates in a dredging plume. Marine Geology 170, 443-459.

MITCHELL, S.B., WEST, J.R. (2002): Particle size distribution in an estuarine turbidity maximum region. In: Winterwerp, J.C., Kranenburg, C. (Eds.), Fine sediment dynamics in the marine environment. Elsevier, Amsterdam, 251-263.

MITCHENER, H., TORFS, H. (1996): Erosion of mud/sand mixtures. Coastal Engineering 29, 1-25.

NASNER, H. (1992): Injektionsbaggerung von Tideriffeln. Hansa 129: (2), 195-196.

NASNER, H., PIEPER, T., TORN, P., KUHLENKAMP, H. (2007): Properties of fluid mud and prevention of sedimentation. Gobal Dredging Conference, 27.05.-01.06.2007, Orlando, 14 p.

NETZBAND, A., GÖNNERT, G., CHRISTIANSEN, H. (1999): Water injection dredging in Hamburg - application and research. Dredging challenged: Proceedings of the CEDA dredging days 1999, 18.-19. November 1999, Amsterdam, 10 p.

NICHOLS, M. (1984): Fluid mud accumulation processes in an estuary. Geo-Marine Letters 4: (3), 171-176.

NLWKN (2008): Deutsches Gewässerkundliches Jahrbuch - Weser und Emsgebiet 2005. Niedersächsischer Landesbetrieb für Wasserwirtschaft, Küsten- und Naturschutz, Norden, 288 p.

NLWKN (2009): Deutsches Gewässerkundliches Jahrbuch - Weser und Emsgebiet 2006. Niedersächsischer Landesbetrieb für Wasserwirtschaft, Küsten- und Naturschutz, Norden, 288 p.

NLWKN (2011): Deutsches Gewässerkundliches Jahrbuch - Weser und Emsgebiet 2007. Niedersächsischer Landesbetrieb für Wasserwirtschaft, Küsten- und Naturschutz, Norden, 288 p.

PAPENMEIER, S., SCHROTTKE, K., BARTHOLOMÄ, A. (2009): Wirkungskontrolle von Wasserinjetkionsbaggerungen auf subaquatischen Dünenfeldern in der Unterweser auf der Basis von hydroakustischen, optischen und laseroptischen Messungen. Deutsche Gesellschaft für Limnologie (DGL), Erweiterte Zusammenfassung der Jahrestagung 2009 (Oldenburg), 6 p.

PAPENMEIER, S., SCHROTTKE, K., BARTHOLOMÄ, A. (2010): Toatal volume concentration and size distribution of suspended matter at sites affected by water injection dredging of subaqueous dunes in the German Weser Estuary. Coastline Reports 16, 71-76.

PAPENMEIER, S., SCHROTTKE, K., BARTHOLOMÄ, A., FLEMMING, B. (2011, accepted): Sedimentological and rheological properties of the water-solid bed interface in the Weser and Ems estuaries, North Sea, Germay: Implication for fluid mud classification. Journal of Coastal Research X: (X), X-X.

PIECHOTTA, F. (2011): Gewässerkundliche Untersuchungen im Rahmen der WI-Wirkungskontrolle. Umweltauswirkungen von Wasserinjektionsbaggerungen. In: Umweltauswirkungen von Wasserinjektionsbaggerungen. WSV-Workshop am 21./22. Juni 2010 in Bremerhaven. BfG, Koblenz, 18-31.

PROJEKTBÜRO FAHRRINNENANPASSUNG, P. (2007): Fahrrinnenanpassung Unter- und Außenelbe. Das Projekt im Überblick. Wasser- und Schifffahrtsamt Hamburg, Hamburg, 44 p.

PULS, W., KUEHL, H., HEYMANN, K. (1988): Settling velocity of mud flocs: results of field measurements in the Elbe and the Weser Estuary. In: Dronkers, J., van Leussen, W. (Eds.), Physical processes in estuaries. Springer, Berlin, 404-424.

PYE, K., BLOTT, S.J. (2004): Particle size analysis of sediments, soils and related particulate materials for forensic purposes using laser granulometry. Forensic Science International 144: (1), 19-27.

ROSS, M.A., MEHTA, A. (1989): On the mechanics of lutoclines and fluid mud. Journal of Coastal Research SI 5, 51-61.

SAVENIJE, H.H.G. (2005): Salinity and tides in alluvial estuaries. Elsevier, Amsterdam, 194 p.

SCHRAMM, G. (2000): A practical approach to rheology and rheometry. Gebrueder HAAKE GmbH, Karlsruhe, 291 p.

SCHROTTKE, K., BARTHOLOMÄ, A. (2008): Detaillierte Einblicke in die ästuarine Schwebstoffdynamik mittels hochaufläsender Hydroakustik. Ultraschall in der Hydrometrie: neue Technik - neuer Nutzen!?, 3.-4. Juni 2008, Koblenz, 75-82.

SCHROTTKE, K., BARTHOLOMÄ, A., BECKER, M., FLEMMING, B.W., HEBBELN, D. (2007): Tidally forced dynamics of fluid mud interfaces in tidal estuaries. International Conference 2007 and 97th Annual Meeting of the Geologische Vereinigung e.V. (GV), Bremen, 208.

SCHROTTKE, K., BECKER, M., BARTHOLOMÄ, A., FLEMMING, B.W., HEBBELN, D. (2006): Fluid mud dynamics in the Weser estuary turbidity zone tracked by high-resolution side-scan sonar and parametric sub-bottom profiler. Geo-Marine Letters 26, 185 - 198.

SCHUCHARDT, B., HASELOOP, U., SCHIRMER, M. (1993): The tidal freshwater reach of the Weser estuary: riverine or estuarine? Netherlands Journal of Aquatic Ecology 27: (2-4), 215-226.

SCHUCHARDT, B., SCHOLLE, J., SCHULZE, S., BILDSTEIN, T. (2007): Vergleichende Bewertung der ökologischen Situation der inneren Ästuare von Eider, Elbe, Weser und Ems: Was hat sich nach 20 Jahren verändert? Coastaline Reports 9, 15-26.

SEEDORF, H.H., MEYER, H.H. (1992): Landeskunde Niedersachsen - Natur- und Kulturgeschichte eines Bundeslandes, Band 1: Historische Grundlagen & naturräumliche Ausstattung. Karl Wachholtz Verlag, Neumünster, 517 p.

SHOLKOVITZ, E.R. (1976): Flocculation of dissolved organic and inorganic matter during the mixing of river water and seawater. Geochimica et Cosmochimica Acta 40: (7), 831-845.

SMITH, T.J., KIRBY, R. (1989): Generation, stabilization and dissipation of layered fine sediment suspensions. Journal of Coastal Research SI 5, 63-73.

SPENCER, K.L., DEWHURST, R.E., PENNA, P. (2006): Potential impacts of water injection dredging on water quality and ecotoxicity in Limehouse Basin, River Thames, SE England, UK. Chemosphere 63: (3), 509-521.

SPINGAT, F.M. (1997): Analyse der Schwebstoffdynamik in der Trübungszone eines Tideflusses. Leichtweiss-Institut für Wasserbau der Technischen Universität Braunschweig, Braunschweig, 187 p.

SPINGAT, F.M., OUMERACI, H. (2000): Schwebstoffdynamik in der Trübungszone des Ems-Ästuars - Anwendung eines Analysekonzeptes für hoch aufgelöste und dauerhaft betriebene Gewässergütemessungen. Die Küste 62, 159-221.

STREIF, H. (1990): Das ostfriesische Küstengebiet: Nordsee, Inseln, Watten und Marschen. Borntraeger, Hannover, 376 p.

STREIF, H. (2004): Sedimentary record of Pleistocene and Holocene marine inundations along the North Sea coast of Lower Saxony, Germany. Quaternary International 112: (1), 3-28.

SYLVESTER, A.J., WARE, G.C. (1976): Anaerobiosis of fluid mud. Nature 264: (5587), 635-635.

SYVITSKI, J.P.M. (1991): Principles, methods, and application of particle size analysis. Cambridge University Press, Cambridge.

SYVITSKI, J.P.M., ASPREY, K.W., CLATTENBURG, D.A. (2007): Principles, design and calibration of settling tubes. In: Syvitski, J.P.M. (Ed.), Principles, methods and application of particle size analysis. Cambridge University Press, Cambridge, 45-63.

TABILO-MUNIZAGA, G., BARBOSA-CÁNOVAS, G.V. (2005): Rheology for the food industry. Journal of Food Engineering 67: (1-2), 147-156.

TALKE, S.A., DE SWART, H.E. (2006): Hydrodynamics and morphology in the Ems/Dollard Estuary: Review of models, measurements, scientific literature, and the effects of changing conditions. University of Utrecht, Utrecht, 78 p.

THILL, A., MOUSTIER, S., GARNIER, J.-M., ESTOURNEL, C., NAUDIN, J.-J., BOTTERO, J.-Y. (2001): Evolution of particle size and concentration in the Rhône river mixing zone: influence of salt flocculation. Continental Shelf Research 21: (18-19), 2127-2140.

TRAYKOVSKI, P., GEYER, W.R., IRISH, J.D., LYNCH, J.F. (2000): The role of wave-induced density-driven fluid mud flows for cross-shelf transport on the Eel River continental shelf. Continental Shelf Research 20: (16), 2113-2140.

TRAYKOVSKI, P., LATTER, R.J., IRISH, J.D. (1999): A laboratory evaluation of the laser in situ scattering and transmissometery instrument using natural sediments. Marine Geology 159: (1-4), 355-367.

UNCLES, R.J., ELLIOTT, R.C.A., WESTON, S.A. (1985): Observed fluxes of water, salt and suspended sediment in a partly mixed estuary. Estuarine, Coastal and Shelf Science 20: (2), 147-167.

UNCLES, R.J., STEPHENS, J., HARRIS, C. (2006a): Properties of suspended sediment in the estuarine turbidity maximum of the highly turbid Humber Estuary system, UK. Ocean Dynamics 56: (3), 235-247.

UNCLES, R.J., STEPHENS, J.A., LAW, D.J. (2006b): Turbidity maximum in the macrotidal, highly turbid Humber Estuary, UK: Flocs, fluid mud, stationary suspensions and tidal bores. Estuarine, Coastal and Shelf Science 67: (1-2), 30-52.

USACE (2002): Depth measurement over irregular or consolidated bottoms. In: USACE (Ed.), Hydrographic engineering. US Army Corps of Engineers, Washington, 21/21-21/22.

VAN DE KREEKE, J., DAY, C.M., MULDER, H.P.J. (1997): Tidal variations in suspended sediment concentration in the Ems estuary: origin and resulting sediment flux. Journal of Sea Research 38: (1-2), 1-16.

VAN DER LEE, W. (2001): Parameters affecting mud floc size on a seasonal time scale: The impact of a phytoplankton bloom in the Dollard estuary, the Netherlands. In: McAnally, W.H., Mehta, A.J. (Eds.), Coastal and estuarine fine sediment processes. Elsevier, Amsterdam, 403-421.

VAN LEUSSEN, W. (1988): Aggregation of particles, settling velocity of mud flocs. A review. In: Dronkers, J., van Leussen, W. (Eds.), Physical processes in estuaries. Springer, Berlin, 348-403.

VAN LEUSSEN, W. (1999): The variability of settling velocities of suspended fine-grained sediment in the Ems Estuary. Journal of Sea Research 41: (1-2), 109-118.

VAN MAREN, D.S., WINTERWERP, J.C., WANG, Z.Y., PU, Q. (2009): Suspended sediment dynamics and morphodynamics in the Yellow River, China. Sedimentology 56, 785-806.

VAN OLPHEN, H. (1991): An introduction to clay colloid chemistry: For clay technologists, geologists, and soil scientists. Wiley, New York, 318 p.

VANTORRE, M. (2001): Nautical Bottom Approach - application to the access to the harbour of Zeebrugge. Hansa 138: (6), 93-97.

WELLERSHAUS, S. (1981): Turbidity maximum and mud shoaling in the Weser estuary. Archiv für Hydrobiologie 92, 161-198.

WELLS, J.T. (1983): Dynamics of coastal fluid muds in low-, moderate and high tide-range environments. Canadian Journal of Fischeries and Aquatic Sciences 40: (1), 130-142.

WELLS, J.T., COLEMAN, J.M. (1981): Physical processes and fine-grained sediment dynamics, coast of Surinam, South America. Journal of Sedimentary Research 51: (4), 1053-1068.

WHITEHOUSE, R., SOULSBY, R., ROBERSTS, W., MITCHENER, H. (2000): Dynamics of estuarine muds. Thomas Telford Publishing, London, 210 p.

WIENBERG, C. (2003): Korrigiert und ausgebaggert - Die Außenweser im Wandel der Zeit. In: Heidbrink, I. (Ed.), Konfliktfeld Küste: ein Lebensraum wird erforscht. Bilbliotheks- und Informationssystem der Universität Oldenburg, Oldenburg, 139-160.

WILLIAMS, N.D., WALLING, D.E., LEEKS, G.J.L. (2007): High temporal resolution in situ measurement of the effective particle size characteristics of fluvial suspended sediment Water Research 41: (5), 1081-1093.

WINTERWERP, J.C. (2002): On the flocculation and settling velocity of estuarine mud. Continental Shelf Research 22: (9), 1339-1360.

WINTERWERP, J.C., VAN KESTEREN, W.G.M. (2004): Introduction to the physics of cohesive sediment in the marine environment. Elsevier, Amsterdam, 205 p.

WOLANSKI, E., ASAEDA, T., IMBERGER, J. (1989): Mixing across a lutocline. Limnology and Oceanography 34: (5), 931-938.

WOLTERING, S. (1996): Einsatz eines Wasserinjektionsgerätes zur Hafenunterhaltung. Hansa 133: (12), 62-66.

WRIGHT, J., KRONE, R. (1989): Aggregate structure in hyperconcentrated mud flows. Journal of Coastal Research SI 5, 117-125.

WUNDERLICH, J., MÜLLER, S., ERDMANN, S., HÜMBS, P., BUCH, T., ENDLER, R. (2005): High-resolution acoustical site exploration in very shallow water - a case study. EAGE Near Surface, 5.-8.September 2005, Palermo, 4 p.

WURPTS, R. (2005): Hyperconcentratred flow. Hansa 142: (9), 75-88.

WURPTS, R., TORN, P. (2005): 15 Years Experience with fluid mud: Definition of the nautical bottom with rheological parameters. Terra et Aqua 99, 22-32.

ZORNDT, A., WURPTS, A., SCHLURMANN, T. (2011): The influence of hydrodynamic boundary conditions on characteristics, migration, and associated sand transport of sand dunes in a tidal environment. Ocean Dynamics 61: (10), 1629-1644.

Ich versichere an Eides statt, dass:

1) Ich bis zum heutigen Tage weder an der Christian-Albrechts-Universität zu Kiel noch an einer anderen Hochschule ein Promotionsverfahren endgültig nicht bestanden habe oder mich in einem entsprechenden Verfahren befinde oder befunden habe.

2) Ich die Inanspruchnahme fremder Hilfen aufgeführt habe, sowie, dass ich die wörtlich oder inhaltlich aus anderen Quellen entnommenen Stellen als solche gekennzeichnet habe.

3) Die Arbeit unter Einhaltung der Regeln guter wissenschaftlicher Praxis der Deutschen Forschungsgemeinschaft entstanden ist.

Kiel, Unterschrift